

Doctoral thesis

Doctoral theses at NTNU, 2020:307

Marit Fladvad

# OPTIMAL UTILISATION OF UNBOUND CRUSHED AGGREGATES FOR ROAD CONSTRUCTION

**NTNU**  
Norwegian University of Science and Technology  
Thesis for the Degree of  
Philosophiae Doctor  
Faculty of Engineering  
Department of Geoscience and Petroleum



**NTNU**

Norwegian University of  
Science and Technology



Marit Fladvad

# **OPTIMAL UTILISATION OF UNBOUND CRUSHED AGGREGATES FOR ROAD CONSTRUCTION**

Thesis for the Degree of Philosophiae Doctor

Trondheim, October 2020

Norwegian University of Science and Technology  
Faculty of Engineering  
Department of Geoscience and Petroleum

**NTNU**

Norwegian University of Science and Technology

Thesis for the Degree of Philosophiae Doctor

Faculty of Engineering  
Department of Geoscience and Petroleum

© Marit Fladvad

ISBN 978-82-326-4962-4 (printed ver.)  
ISBN 978-82-326-4963-1 (electronic ver.)  
ISSN 1503-8181

Doctoral theses at NTNU, 2020:307

Printed by NTNU Grafisk senter

Durch Stolpern kommt man bisweilen weiter,  
man muß nur nicht fallen und liegen bleiben.

— Johann Wolfgang von Goethe, 1831



## ABSTRACT

---

Aggregates are construction materials produced from non-renewable rock resources. Because high-quality aggregate resources have limited availability, utilisation of aggregates should be considered carefully to prevent resource scarcity. When suitable aggregate resources are encountered at or close to construction sites, e.g. surplus material from tunnelling, they should be utilised in construction rather than landfilled or used for less quality-demanding purposes. To obtain optimal utilisation, we must ensure that the best possible construction materials are produced from the available resources.

Climate changes are expected to represent a shift towards increased precipitation and more intense rainfall events. This development may cause increased moisture levels in pavement structures, which in turn may affect pavement performance. The Norwegian pavement design system is empirical, and thus not suited for adaptation to new environmental conditions. To adapt the pavement design to changing climatic conditions, the behaviour of typical road materials must be understood.

The research presented in thesis concerns three subjects:

- Use of large-size aggregates in pavement structures
- Production methods affecting aggregate quality
- Influence of aggregate gradation and moisture on pavement performance

A construction practice of using large-size aggregates is uncommon outside the Nordic countries. European standards do not cover large-size aggregates with upper particle size over 90 mm. The main concern regarding the use of large-size aggregates is the lack of suitable quality assessment methods.

The research design focussed on testing large-size aggregates using two full-scale studies. A full-scale crushing test examined the influence of crusher and feed parameters on the quality of primary crushed aggregates. The results showed that through adjustments to the crushing process, product quality measured as gradation and particle shape can be controlled. Optimising mechanical properties requires more than one crushing stage.

An accelerated pavement test investigated the performance of two instrumented pavement structures constructed using large-size subbase aggregates. The stress and strain response and performance of the unbound pavement materials were modelled using multi-layer elastic theory. Increased moisture content in unbound pavement materials leads to a substantial acceleration of permanent deformations from traffic. The stiffness of the unbound materials decreases as moisture content increases.

The research showed that the utilisation of aggregate resources in pavement structures have a clear potential for increase without compromising long-term pavement performance. There is room for optimisation of aggregate utilisation even within current quality requirements.

Adapting pavement structures to future climate changes leads to a more reliable and resilient transport infrastructure. Making efforts for optimal utilisation of available aggregate resources will reduce the consumption of non-renewable resources. By using more local resources, aggregate transport can be reduced, which will reduce the carbon footprint of the construction projects. Combined, these effects will help ensure a more sustainable infrastructure development.

Steinmaterialene omtalt i denne avhandlingen er byggeråstoff som produseres fra ikke-fornybare bergressurser. Siden tilgangen på høykvalitetsmaterialer er begrenset bør utnyttelsen av steinmaterialer planlegges nøye, slik at riktig kvalitet blir brukt til riktig formål. Når egnede steinmaterialer er tilgjengelig i eller nært et anleggsprosjekt, f.eks. overskuddsmaterialer fra tunnelbygging, bør de utnyttes i vegkonstruksjonen heller enn å bli brukt til fyllinger eller andre mindre kvalitetskrevenne formål. For å oppnå optimal utnyttelse må vi sørge for at tilgjengelige steinressurser blir bearbeidet til byggeråstoff av beste mulige kvalitet.

Det er ventet at klimaendringer vil føre til økte nedbørsmengder og mer intens nedbør. Denne utviklingen kan føre til økt fuktinnhold i vegbyggingmaterialene, som igjen kan påvirke nedbrytningen av vegkonstruksjonene. Det norske dimensjoneringsystemet for veger er erfaringsbasert, og lite egnet for tilpasning til nye klimatiske forhold. For å kunne tilpasse dimensjoneringen av veger til klimaendringene er det nødvendig med økt kunnskap om materialeegenskapene til typiske vegbyggingsmaterialer.

Forskningen som blir presentert i denne avhandlingen omhandler i hovedsak tre tema:

- Bruk av grove steinmaterialer i vegkonstruksjoner
- Hvordan produksjonsmetoden påvirker kvaliteten på byggeråstoffet
- Hvordan steinmaterialenes gradering og fuktinnhold påvirker vegkonstruksjoners tilstandsutvikling

Bruken av grov pukk og kult i vegbygging er uvanlig utenfor Norden, og grove materialer med øvre steinstørrelse over 90 mm dekkes ikke av europeiske standarder. Hovedutfordringen knyttet til bruken av grove steinmaterialer er mangelen på gjennomførbare testmetoder.

Forskningsarbeidet ble planlagt med vekt på å kunne teste grove steinmaterialer i fullskalaforsøk. Innvirkningen av knuserinnstillinger og pågangsegenskaper på kvaliteten til førstegangsknust materiale ble undersøkt ved hjelp av en fullskala knusetest. Resultatene viste hvordan det er mulig å innrette produksjonen for å tilpasse produktkvalitet i form av kornform og gradering. For å forbedre mekaniske egenskaper kreves flere knusetrinn.

Nedbrytningen av to instrumenterte vegkonstruksjoner bygd med grove steinmaterialer ble undersøkt med akselerert trafikk under ulike grunnvannsførhold. Spenninger, tøyninger og tilstandsutvikling ble modellert med elastisitetsteori for lagdelte konstruksjoner. Økt fuktinnhold i de ubundne vegbyggingsmaterialene fører til en kraftig akselerasjon av nedbrytningen av vegkonstruksjonene. Nedbrytningen ble målt som permanente deformasjoner og sporutvikling på overflaten. Årsaken til at nedbrytningen øker er at stivheten til de ubundne materialene minker når fuktinnholdet øker.

Forskningsarbeidet har vist at utnyttelsen av steinmaterialer i vegkonstruksjoner har potensiale for forbedring uten at det går på akkord med langsiktig tilstandsutvikling. Det er rom for optimalisering av utnyttelsen av steinmaterialer også innenfor begrensningene i dagens kvalitetskrav.

Ved å tilpasse dimensjoneringen av vegkonstruksjoner til framtidige klimaendringer bidrar vi til en mer pålitelig og motstandsdyktig transportinfrastruktur. Å gjøre innsats for å optimalisere utnyttelsen av tilgjengelige steinmaterialer vil redusere forbruket av ikke-fornybare ressurser. Ved å utnytte lokale bergressurser – kortreist stein – kan transporten av steinmaterialer reduseres, noe som kan redusere karbonfotavtrykket fra anleggsprosjekter. Til sammen vil disse virkningene bidra til en mer bærekraftig infrastrukturutvikling.

## PREFACE

---

The work presented in this thesis has been conducted at the Norwegian University of Science and Technology (NTNU), Department of Geoscience and Petroleum, in the PhD programme for Geology and Mineral Resources Engineering. The duration of the study was the period from January 2016 to May 2020. The Norwegian Public Roads Administration (NPRA) has financed the research and employment, with research contributions from Metso Minerals and Veidekke Industri. The study has been part of the project *Kortreist stein* [Local use of rock materials], an industrial innovation project financed through the Research Council of Norway.

The aim of the PhD study was to investigate opportunities and challenges regarding use of large-size unbound aggregates in road construction projects, with special emphasis on aggregates produced from surplus materials at road construction sites.

The study was initiated by the NPRA, and adjunct professor Børge Johannes Wigum from NTNU has been the main supervisor. Technical advisor Lillian Uthus Mathisen (Veidekke Industri), researcher Elena Scibilia (NTNU) and professor Rolf Arne Kleiv (NTNU) have been co-supervisors. Nils Uthus (NPRA) was appointed as mentor for the PhD candidate, and has been the main contact point between NTNU and NPRA throughout the study.

Within this study, six research papers have been prepared for publication. Each research paper is an individual presentation of a part of the research and can be read separately.

## ACKNOWLEDGEMENTS

---

This thesis is the result of a study that commenced in January 2016 when I became a PhD student at the Department of Geology and Mineral Resources Engineering. I want to thank my main supervisor, Børge Johannes Wigum, for agreeing to supervise my studies even though I am no geologist. Børge has given me a lot of freedom in the process, telling me that his role was to stay in the background and make adjustments to a direction I was to point out on my own. Consequently, this thesis is a true mirror of my broad interest in the field of road construction.

Lillian Uthus Mathisen deserves great thanks for always believing in me and giving me pep-talks even when I was not aware I needed them. Lillian has been a key person in organising my field studies with Metso Minerals and the Swedish National Road and Transport Research Institute (VTI).

I am grateful to my employer, the Norwegian Public Roads Administration (NPRA), for giving me the opportunity to do a PhD study as part of my job. I would particularly like to acknowledge my now retired boss Svein Ryan for making this possible. I could not have conducted the extensive full-scale studies in this study without the solid financial support provided by NPRA. I am also grateful to Nils Uthus, who has always looked after me and supported my work. My colleagues in the road administration have all been encouraging and patient throughout this period. Among my colleagues, I particularly want to thank Arnhild Ulvik for solving all lab-related challenges. I am grateful to Joralf Aurstad for his contributions to my research, but just as much for his endless supply of quizzes.

Veidekke Industri deserves thanks for providing me with a supervisor, test material, and an office for part of the study period. Veidekke was the owner of the *Kortreist stein* project, and our cooperation in the project enabled my full-scale studies. I am also very grateful to Metso Minerals, who made their test facility in Tampere available for me and supplied test material. I personally want to thank Tero Onnela and Ville Viberg from Metso Minerals for making my full-scale crushing test possible. Thanks to Sigurður Erlingsson for organising the accelerated pavement test at VTI. Above all, Sigurður deserves special thanks for being a de facto supervisor for the final period of this study and spending many hours patiently guiding me through the world of stress, strain and deformation.

I thank my friends in Puffinbiff for keeping up my social life throughout these years. The company of my PhD colleagues has been helpful, not least for ventilating all kinds of big and small frustrations over a cup of coffee. Thanks to Marte for walking up the path before me, and Anette for walking it with me.

I am especially grateful to my partner Eivind, who has been by my side all through this period. Eivind has always been supportive and patient, and eager to spend his holidays joining me at work travels abroad.

I thank my parents and my brothers for showing interest and support even though I have not always given answers when they have asked how the work is going. My family has provided me with a stable platform which all my achievements are built on. I owe a lot to my late grandmother Brita, who taught me many lessons that still spring to mind surprisingly often.

My father taught me to finish what I have started, but also that it is allowed to change course if I feel it is necessary. I have followed this advice several times, but I am happy that I found a research topic that was interesting enough for me to stick to it and finish this thesis even though my motivation has varied during these four years.

A PhD study is a solo journey, but I could not have completed it without the support from research partners, colleagues, family and friends – many more than those named here. Warm thanks to you all!

*Trondheim, May 2020*

*Marit Fladvad*



## PUBLICATIONS

---

The thesis is based on the following publications, which are included as appendixes. The specific contributions from each author to the papers are described in section 1.6 of the thesis.

### PAPER A

Fladvad, M., Aurstad, J. & Wigum, B.J. (2017) Comparison of practice for aggregate use in road construction – results from an international survey. In Loizos, A., Al-Qadi, I., Scarpas, T. (eds.) *Bearing Capacity of Roads, Railways and Airfields* (pp. 563–570). CRC Press. doi: 10.1201/9781315100333-74

### PAPER B

Fladvad, M. & Ulvik, A. (2019). Large-size aggregates for road construction – a review of standard specifications and test methods. *Bulletin of Engineering Geology and the Environment*. doi: 10.1007/s10064-019-01683-z

### PAPER C

Fladvad, M. & Onnela, T. (2020). Influence of jaw crusher parameters on the quality of primary crushed aggregates. *Minerals Engineering* 151(2020)106338. doi: 10.1016/j.mineng.2020.106338

### PAPER D

Fladvad, M. & Erlingsson, S. (2020). Performance of unbound pavement materials in changing moisture conditions. In Chabot A., Hornych P., Harvey J., Loria-Salazar L. G. (eds) *Accelerated Pavement Testing to Transport Infrastructure Innovation* (pp. 70-79). Lecture Notes in Civil Engineering vol 96, Springer. doi: 10.1007/978-3-030-55236-7\_8

### PAPER E

Fladvad, M. & Erlingsson, S. (2020). Modelling the response of large-size subbase materials tested under varying moisture conditions in a heavy vehicle simulator. Submitted manuscript.

### PAPER F

Fladvad, M. & Erlingsson, S. (2020). Permanent deformation modelling of large-size unbound pavement materials tested in a heavy vehicle simulator under different moisture conditions. Submitted manuscript.



# CONTENTS

---

ABSTRACT	v
PREFACE	ix
ACKNOWLEDGMENTS	x
PUBLICATIONS	xiii
PART I THE THESIS	
1 INTRODUCTION	3
1.1 Motivation . . . . .	3
1.2 Aim and scope . . . . .	5
1.2.1 Aim and objectives . . . . .	5
1.2.2 Scope of the thesis . . . . .	6
1.3 Research questions . . . . .	7
1.4 Research design . . . . .	7
1.5 Structure of the thesis . . . . .	8
1.6 Publications included in the thesis . . . . .	8
2 THEORY	13
2.1 Aggregate production . . . . .	13
2.1.1 Basic principles of comminution . . . . .	13
2.1.2 Crusher principles . . . . .	14
2.1.3 The aggregate production process . . . . .	16
2.1.4 Quality parameters . . . . .	18
2.2 Pavement design . . . . .	21
2.2.1 Typical Norwegian pavement structures . . . . .	22
2.2.2 The basis of pavement design . . . . .	22
2.2.3 Stress and strain under traffic load . . . . .	25
2.2.4 Influence of traffic and loading . . . . .	26
2.2.5 Influence of climate . . . . .	27
2.2.6 Modelling the response behaviour of unbound pavement materials . . . . .	28
2.2.7 Modelling the permanent deformation behaviour of unbound pavement materials . . . . .	30
2.3 Sustainability in aggregate production and use . . . . .	32
3 METHODS	37
3.1 Survey of practice for aggregate use . . . . .	37
3.2 Literature review of standards and quality assessment methods . . . . .	38
3.3 Full-scale crushing test . . . . .	38
3.3.1 Full-scale test setup . . . . .	39
3.3.2 Selection of test material . . . . .	40

3.3.3	Laboratory test programme . . . . .	41
3.3.4	Statistical analysis . . . . .	44
3.4	Accelerated pavement test . . . . .	45
3.4.1	Pavement design and selection of materials . . . . .	46
3.4.2	Instrumentation of pavement structures . . . . .	47
3.4.3	Accelerated traffic . . . . .	47
3.4.4	Climatic conditions . . . . .	48
3.4.5	Measurements . . . . .	49
3.4.6	Modelling of pavement response and performance . . . . .	50
4	KEY FINDINGS – SUMMARY AND DISCUSSION . . . . .	53
4.1	Use of large-size aggregates in pavement structures . . . . .	53
4.1.1	Paper A . . . . .	53
4.1.2	Paper B . . . . .	55
4.1.3	Joint discussion for papers A–B . . . . .	56
4.2	Production methods affecting aggregate quality . . . . .	57
4.3	Influence of gradation and moisture on pavement performance . . . . .	61
4.3.1	Paper D . . . . .	61
4.3.2	Paper E . . . . .	63
4.3.3	Paper F . . . . .	68
4.3.4	Joint discussion for papers D–F . . . . .	71
4.4	General findings . . . . .	72
5	CONCLUSIONS AND FURTHER WORK . . . . .	75
5.1	Conclusions . . . . .	75
5.2	Possibilities for continuation of the research . . . . .	78
5.3	Future research needs . . . . .	78
	 BIBLIOGRAPHY . . . . .	 81
	 PART II APPENDIXES . . . . .	
A	PAPER A . . . . .	91
B	PAPER B . . . . .	101
C	PAPER C . . . . .	117
D	PAPER D . . . . .	133
E	PAPER E . . . . .	145
F	PAPER F . . . . .	175

## LIST OF FIGURES

---

Figure 1.1	Relation between research questions and research papers	9
Figure 2.1	Crushing principles – impact crushing, single-particle compressive crushing, and inter-particle compressive crushing . . . . .	14
Figure 2.2	The principles of common compressive crushers . . .	15
Figure 2.3	Example aggregate production process flowchart for 0/90 mm subbase . . . . .	16
Figure 2.4	Example of process optimisation for either capacity or quality . . . . .	17
Figure 2.5	Classification of particle shape . . . . .	19
Figure 2.6	Outline of typical Norwegian pavement structures . .	23
Figure 2.7	Flowchart for mechanistic-empirical pavement design procedure . . . . .	25
Figure 2.8	Development of stress in unbound layers beneath a moving wheel load . . . . .	26
Figure 2.9	Development of resilient and permanent strain during traffic loading . . . . .	27
Figure 2.10	Stress-strain behaviour of unbound granular materials	29
Figure 2.11	Ratio of resilient modulus as a function of change in degree of saturation . . . . .	30
Figure 2.12	Permanent deformation behaviour depending on stress level . . . . .	31
Figure 2.13	The time hardening approach . . . . .	32
Figure 2.14	Aggregate consumption in Europe . . . . .	33
Figure 2.15	Aggregate quality depending on application . . . . .	34
Figure 3.1	Process flowchart for the full-scale crushing test . . .	40
Figure 3.2	Examples of photos used in digital image processing of feed particle size distributions . . . . .	42
Figure 3.3	Method for collection of product samples from wheel loader bucket . . . . .	43
Figure 3.4	Multiple linear regression example . . . . .	44
Figure 3.5	Outline of HVS test pit seen from above . . . . .	46
Figure 3.6	Outline of pavement structures in APT . . . . .	47
Figure 3.7	Instrumentation of pavement structures in APT . . .	48
Figure 4.1	Minimum and maximum pavement thicknesses for AADT $\approx 10\,000$ . . . . .	54
Figure 4.2	Upper sieve size limits for subbase materials . . . . .	54
Figure 4.3	Specific energy consumption vs. lower size of feed material . . . . .	58
Figure 4.4	The impact of sample preparation by laboratory crushing on measured mechanical properties . . . . .	58

Figure 4.5	Mechanical properties vs. flakiness index . . . . .	59
Figure 4.6	Particle shape measured as FI for individual particle size fractions . . . . .	60
Figure 4.7	Registered volumetric water content during APT . . . . .	62
Figure 4.8	Back-calculated deflection from FWD . . . . .	63
Figure 4.9	Development of induced vertical stress and strain in subbase during APT . . . . .	64
Figure 4.10	Rut development during APT . . . . .	64
Figure 4.11	Comparison between measured and modelled induced vertical elastic strain as a function of depth . . . . .	66
Figure 4.12	Comparison between measured and modelled induced vertical stress as a function of depth . . . . .	67
Figure 4.13	Modelled and measured permanent deformations for unbound base, subbase and subgrade . . . . .	69
Figure 4.14	Modelled rut development compared to surface laser measurements . . . . .	70
Figure 4.15	Modelled and measured rut profiles at the end of each groundwater phase . . . . .	70

## LIST OF TABLES

---

Table 2.1	Particle size ranges used in test methods for aggregate quality . . . . .	20
Table 2.2	Guidelines for producing cubical product . . . . .	20
Table 2.3	Amount of aggregates in pavement structures . . . . .	23
Table 3.1	Summary of available settings of the feed and crusher parameters . . . . .	40
Table 3.2	Parameter combinations used in full-scale crushing test . . . . .	41
Table 3.3	Declared values for mechanical properties . . . . .	41

## ACRONYMS

---

AADT	annual average daily traffic
AC	asphalt concrete
APT	accelerated pavement test
ASG	asphalt strain gauge

CEN	European Committee for Standardization
CSS	closed side setting
DIP	digital image processing
ESAL	equivalent single axle load
FI	flakiness index
FWD	falling weight deflectometer
GWT	groundwater table
HMA	hot mix asphalt
HVS	heavy vehicle simulator
LCA	life cycle assessment
LE	linear elastic
MEPDG	mechanistic-empirical pavement design guide
MLET	multi-layer elastic theory
MSRLT	multi-stage repeated load triaxial
NLE	non-linear elastic
NPRA	Norwegian Public Roads Administration
NTNU	Norwegian University of Science and Technology
NVF	Nordic Road Association
OSS	open side setting
PIARC	World Road Association
PSD	particle size distribution
RQ	research question
SEC	specific energy consumption
SI	shape index
SPC	soil pressure cell
VTI	Swedish National Road and Transport Research Institute
$\epsilon$ MU	strain measuring unit



Part I

THE THESIS



## INTRODUCTION

---

In this chapter, the motivation for the choice of research topic is described (1.1). The research topic is then specified by defining the aim and scope of the thesis (1.2). Further, verifiable research questions covering the research topic are defined (1.3), and a research design suited to answer the defined research questions is outlined (1.4). Additionally, the structure of the thesis is outlined (1.5), and the contributions to the publications included in the thesis are described (1.6).

### 1.1 MOTIVATION

Road pavements are built to strengthen the ground and supply an even and serviceable surface for traffic. A road pavement typically consists of one or more bound layers over one or more unbound layers (Dawson and Mundy, 1999). Aggregates are the most important construction materials for roads, as they represent 95 % of the mass in hot mix asphalt (HMA), about 70 % of the mass in concrete and they are additionally used in unbound form (i.e. not mixed with a binding agent) in the layers beneath the concrete or HMA surfaces (Mamlouk, 2006). Aggregates are produced from natural sediments or hard rock resources.

Figures from the Norwegian mineral statistics underline the importance of crushed aggregates for the Norwegian construction industry (Directorate of Mining, 2019):

- The Norwegian aggregate industry sold 94 million tonnes of aggregates at a value of 6.8 billion NOK in 2018. These numbers have been growing steadily over the last 10 years. Export represents about 22 % of the sale, while the remaining is sold within Norway.
- Of the total sold amount domestic and abroad, 55 % was used in road construction, 18 % for concrete production, and the remaining for other construction purposes.
- Of the total 94 million tonnes, 85 % were crushed rock aggregates.
- In total, 53 million tonnes of aggregates from Norway were used for road construction purposes in 2018, of which 73 % in unbound form.

Aggregates are non-renewable resources, and suitable high-quality aggregate resources have limited availability. Although vast amounts of aggregate resources are available in the world, they are not necessarily available for use. Some resources are tied up by buildings and infrastructure, while others are

unavailable due to environmental concerns. Transport of aggregates increases the product price significantly, and the transport price alone make some deposits uneconomical (Langer et al., 2004). For the Norwegian market, it is estimated that when aggregates are transported longer than 30 km by truck, the cost of transport is higher than the price of the products (Wolden, 2014).

To prevent resource scarcity, utilisation of aggregates should be considered carefully. When suitable aggregate resources are encountered at a construction site, e.g. in the form of surplus material from tunnelling, they should be utilised in construction rather than landfilled or used for less quality-demanding purposes. To obtain optimal utilisation, we must ensure that we produce the best possible construction material from the available resources.

A starting point for the research was the notion that the Norwegian or Nordic practice for aggregate use, where large-size aggregates are commonplace, differ from the practice in other parts of the world. Part of the background for this presumption is the fact that aggregate sizes over 90 mm are not covered by European standards, even though these aggregate sizes are routinely used in Norway.

Large-size aggregates for unbound use are often produced from one single crushing in a jaw crusher, as opposed to concrete or asphalt aggregates, where at least two and often three or four crushing steps are used, employing several crusher types. Most published literature found is focused on the use of cone crushers and several types of impact crushers. There is a gap of knowledge regarding the quality of large-size aggregates, especially large-size aggregate products from primary crushing. A specific reason for the current interest in the production of large-size aggregates is the change in requirements implemented from 2014, where the Norwegian Public Roads Administration (NPRA) demands all aggregates used in subbase and frost protection layers to be produced by crushing (Norwegian Public Roads Administration, 2014). Previously, materials for these purposes could be used directly after blasting and screening/sorting. The increased focus on the production of these aggregates has also spurred interest in the impact of production methods on the quality of the construction materials. The single crusher productions are particularly relevant in the perspective that they are easily employable in mobile crushing plants working temporarily at a construction site. For utilisation of local aggregates, an important prerequisite is the ability to produce construction aggregates from rock materials found at or in connection with planned construction sites. Road construction sites are geographically widespread and can be located far from established quarries. This means that the transport distances can be long, and the cost related to transportation will raise the cost of the aggregates.

On a more overarching level, climate changes are expected to represent a shift towards increased precipitation and more intense rainfall events in the coming years (Seneviratne et al., 2012). This development may cause increased moisture levels in pavement structures. The Norwegian pavement design system is empirical, thus not suited to adapt to new environmental conditions. Research is needed to enable pavement design methods to predict

the behaviour of pavement materials at increased moisture levels. Since the materials used in the Norwegian and Nordic pavement design differ from the norms in the rest of the world, new pavement design systems developed in other countries must be calibrated to our local conditions.

The research subject is related to UNs Sustainable Development Goals (United Nations, 2015):

GOAL 9.1: Develop quality, reliable, sustainable and resilient infrastructure, including regional and transborder infrastructure, to support economic development and human well-being, with a focus on affordable and equitable access for all

GOAL 12.2: By 2030, achieve sustainable management and efficient use of natural resources

Reliable and resilient pavement structures must be adapted to the effects of future climate changes. The consumption of non-renewable resources can be reduced by optimising the utilisation of available aggregate resources. By using more local resources, the aggregate transport can be reduced, which will reduce the carbon footprint of the construction projects.

## 1.2 AIM AND SCOPE

### 1.2.1 *Aim and objectives*

The aim of the current PhD research was to conduct full-scale tests on large-size aggregate materials currently used in the Norwegian road construction industry to gather knowledge on their performance. The overarching vision was to increase sustainability in road construction projects through increased utilisation of local aggregate materials.

One of the main objectives of the research was to show that production methods for aggregates have impact on the aggregate properties as a raw material for road construction. As a consequence, it will be possible to achieve better utilisation of aggregate resources through adjusting the production process according to local geological conditions and construction needs. Another main objective was to contribute to closing the knowledge gap regarding the performance of large-size aggregates in pavement structures. The existing knowledge on this subject is primarily empirical, and thus difficult to adapt to new conditions.

The research investigated whether utilisation of local aggregates for road construction can be increased through adjustment of production methods and pavement design.

The specific objectives of the research were the following:

- To gather knowledge about the varying practices for aggregate use and pavement design, in order to enable better interpretation of international research on the topic

- To associate variations in material characteristics for aggregates with variations in the production conditions
- To associate the performance of large-size aggregates in pavement structures with variations in material characteristics
- To evaluate whether established knowledge about aggregate properties from research on finer aggregates is valid for large-size aggregates

### 1.2.2 Scope of the thesis

The specific focus of the project was crushed aggregates used in unbound form in the main layers of a pavement structure: base, subbase, and frost protection layer.

The European Committee for Standardization (CEN) defines aggregates as *granular material of natural, manufactured or recycled origin used in construction* (EN 13242, 2007). Within the purview of this research project, the definition of aggregates was additionally confined to *granular material of crushed rock used in road construction*. The aggregates used in the testing were of sizes relevant for use in subbase and frost protection layers in a Norwegian pavement structure, with  $D \geq 90$  mm. Any aggregate production and handling process will also generate fines and fine aggregates. When the mass balance in the production is evaluated, excess fines are often considered as waste. Thus the properties of the complete particle size distribution were an important part of the research scope, as the objective of the production is to produce quality coarse aggregates without losing a large share of the processed volume as waste.

The research aimed to employ a comprehensive view of aggregate production – planning for the best possible utilisation of available geological resources at or close to construction sites. The research was limited to aggregates produced by blasting, crushing and screening bedrock, and covered aggregates processed from both tunnel blasting and traditional quarrying.

The research did not cover recycled aggregates, natural uncrushed aggregates or aggregates for use in bound forms such as asphalt or concrete. Aggregates used in asphalt and concrete do generally have finer gradations and more specific quality requirements than the materials covered in this research project. The research was further limited to primary production of aggregates, not considering the recycling or reuse of aggregates from previous use for other purposes. Although reuse and recycling of aggregates can make significant contributions to reduce the need for producing new crushed aggregates, the demand for aggregates cannot be covered entirely by recycled material. It is, therefore, still important to improve the resource efficiency of traditional aggregate production.

The scope of the thesis was further limited to aggregates used in road construction only, excluding use in railways, dams, and other construction purposes. These limitations do not imply that the research results are not applicable for other purposes, but rather that the materials chosen for the

research were selected among those known to be used in road construction. For aggregates of similar size subject to similar quality demands, the research results regarding quality and sustainability impact from aggregate production can be relevant for any intended area of application.

### 1.3 RESEARCH QUESTIONS

In order to achieve the described research aims within the limitation of the scope of the thesis, the research topic was narrowed down to five verifiable research questions (RQs). These RQs will together provide answers to the overall research problem regarding sustainable use of local aggregate resources.

- RQ1 How does the Norwegian practice for aggregate use, with large-size unbound aggregates in subbase and frost protection layers, differ from other countries?
- RQ2 How are large-size unbound aggregates currently described, specified, and quality assessed?
- RQ3 How do production methods affect the quality of large-size unbound aggregates?
- RQ4 How does variation in characteristics of large-size unbound aggregates affect pavement performance?
- RQ5 How do changing moisture conditions affect the performance of large-size unbound aggregates?

### 1.4 RESEARCH DESIGN

The research consisted of a combination of literature review, field studies and laboratory testing. Field methods were chosen with the goal of testing materials in full scale or with as little downscaling as possible.

Review of relevant literature formed the basis of all parts of the research. Moreover, literature review was an essential tool to answer RQ1 and RQ2, where the focus was on the current practice and standards. The theoretical studies answering RQs 1 and 2 formed the basis for the test programmes used to answer RQs 3–5.

The first stage of the practical research was a parameter study regarding jaw crusher performance conducted in full scale, examining how aggregate quality is affected by changing crusher properties. Relevant properties were among others feed size, reduction rate, crusher speed, and feed level into the crusher. Material samples for laboratory studies were gathered from the parameter study and analysed using common quality assessment methods for pavement aggregates. The parameter study was limited to one rock type, as the focus was on the crushing parameters and revealing their specific

impact on the produced aggregates. The results from this study provided answers to RQ3.

The next full-scale study was an accelerated pavement test (APT) studying the impact of varying moisture levels and subbase gradation on the performance of pavement structures subjected to traffic loading from a heavy vehicle simulator (HVS). A HVS can simulate accelerated deterioration of a pavement structure by running a heavy wheel load over a pavement during a concentrated period of time (Wiman, 2001). Accelerated traffic was applied to two instrumented pavement structures, where the difference between them was the gradation of the subbase layers. Relevant pavement responses were stresses, strains and permanent deformations. The results from this study provided answers to RQ4 and RQ5.

Material for both full-scale tests was collected from production lines at ongoing road construction or aggregate production sites. Comparing the results from the full-scale tests to known literature from research on finer aggregates, it was possible to gain knowledge about whether research results from fine aggregates are valid also for large-size aggregates.

The choice of research methods are described in chapter 3.

## 1.5 STRUCTURE OF THE THESIS

The thesis is comprised of five chapters, in addition to appendices containing the full research papers.

CHAPTER 1 introduces the topic of the thesis, including the motivation for the project and the limitations to the research. Specific research questions are formulated in this chapter, and the contribution to each publication is described.

CHAPTER 2 describes the theoretical background for the conducted research.

CHAPTER 3 outlines the choice of research methods to obtain data for the analyses conducted for this thesis. Methods include literature review, field methods and laboratory methods.

CHAPTER 4 summarises and discusses the main results and key findings from the research.

CHAPTER 5 presents the main conclusions from the research, and gives recommendations for further research on the topics covered by this thesis. This chapter connects the results of the research to the RQs defined in section 1.3.

## 1.6 PUBLICATIONS INCLUDED IN THE THESIS

Six research papers are included in the thesis. The contributions to each paper are described below. The full papers are appended to the thesis in appendix A–F. Figure 1.1 illustrates the relation between each research paper and the

RQs. Solid lines show the main connections, while additional relations are illustrated by dashed lines.

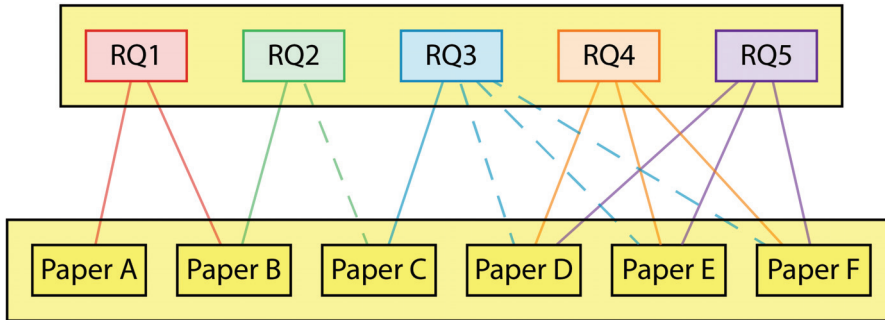


Figure 1.1: Relation between research questions and research papers.

**PAPER A** Comparison of practice for aggregate use in road construction – results from an international survey

**AUTHORS** Marit Fladvad, Joralf Aurstad & Børge Johannes Wigum

**STATUS** Published in proceedings from the 10th International Conference on the Bearing Capacity of Roads, Railways and Airfields (BCRRA2017)

**CONTRIBUTIONS** Marit Fladvad designed the survey, analysed the collected data and wrote the manuscript. Joralf Aurstad contributed to the survey design, provided the contacts for the survey and revised and approved the manuscript. Børge Johannes Wigum revised and approved the manuscript.

**PAPER B** Large-size aggregates for road construction – a review of standard specifications and test methods

**AUTHORS** Marit Fladvad & Arnhild Ulvik

**STATUS** Published in Bulletin of Engineering Geology and the Environment

**CONTRIBUTIONS** Marit Fladvad conducted the literature review and wrote the manuscript. Arnhild Ulvik provided background information for standard development and knowledge about test methods, and revised and approved the manuscript.

**PAPER C** Influence of jaw crusher parameters on the quality of primary crushed aggregates

**AUTHORS** Marit Fladvad & Tero Onnela

**STATUS** Published in Minerals Engineering

**CONTRIBUTIONS** The full scale test was designed by Tero Onnela and Marit Fladvad. Data collection during full scale testing was conducted by employees at Metso Minerals (Tampere, Finland). The laboratory test programme was designed by Marit Fladvad and Arnhild Ulvik. Part of the laboratory testing was conducted by Marit Fladvad, otherwise by Master student Nils Arne Fjeldstad Luke and employees at the NPRA laboratory (Trondheim, Norway). Data analysis was conducted by Marit Fladvad. The manuscript was written by Marit Fladvad, and revised by Tero Onnela, Børge Johannes Wigum and Rolf Arne Kleiv.

**PAPER D** Performance of unbound pavement materials in changing moisture conditions

**AUTHORS** Marit Fladvad & Sigurdur Erlingsson

**STATUS** Published in proceedings from the 6th International Conference on Accelerated Pavement Testing

**CONTRIBUTIONS** The accelerated pavement test setup was designed by Sigurdur Erlingsson and Marit Fladvad. Data collection was handled by employees at the Swedish National Road and Transport Research Institute (VTI). Data analysis was conducted by Marit Fladvad. The manuscript was written by Marit Fladvad and revised by Sigurdur Erlingsson.

**PAPER E** Modelling the response of large-size subbase materials tested under varying moisture conditions in a heavy vehicle simulator.

**AUTHORS** Marit Fladvad & Sigurdur Erlingsson

**STATUS** Submitted to Road Materials and Pavement Design

**CONTRIBUTIONS** The accelerated pavement test setup was designed by Sigurdur Erlingsson and Marit Fladvad. Data collection was handled by employees at VTI. Data analysis was conducted by Marit Fladvad. The manuscript was written by Marit Fladvad and revised by Sigurdur Erlingsson.

**PAPER F** Permanent deformation modelling of large-size unbound pavement materials tested in a heavy vehicle simulator under different moisture conditions

**AUTHORS** Marit Fladvad & Sigurdur Erlingsson

**STATUS** Submitted to Road Materials and Pavement Design

CONTRIBUTIONS The accelerated pavement test setup was designed by Sigurdur Erlingsson and Marit Fladvad. Data collection was handled by employees at VTI. Data analysis was conducted by Marit Fladvad. The manuscript was written by Marit Fladvad and revised by Sigurdur Erlingsson.



## THEORY

---

The theoretical background for the research is divided in two separate subjects; aggregate production described in section 2.1 and pavement design described in section 2.2. Some additional considerations regarding the sustainability of aggregate production and use are described in section 2.3.

### 2.1 AGGREGATE PRODUCTION

The construction aggregates studied in this thesis were produced from hard rock by blasting, crushing and screening. Blasting is sometimes called the first crushing stage, as it is through blasting the rock particles are liberated from the surrounding hard rock, and the first size reduction takes place. The crushing is the process where the blasted rock particles are reduced to the desired size. An aggregate production plant usually implements several crushing stages with different crushers at each stage. Screening is used both to separate material flows in the crushing circuit and to separate the crushed materials into product gradations.

#### 2.1.1 *Basic principles of comminution*

Comminution is the collective term for the size reducing processes which have one or more of the following objectives (Rothery and Mellor, 2007):

- to improve the handleability of the material
- to liberate valuable minerals from ores prior to mineral separation
- to produce particles of a given size or size distribution

Classical comminution theory describes the relationship between energy consumption and size reduction. The energy consumption during size reduction can be related to the increase in surface area when large particles are divided into several smaller particles. The energy exerted by the crusher on the particles induces tensile stress within the rock. Rock fractures occur when the tensile stress becomes higher than the internal strength of the rock material (Jern, 2004). As more compression is added, these fractures propagate into new surfaces dividing the particles into pieces. As rock is an inhomogeneous material, particle breakage often starts in existing cracks in the particles. The crushability of rock relies on the propagation of internal flaws within the rock (Ruuskanen, 2006).

The goal of comminution in mineral processing is most often to liberate a valuable mineral from its host rock, thus reducing all particles to the

liberation size. The liberation size depends on the mineral grain size, often  $< 1$  mm. Aggregate production differs from this approach, as the goal of the size reduction process is not to reduce all particles to a certain size, but to produce particles in a given range of sizes suited to a construction purpose. The desired size range varies depending on the intended use of the material, exemplified for road construction: 0/11 mm for hot mix asphalt (HMA), 0/32 mm for unbound base, 22/125 mm for use in a subbase layer.

### 2.1.2 Crusher principles

The crushing of rock particles can follow three principles; impact crushing, single-particle compressive crushing and inter-particle compressive crushing, illustrated in Figure 2.1 (Bengtsson, 2009). During crushing, the rock particles can be subjected to several of these mechanisms. As the goal of aggregate production is to reduce particles to a desired size distribution, the amount of fines produced during crushing should be limited. This can be achieved by ensuring that inter-particle crushing is the main crushing mechanism.

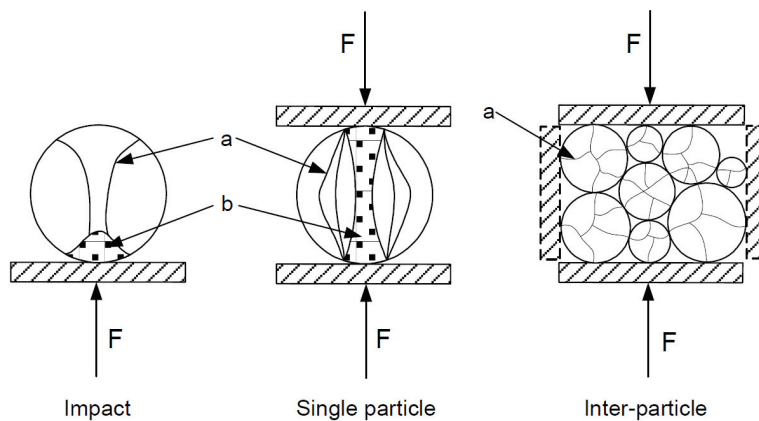


Figure 2.1: Crushing principles – impact crushing, single-particle compressive crushing, and inter-particle compressive crushing (Bengtsson, 2009). a = principal cracks; b = fines generated on account of breakage.

Crushers can mainly be divided in two groups, pending their breakage mechanism: impact crushers and compressive crushers. In the first stages of aggregate production, compressive crushers are most widely used. Jaw, gyratory, cone and roller crushers are types of compressive crushers. Jaw crushers are most commonly used in primary crushing. In a jaw crusher, the material is crushed between a fixed and a moving jaw, as illustrated in Figure 2.2a. Gyratory and cone crushers can be used both as primary crushers and in subsequent crushing stages. These crushers compress the material between a rotating mantle and an outer casing (Figure 2.2b). A central difference between the jaw crusher and cone/gyratory crushers is

that a jaw crusher alternately compresses and releases the full width of the chamber, whereas in a cone/gyratory crusher, there is always a section of the crushing chamber in compression as the mantle rotates. In both machines, however, rock particles are subjected to the same pulsing compression and release.

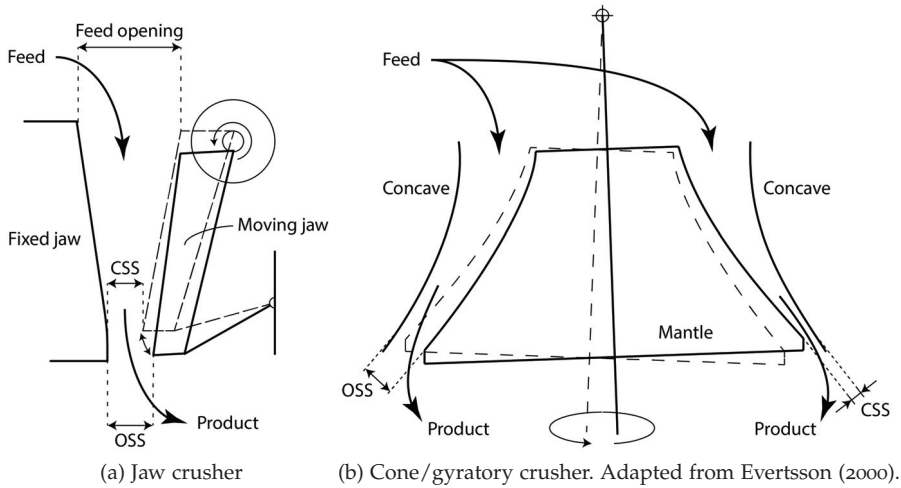


Figure 2.2: The principles of common compressive crushers.

The closed side setting (CSS) is the smallest distance between the moving and fixed piece when the crusher is compressing. Conversely, the open side setting (OSS) is the largest discharge opening that occurs through the compression cycle. The difference between CSS and OSS is called the stroke, or throw, of the crusher. The crusher speed is called eccentric speed or the gyration frequency and is the speed of the rotation of the eccentric axle running the movement of the crusher. The eccentric speed is measured in revolutions per minute (rpm).

The size reduction from feed material to product is usually quantified using the reduction ratio  $R_{80}$ , defined as the ratio between the respective screen sizes through which 80 % of the feed and product distribution passes, calculated by Eq. 2.1 (Wills and Finch, 2015).

$$R_{80} = \frac{F_{80}}{P_{80}} \quad (2.1)$$

The energy efficiency of the crushing process can be measured as specific energy consumption (SEC); consumed power per tonne of crushed material (Eq. 2.2).

$$SEC = \frac{\text{Power draw}}{\text{Throughput}} \quad (2.2)$$

Only a fraction of the power consumed by a crusher is actually used for size reduction (Legendre and Zevenhoven, 2014). Most of the energy is lost through noise, heat, vibration and ductile particle deformation.

### 2.1.3 The aggregate production process

Figure 2.3 shows a possible setup of a aggregate production process for a 0/90 mm subbase material for road construction. A 600 mm feed material (1) is fed to the crusher over a combined feeder and screen (2) which removes materials < 100 mm and provides a constant flow of material into the jaw crusher (3). The process of removing fine material from the feed is called scalping. The 0/100 mm material is bypassed the primary crusher and combined with the jaw crusher output. The material is then transported to a screen (4), where two size fractions are separated: 0/90 mm material is transported directly to the product stockpile (6), while material > 90 mm is fed to the secondary gyratory crusher (5). The gyratory crusher is installed in a closed circuit, meaning that the product material > 90 mm is fed back to the crusher. This process results in a single 0/90 mm product stockpile, where some material has been bypassed both crushers, some is product from the primary crusher, while the rest is crushed at least once in the secondary crusher. Subbase materials can also be produced in simple setups using only one crusher, especially when aggregates are produced from local resources at construction sites, where space is limited.

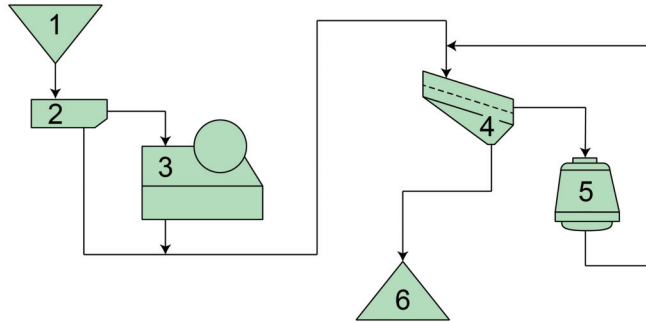


Figure 2.3: Example aggregate production process flowchart for 0/90 mm subbase. 1 – Feed stockpile; 2 – Feeder; 3 – Primary jaw crusher; 4 – Screen; 5 – Secondary gyratory crusher; 6 – Product stockpile. Adapted from Eloranta (2009).

The planning of a production process is based on the properties of the rock material, capacity requirements and product quality requirements. While a subbase production process can have a relatively simple process as shown in Figure 2.3, production of aggregates for HMA or concrete may employ both three and four crushing steps. Generally, the aggregate quality is improved for each crushing step, as the rock particles are broken along their weaknesses, and the resulting particles have fewer faults in their rock mass.

The process planning must always balance capacity, costs and product quality. Mass balance is also an important issue, as excess fines often become a challenge in quarries. The end products may have strict requirements for fines content, while requirements for particle shape can be hard to achieve without generating more fines. As a result, an excess of fine material, e.g.  $0/4$  mm, may be produced which eventually become waste because the demand for such products is smaller than the supply.

Figure 2.4 compares two different combinations of three crushers and two screens, where one alternative is optimised for capacity, and the other is optimised for quality. The alternative which gives higher capacity (Figure 2.4a) has only the tertiary crusher in closed circuit and combines output from all three crushers in the product stockpiles. Releasing the product from the production circuit as soon as the particles reach a certain particle size ensures high capacity, but does not ensure cubical particle shape. The maximum quality alternative (Figure 2.4b) has both the secondary and tertiary crushers in closed circuits. This setup increases the time the material stays in the production circuit and thus reduces the capacity. This production separates the products in stockpiles of different quality, where the larger-sized material in the first stockpile has been subject to less size reduction and likely less shape improvement. The products gathered in the three final product stockpiles, which are output from the tertiary crusher only, have improved shape properties.

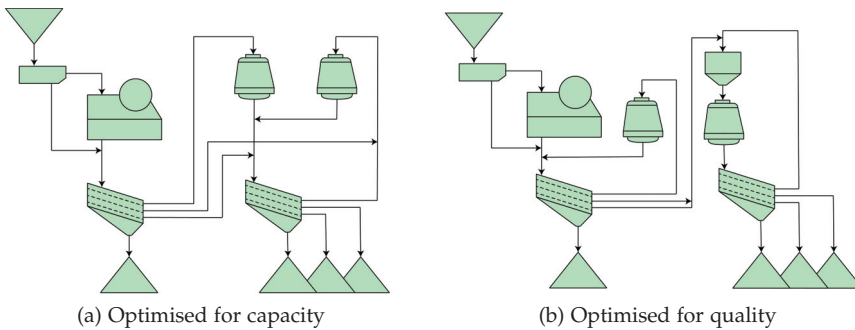


Figure 2.4: Examples of process optimisation for either capacity or quality. Adapted from Eloranta (2009).

The output from primary crushing has generally not been considered end products, as can be illustrated by these definitions of the purpose of the primary crusher:

- To reduce the material to a size that allows its transportation on a conveyor belt (Eloranta, 2009)
- To reduce rock size to prepare a feed material for down stream processing (Bengtsson, 2009)

These definitions are of course correct for multi-stage crushing processes, but not for the single-stage crushing processes investigated in this thesis. As multi-stage processes are the common alternative, less research can be found regarding the products from primary crushing.

#### 2.1.4 *Quality parameters*

The quality of the crushing process is often considered in terms of process capacity, reduction rate and energy efficiency. Deviating from the classical comminution theory focussing on energy consumption in size reduction, modern aggregate production has transitioned towards a quality-driven approach where size reduction is no longer the sole objective of the crushing process. Although the main objective of the crushing process is size reduction, there are several ways to describe the quality of the crushed product. Here, it is important to distinguish between the intrinsic physical properties of the material that are related to basic geologic origin, mineralogy, and other properties such as hardness and durability, and the properties which can be influenced in the production process (Xiao and Tutumluer, 2012).

The primary quality descriptors of the products are still related to the size of the material, such as fines content and particle size distribution. Another common descriptor of aggregate quality is particle shape (Eloranta, 1995; Briggs and Evertsson, 1998; Räsänen and Mertamo, 2004; Bengtsson, 2009).

An early classification of particle shape was made by Zingg (1935), who defined four particle shape classes depending on the relationship between length (L), width (I) and thickness (S). The classes are illustrated in Figure 2.5: d – disc; e – equant (cubical); b – blade; r – rod-shaped. In the current aggregate standards, particle shape can be described as flakiness or elongation. A flaky particle has a thickness less than half of its width (EN 933-3, 2012), while an elongated particle has a length more than three times its width (EN 933-4, 2008). Particles which are neither flaky nor elongated can be classified as cubical.

Particle shape is of interest because it affects the amount of voids in the material, hence affecting the density and degree of compaction in addition to stability (Lekarp et al., 2000a; Hansson and Svensson, 2001; Uthus, 2007; Cook et al., 2017). Particle shape also affects the degradation of aggregate particles under compaction and traffic, as flaky and elongated particles tend to break more easily than cubical particles (Grønhaug, 1967). Furthermore, particle shape influences the particle size distribution. Lees (1964) showed that a rod-shaped particle can have 2.5 times the volume of a disc-shaped particle classified as the same size. Generally, cubical particles are considered well-shaped, while both elongation and flakiness is regarded as poorer shape.

Bengtsson (2009) listed a number of problems associated with quality-driven production, such as:

- methods for quality assessment is defined depending on the intended use of the aggregates

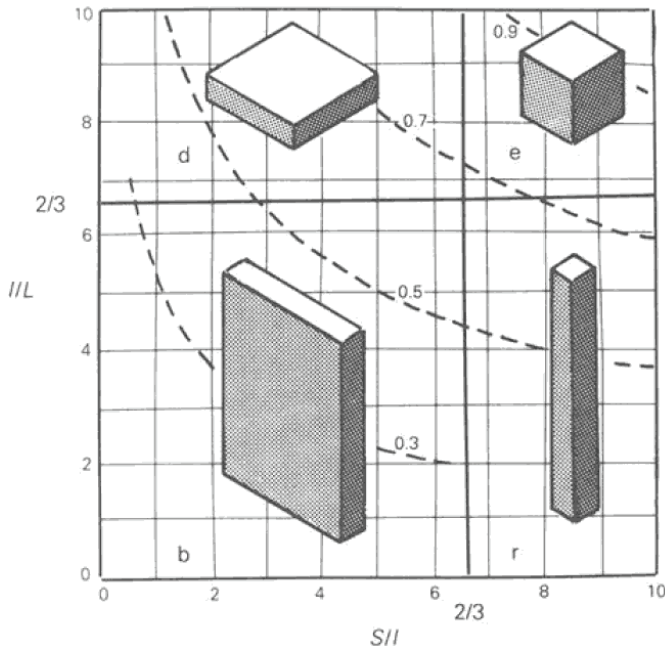


Figure 2.5: Classification of particle shape depending on the length of long (L, length), intermediate (I, width) and short (S, thickness) axes (Lindholm 2012, after Zingg 1935).

- methods for quality assessment can be difficult to put into practice
- methods for quality assessment cannot be used for certain size ranges

A main challenge for the aggregate producers is that the assessment of quality is dependent on the intended use of the aggregates. This means that different customers have different demands for quality, and the products are specified according to different standards and specifications pending their end use. Additionally, the standards describing test methods are limited to certain size ranges, meaning that the products can be quality assessed in relation to other size ranges than their actual size (Table 2.1). An example of this is the European standards for mechanical properties which are tested on the 10–14 mm size range (EN 1097-2, 2010; EN 1097-1, 2011). These standards apply for subbase materials in road construction, where a commonly used material in Norway is 22/125 mm (Norwegian Public Roads Administration, 2018). When the customer wants to sample and test the delivered product according to the standard, the material must be processed in order to obtain the correct particle sizes for testing. This processing may affect the test result and can become a source of conflict between the producer and customer.

Over the years, numerous studies have attempted to determine the relationships between rock properties, feed properties, crusher properties and product particle shape, with varying and sometimes contradicting conclusions summarized thoroughly by Ruuskanen (2006).

Table 2.1: Particle size ranges used in test methods for aggregate quality.

AGGREGATE PROPERTY	TEST METHOD	SIZE RANGE
Particle shape	Flakiness index (EN 933-3)	4–100 mm
Particle shape	Shape index (EN 933-4)	4–63 mm
Resistance to fragmentation	Los Angeles test (EN 1097-2)	10–14 mm
Resistance to wear	micro-Deval test (EN 1097-1)	10–14 mm

Shergold (1959) found that the most important factor deciding particle shape was the reduction ratio. Larger feed sizes resulted in poorer shaped products, but at the same time, the smaller sizes in a product gradation had poorer shape than the larger particles (Shergold 1959, as cited by Grønhaug 1967). Szczelina (2000) tested crushing of coarse feed materials in the sizes from 22/40 mm to 450/560 mm, and found that larger product particles had better shape in terms of elongation than smaller product particles. Bengtsson (2009) tested crusher impact on particle shape after secondary and tertiary crushing. Among his findings were empirical models showing that crusher setting, feed size, crusher speed and throw affects particle shape in products from cone crushers. Increased average feed size increases flakiness index (FI), likewise does decreased crusher speed. Further, Bengtsson states that in full-scale crushing, there is no evidence that feed shape affects product shape. Eloranta (1995) provided a set of guidelines for how to produce cubical aggregates, differentiated on whether fines are included in the feed to the crusher (Table 2.2). Regardless of fines, choke feeding is a must to obtain a cubical product. Choke feeding means ensuring that the crushing chamber is full at all times so that inter-particle crushing is possible.

Table 2.2: Guidelines for producing cubical product, excerpt from Eloranta (1995).

PARAMETER	TARGET	
	Feed containing fines	No fines in feed
Stroke	Higher	Lower
Setting	Smaller	–
Reduction ratio	Higher	Lower
Crushing force	Higher	Lower

Briggs and Evertsson (1998) found that efficient size reduction and improvement of shape are two mutually excluding objectives. When the single goal of the crushing operation is size reduction, undersize is scalped and bypassed the crusher to optimise the capacity of the crushing operation. However, if well-shaped aggregates are the goal of the crushing operation, undersize can be included in the crusher feed, ensuring more rock-to-rock

contact points in the crushing chamber. Including undersize will reduce the capacity of the crushing process and add more fines in the product gradation, but provide a better-shaped product.

The fundamental knowledge of these relations may be used in mathematical models of the crushing process. Modelling of crusher operation can be used in process planning for a specific quarry or by crusher producers in product development. Traditionally, crusher operation modelling has focussed on capacity and energy consumption (Gupta and Yan, 2016). Increasing computer power has allowed the development of more comprehensive models (Morrison and Cleary, 2008). Recent developments in crusher modelling utilise discrete element method modelling, where the behaviour of individual particles passing through a crusher can be calculated (Quist and Evertsson, 2016; Cleary et al., 2017; Bhadani et al., 2020). However, all modelling relies on experimental test data to verify the modelled results (Legendre and Zevenhoven, 2014).

Particle breakage is usually modelled as a series of repeated crushing events (Evertsson, 2000). For each event, a share of the particles is broken into daughter particles which are included in the next event. Johansson et al. (2017) have developed a fundamental model for a jaw crusher, calculating capacity, particle size distribution and power consumption from crusher geometry and material parameters. The particle size distribution is calculated from a breakage model where both single particle breakage and inter-particle breakage is included. Another important parameter to model is the wear of the crusher (Lindqvist and Evertsson, 2003).

In a multi-stage crusher operation with closed-circuit installations, the particle shape of the larger particles from the early crushing stages are of less importance, as these particles will be crushed again at a later stage. Here, the primary crushed large-size aggregates differ from the products studied in the literature. In the productions studied in this thesis, the feed materials are crushed only once, and the large particles have a great impact on the overall product particle shape. It is also important to note that although including fines in the feed will improve particle shape due to increased inter-particle crushing, the inclusion of fines also means that some undersize particles will pass through the crusher without size reduction, possibly making the product particle shape dependent on the feed particle shape.

## 2.2 PAVEMENT DESIGN

Yoder and Witczak (1975) gave a general definition of pavement design :

The design of airport and highway pavements involves a study of soils and paving materials, their behaviour under load, and the design of a pavement to carry that load under all climatic conditions.

Ahlvin (1991) defined three simple requirements which the pavement design must cover:

- Each layer must be thick enough to distribute the stresses induced by traffic resulting in a stress level which will not overstress and produce shear deformation in the next underlying layer
- Each layer must be compacted well enough so that traffic does not produce an intolerable amount of added compaction
- The flexible pavement must have a wear- and weather-resistant medium as a surface that will not displace under traffic

A successful pavement design limits damage from traffic both in the pavement itself and in the subgrade beneath the pavement structure.

### 2.2.1 *Typical Norwegian pavement structures*

A typical Norwegian pavement structure is constructed from relatively thin HMA layers over bound or unbound base layers, and  $\geq 30$  cm subbase layer, depending on subgrade materials and the need for frost protection (Figure 2.6). The need for frost protection is controlled by the frost volume and subgrade frost susceptibility. For a fully frost protected low-volume road, the total pavement thickness can be up to 1.8 m. For high-volume roads (annual average daily traffic (AADT)  $> 8000$ ), the maximum thickness is extended to 2.4 m (Norwegian Public Roads Administration, 2018).

A new low-volume road (AADT  $< 6000$ ) can have a width of up to 9 m following the Norwegian design manual (Norwegian Public Roads Administration, 2019). A simple geometrical calculation using a side slope of 1:2 together with layer thicknesses corresponding to Figure 2.6 gives an amount of aggregates per metre of constructed pavement as shown in Table 2.3.

The values calculated in Table 2.3 are examples of possible structures, and show how the lower unbound layers in the pavement structures dominate the mass balance. On frost susceptible subgrade, a frost protection layer is required, and the total volume of the pavement structure increases by a factor 3. The introduction of a frost protection layer allows for a reduction of the subbase layer.

### 2.2.2 *The basis of pavement design*

Flexible pavements are layered structures where the material stiffness gradually increases from the bottom upwards, and HMA layers are placed at the top. The central inputs to pavement design are knowledge regarding:

- Traffic – amount and load levels, configuration, growth
- Foundation – subgrade materials, variation
- Climate – moisture, temperature, frost
- Material properties

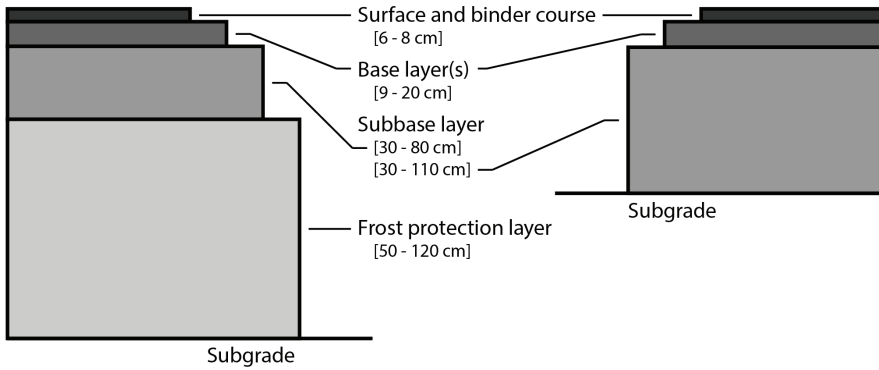


Figure 2.6: Outline of typical Norwegian pavement structures with and without frost protection layer.

Table 2.3: Amount of aggregates per metre of constructed pavement structure.

LAYER	THICKNESS [cm]	AVERAGE WIDTH [m]	VOLUME [m <sup>3</sup> ]	WEIGHT [tonnes]
Surface layer	7	9.14	0.64	1.52
Bound base	7	9.42	0.66	1.57
Unbound base	10	9.76	0.98	2.02
Subbase	27	10.10	2.73	5.65
Frost protection layer	129	13.22	17.05	35.31
Total	180		22.06	46.06

(a) Fully frost protected structure

LAYER	THICKNESS [cm]	AVERAGE WIDTH [m]	VOLUME [m <sup>3</sup> ]	WEIGHT [tonnes]
Surface layer	7	9.14	0.64	1.52
Bound base	7	9.42	0.66	1.57
Unbound base	10	9.76	0.98	2.02
Subbase	45	10.86	4.89	10.12
Total	69		7.16	15.22

(b) Structure without need for frost protection

Pavement design has traditionally been conducted with empirical methods based on past experience with certain sets of conditions. The main drawback of empirical models is their lack of adaptability to new and changing conditions. Examples of changing conditions in pavement design are:

- Increased traffic loads
  - Increased axle load allowances → higher loads
  - Increased number of axles per vehicle → less time between each axle load passing, more intense loading
  - Less strict tyre pressure limitations → higher tyre pressure leads to increased stress
  - Increased use of super-single tyres instead of dual tyres → reduced contact surface leads to increased stress
  - Platooning of future automated vehicles → less lateral wander of traffic loads, more concentrated loading
- Climate changes
  - Increased precipitation → higher moisture level in pavement materials
  - More intense rainfall events → increased risk of flooding
  - Changing frost conditions → less stable winter conditions can lead to more frequent and longer thawing periods
  - Warmer temperatures → Reduced asphalt stiffness
- Introduction of new materials with unknown properties
  - Unusual particle sizes and gradations
  - Recycled materials, e.g. crushed concrete or steel slag
  - Additives

The alternative to empirical design is analytical design. Numerous mechanistic or mechanistic-empirical pavement design models have been under development in the last decades, facilitated by increasing computational power. Mechanistic-empirical methods are analytical methods based on material mechanics which are calibrated to empirical data (Y. H. Huang, 2012). To enable the development of a mechanistic pavement design system, the performance of typical road materials under realistic loading conditions must be understood (Erlingsson, 2012). The response of a pavement subject to traffic load is modelled in terms of stresses, strains and deformation using response models, also called structural models. From the response model, pavement performance over time can be predicted for the relevant distress modes. Common types of distress for flexible pavements are rutting in pavement materials or subgrade, fatigue cracking of the surface material and roughness of the pavement profile (Mamlouk, 2006). To include a distress mode in the pavement design method, a model for calculating the development of the

type of distress is needed, and a quantifiable failure criteria for the distress mode must be defined. Finally, a pavement design system should balance pavement service life against construction costs and maintenance requirements in form of life cycle costs. The process from inputs through pavement performance analysis to life cycle assessment is shown in Figure 2.7 (Ahmed, 2014).

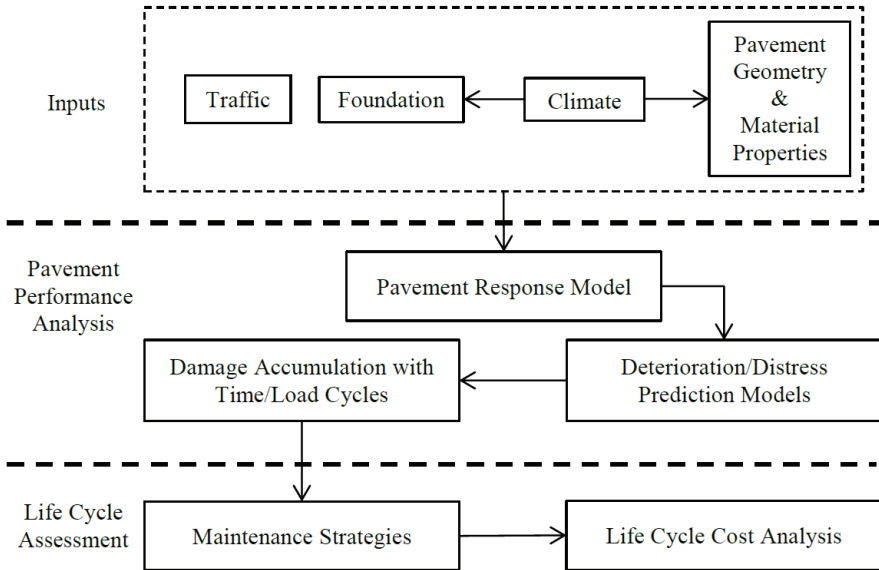


Figure 2.7: Flowchart for a mechanistic-empirical pavement design procedure (Ahmed, 2014).

### 2.2.3 Stress and strain under traffic load

During its service life, a pavement experiences a large number of load pulses induced from traffic, each consisting of vertical, horizontal and shear stress components. Figure 2.8 shows how the stress in unbound materials develop as a wheel load moves over a pavement section (Lekarp and Dawson, 1998).

Unbound granular materials show a complex behaviour under cyclic loads, with a gradual accumulation of permanent strain with each load application, as illustrated in Figure 2.9 (Lekarp and Dawson, 1998; Rahman, 2015). Each vehicle passing causes a small deformation in the pavement structure, and when the vehicle has passed, the deformation recedes. This is called elastic or resilient deformation. However, a small portion of the deformation is not elastic and does not recede. This causes a permanent deformation in the pavement structure which accumulates as more traffic passes the structure. Permanent deformation can be seen on the surface as rutting.

There are two main properties of pavement materials which must be controlled during pavement design and construction (Thom, 2008):

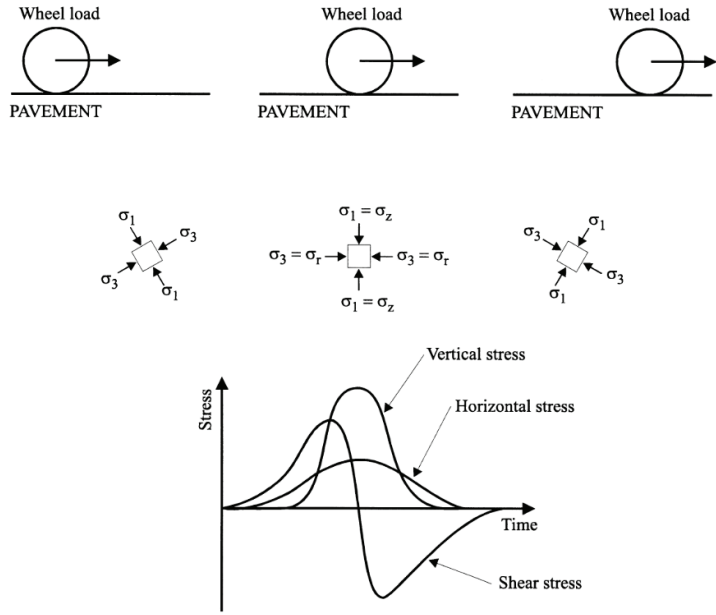


Figure 2.8: Development of stress in unbound layers beneath a moving wheel load (Lekarp and Dawson, 1998).

- Stiffness under rapid traffic load
- Resistance to accumulation of deformation under repeated load

2.2.4 Influence of traffic and loading

The structural degradation of pavement structures is mainly caused by heavy vehicles. The damaging effect of a vehicle axle is not linearly related to the axle load, but related by a power law relationship. Traffic load has traditionally been calculated as a sum of equivalent single axle loads (ESALs) using Eq. 2.3, where  $N_{eq}$  is the equivalent number of load repetitions from a standard axle  $P_{eq}$  corresponding to the damaging effect of  $N$  load repetitions from an axle of load  $P$ . Eq. 2.3 is known as the fourth power rule, and is based on the AASHO Road Test conducted in the 1950s (Dawson, 2008).

$$N_{eq} = N \left( \frac{P}{P_{eq}} \right)^4 \tag{2.3}$$

From Eq. 2.3, increasing an axle load by 20 % more than doubles the damaging effect ( $N_{eq} = N \cdot (1.2)^4 = 2.07N$ ). Meanwhile, halving the axle load results in a reduction to only 6.25 % of the damaging effect of the original axle ( $N_{eq} = N \cdot (0.5)^4 = 0.0625N$ ). These relations show why some pavement design systems, such as the Norwegian, are based on the number

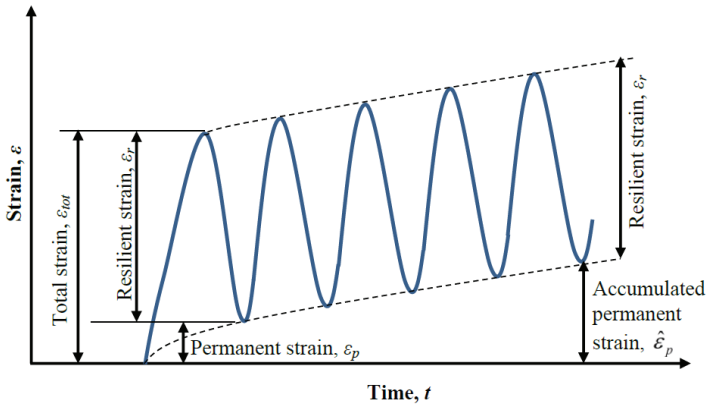


Figure 2.9: Development of resilient and permanent strain during traffic loading (Rahman, 2015).

of heavy vehicles ( $AADT_{\text{heavy}}$ ) instead of the full AADT. Modern analytical pavement design systems take the full axle load spectrum into account directly, without the simplification of ESALs.

Axle load and tyre pressure are two important parameters of the traffic load. At the pavement surface, the vertical stress is equal to the tyre pressure, while the stress decreases with depth. Increasing the axle load while keeping the tyre pressure constant will not change the vertical stress close to the surface, but increase the stress at lower levels in the structure. Increasing the tyre pressure while keeping the axle load constant will, on the other hand, increase stress at and close to the surface, but not affect the stress in lower layers. Hence, load affects deeper layers, while tyre pressure affects the surface layers (Mamlouk, 2006).

The wheel and axle configuration of the vehicles also affects the pavement degradation. Super-single tyres induce about four times larger permanent strain in pavement layers than conventional tyres (Kim et al., 2005). The traditional calculation of ESALs does not take wheel configuration into account. Compared to a single axle/dual wheel configuration, a tandem axle/dual wheel configuration with the same axle load will reduce  $N_{eq}$  by a factor 0.054 (Amorim et al., 2015).

### 2.2.5 Influence of climate

As pavements are constructed in nature, the environmental conditions vary with geography, weather and time of year. Moisture and temperature are the most important climatic properties for pavement materials.

Temperature is of importance because the stiffness of HMA is temperature dependent and decreases with increasing temperature. To ensure long service life of a flexible pavement, the asphalt binder must be designed to ensure necessary stiffness at warm temperatures and avoid cracking at low

temperatures. Furthermore, freezing temperatures cause the pavement and subgrade to freeze, and can result in challenges related to unevenness caused by frost heave and increased moisture levels and loss of bearing capacity during thawing.

Moisture has large impact on subgrade soils and unbound pavement materials. Thin flexible pavement structures, where high stresses are transmitted to the unbound pavement materials and subgrade, are very sensitive to moisture. Granular pavement layers normally show a substantial decrease in stiffness with increasing values of moisture. Increasing moisture in unsaturated materials will reduce strength and elastic and plastic stiffness, and increase the rate of traffic-induced deterioration (Charlier et al., 2009).

In areas subject to seasonal frost, such as the Nordic countries, thawing of frozen materials is a source of moisture in pavement structures. When a pavement structure thaws from the top down, there may be periods during thawing where the drainage system is frozen and blocked, thus hindering water from being drained from the upper unfrozen parts of the structure. Hence, pavement materials may in periods have a higher moisture level than assumed in the pavement design.

### 2.2.6 *Modelling the response behaviour of unbound pavement materials*

Response models are used to calculate stresses, strains and displacements in a pavement structure under traffic load. The calculation is based on material properties and environmental conditions, and the response behaviour can be calculated using methods such as multi-layer elastic theory (MLET), finite element methods and discrete element methods. Finite element methods are less suited due to the discrete and heterogeneous nature of coarse unbound materials. MLET methods have often been preferred because of their high computational speed (Erlingsson and Ahmed, 2013).

In elastic theory, the stiffness of a material can be defined by the resilient modulus  $M_R$  in Eq. 2.4, where  $\sigma_d$  is the deviator stress  $\sigma_1 - \sigma_3$ , and  $\varepsilon_r$  is the resilient strain.

$$M_R = \frac{\sigma_d}{\varepsilon_r} \quad (2.4)$$

However, unbound pavement materials have shown to be non-linear elastic, i.e. there is not a direct linear relationship between stress and strain (Hicks and Monismith, 1971; Rada and Witczak, 1981; Lekarp et al., 2000a). The stiffness of unbound materials is dependent on the stress level. Werkmeister (2003) describes the stress-dependency using Figure 2.10. At a low stress level, the stiffness increases with increasing load levels, meaning that less strain develops per unit of stress increase. At higher stress levels, the material stiffness decreases, i.e. more strain develops per unit of stress increase. As Figure 2.10 shows, the material may be modelled as linear elastic under certain limited stress ranges.

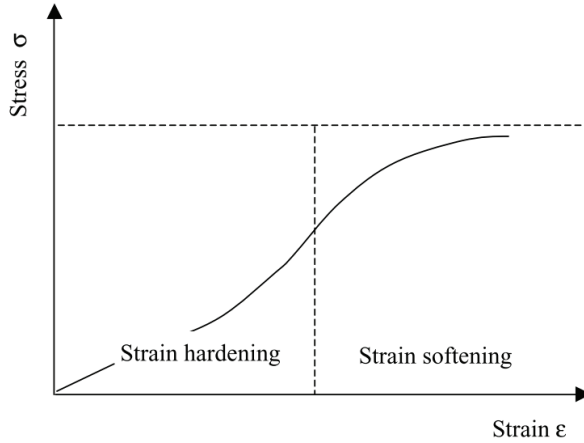


Figure 2.10: Stress-strain behaviour of unbound granular materials (Werkmeister, 2003).

Several models have been developed in attempts to describe the stress-dependent stiffness (Hicks and Monismith, 1971; Uzan, 1985; Kolisoja, 1997). A commonly used model is the  $k$ - $\theta$  model (Eq. 2.5), where the resilient modulus is calculated from the bulk stress  $\theta$  which is the sum of the principal stresses, and the octahedral shear stress  $\tau_{oct}$ .  $p_a$  is a reference pressure (100 kPa), and  $k_1$ ,  $k_2$  and  $k_3$  are experimentally determined constants.

$$M_R = k_1 p_a \left( \frac{\theta}{p_a} \right)^{k_2} \left( \frac{\tau_{oct}}{p_a} + 1 \right)^{k_3} \tag{2.5}$$

Eq. 2.5 is considered a general material model, suitable for both coarse-grained and fine-grained materials. As the material changes from granular to fine-grained,  $k_2$  approaches zero, and the material behaviour is determined by the octahedral shear stress (Lytton et al., 1993). Fine-grained (clayey) materials are weakened by increasing octahedral stress, hence  $k_3 < 0$ . Coarse-grained materials show a strengthening effect of increased confining stress, hence  $k_2 > 0$  (ARA Inc., 2004). For coarse-grained materials,  $k_3$  approaches zero, and the bulk stress determines the material behaviour.

In addition to stress dependency, moisture content is an important factor for the resilient response of unbound materials. At high degrees of saturation,  $M_r$  is highly dependent on moisture content (Lekarp et al., 2000a). Several models incorporate moisture dependency, such as Witczak et al. (2000) and Cary and Zapata (2011). The Witczak et al. (2000) model is implemented in the mechanistic-empirical pavement design guide (MEPDG), and Figure 2.11 shows how  $M_r$  increases with decreasing degree of saturation (ARA Inc., 2004). In Figure 2.11, the x-axis represents the difference between actual saturation ( $S$ ) and optimal saturation ( $S_{opt}$ ), while the y-axis represents the ratio between actual  $M_r$  and resilient modulus at optimal saturation ( $M_{r,opt}$ ).

As implemented in MEPDG, the model differentiates between coarse-grained and fine-grained materials, where fine-grained materials are more affected by changes in saturation. The change in  $M_r$  is most rapid close to optimal saturation.

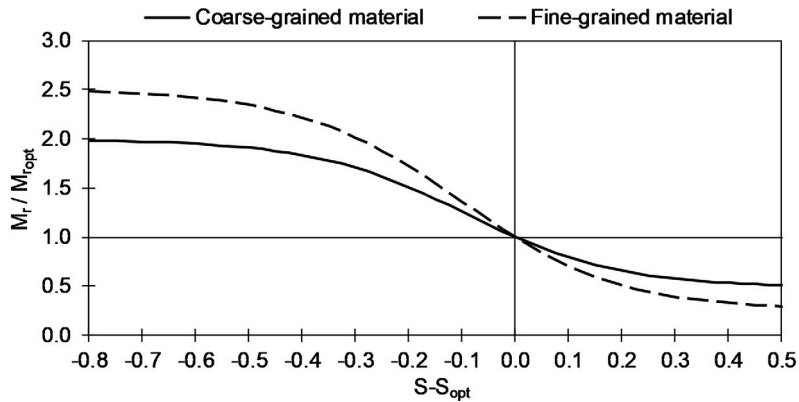


Figure 2.11: Ratio of resilient modulus as a function of change in degree of saturation. Adapted from ARA Inc. (2004).

Although the stress state and moisture level have the greatest influence on the resilient modulus, several properties related to the unbound material have influence as well. Sweere (1990) found that gradation influences the  $M_r$  of unbound materials. For materials with the same maximum particle size, a more coarse grading resulted in a higher degree of stress dependency than a fine grading. For materials with the same amount of fines,  $M_r$  increases with increasing maximum particle size (Kolissoja, 1997). The resilient properties of unbound materials may be influenced by some minerals (Ekblad and Isacsson, 2008). Grading is also affecting the moisture dependency of unbound materials, as well-graded materials are able to hold water in their pores (Ekblad and Isacsson, 2006).

### 2.2.7 Modelling the permanent deformation behaviour of unbound pavement materials

Permanent deformation behaviour is a major characteristic of long-term pavement performance. Numerous models are developed to calculate the accumulation of permanent deformations from traffic. The permanent deformation behaviour is viewed as a function of both the loading and the number of load repetitions. As with the resilient behaviour, other properties such as moisture, density, gradation also impact the permanent deformation behaviour (Lekarp et al., 2000b).

The behaviour of unbound materials under cyclic loading can be described by the shakedown theory, where the permanent deformation behaviour can be classified according to three different stress levels (Werkmeister et al., 2001). The permanent deformation development in three different constant

stress ranges is shown in Figure 2.12. In range A, the stress level is relatively low, and permanent deformations accumulate up to a finite number of load repetitions. After this, the deformation behaviour is purely elastic, and no further permanent deformation is accumulated. In range B, the stress level is higher than range A. As in range A, the accumulation of permanent deformation slows down as the number of load repetitions increases. However, after some finite number of load repetitions, the accumulation of permanent deformation per load repetition becomes close to constant. In range C, the stress level is even higher than in range B, and the accumulation of permanent deformations does not slow down as in range A and B, and the pavement may eventually fail.

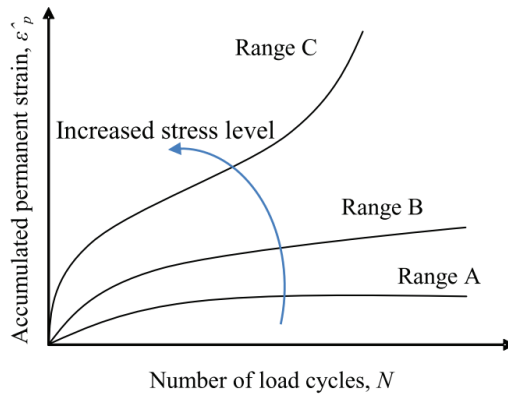


Figure 2.12: Permanent deformation behaviour depending on stress level (Rahman, 2015).

To maintain a long service life, the traffic loads applied to the pavement should mostly cause behaviour in range A and only for limited amounts of traffic cause range B behaviour.

Stress-based models are developed by e.g. Gidel et al. (2001), Werkmeister et al. (2004), Korkiala-Tanttu (2005) and Rahman and Erlingsson (2015). Tseng and Lytton (1989) developed a model based on vertical elastic strain which is implemented in MEPDG (ARA Inc., 2004).

Rahman and Erlingsson (2015) introduced a stress-based empirical model for predicting the permanent deformation behaviour of unbound materials based on the power law presented by Sweere (1990). The model is based on multi-stage repeated load triaxial (MSRLT) testing and is well suited to model the permanent deformations resulting from such tests, but gives wrongful results when applied for cases where negative values for the principal stresses occur from the response model. Hence, Rahman and Erlingsson (2019) proposed a new model, where the stress factor is exchanged for resilient strain.

To replicate traffic loading, the calculation of permanent deformations should include a variety of load levels, not a constant load for all load repetitions. A time-hardening approach can be used to enable the calculation

of permanent deformation from a sequence of stress levels, such as in the MSRLT tests (Lytton et al., 1993; Zhou et al., 2010; Erlingsson and Rahman, 2013). The time-hardening concept takes stress history from previous loading into account when calculating the permanent deformation from the present loading (Figure 2.13).

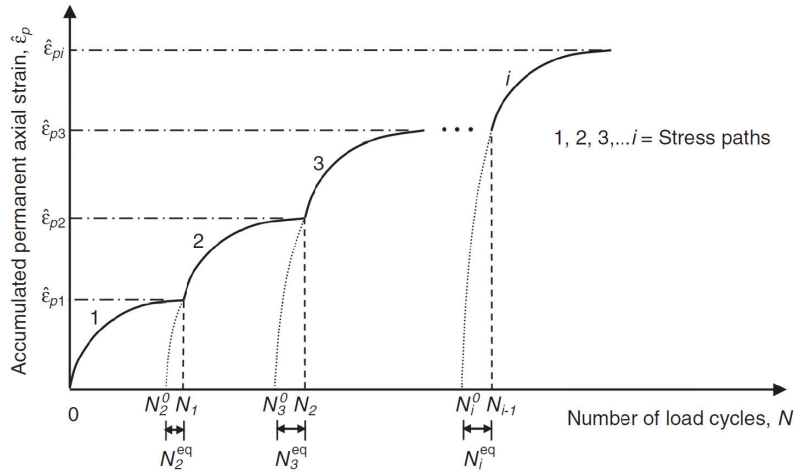


Figure 2.13: Accounting for stress history by using the time hardening approach (Erlingsson and Rahman, 2013).

An equivalent number of load cycles  $N^{eq}$  is added to the number of load cycles at each load level, corresponding to the already accumulated permanent strain at the start of each level. The illustration in Figure 2.13 assumes an increasing stress level from one stress path to the next. If the stress level in one cycle is significantly lower than the previous cycle,  $N^{eq}$  approaches infinity, and no further permanent strain development is calculated from the current cycle.

### 2.3 SUSTAINABILITY IN AGGREGATE PRODUCTION AND USE

Our ever-developing society demands a constant supply of construction aggregates. Even the transition to a greener economy demands construction aggregates; e.g. for the development of new public transport systems and infrastructure for new power sources. As aggregates are non-renewable resources, it is necessary to explore and exploit the resources carefully. Danielsen and Kuznetsova (2015) lists five pressing sustainability issues for the aggregate industry: (1) Mineral resources; (2) Land use; (3) Mass balance and surplus materials; (4) Energy use; (5) Pollution and emissions.

The current annual aggregate consumption in Europe is 6 tonnes per capita (European Aggregates Association, 2020). The consumption varies considerably between countries, as Figure 2.14 shows (Mineral Products Association, 2016). The consumption for Norway alone is 13 tonnes per

capita. In addition to this, Norway is a major exporter of aggregates, and the total annual production of aggregates amounts to 17 tonnes per capita (Directorate of Mining, 2019).

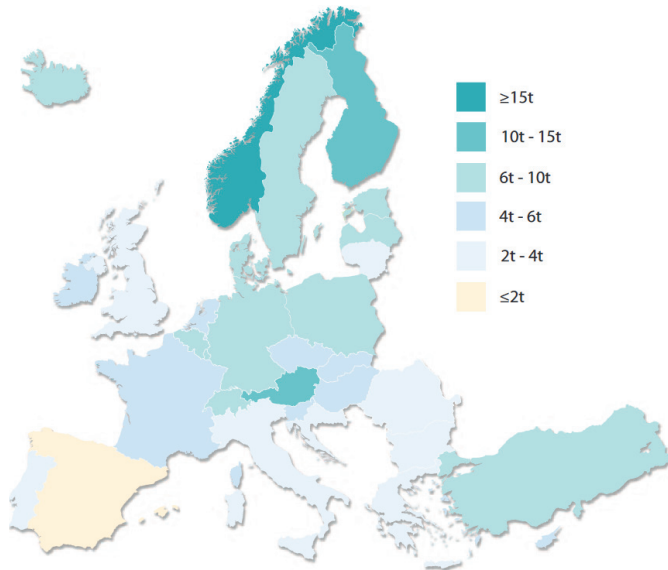


Figure 2.14: Annual aggregate consumption per capita in European countries (Mineral Products Association, 2016).

Hard rock resources vary in quality, and depletion of high-quality resources is a key challenge for the aggregate and construction industry. To obtain a sustainable production, it is essential to assess the required quality correctly in order to avoid overspending high-quality resources. This consideration has two sides;

1. Which quality is “good enough” for the specific application?
2. Are quality assessment methods able to quantify the critical parameters?

Which quality parameter is most important will vary depending on the intended use of the material, as illustrated in Figure 2.15. An example: Flowability is important for the workability of concrete, and to obtain good flow, round and smooth aggregate particles are favourable. For unbound use in a pavement structure, the same aggregate material can cause stability problems. No single parameter can generally determine whether a certain aggregate material is good or poor, because the quality depends on the application.

**UTILISATION OF LOCAL AGGREGATES** In Norway, the term “short-transported aggregates” [*Kortreist stein*] has been rising in importance over the last years. The term illustrates the interest in adjusting existing design and quality

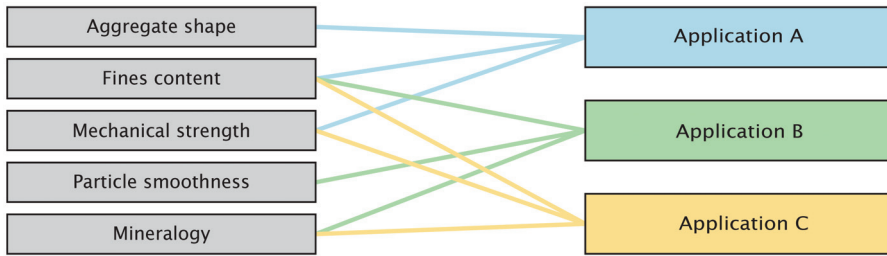


Figure 2.15: Aggregate quality depending on application.

requirements to increase the use of local aggregate materials where these are available. This is called a bottom-up approach, where available resources are mapped and analysed before a structure is designed to utilise the local resources. Traditionally, a top-down approach has been used: a structure is designed based on central guidelines, and local resources are used if they fit the chosen design.

An example of the use of local aggregates is the use of excavated material from tunnels in the production of high-quality concrete and HMA to be used in the same tunnel. These production require a stable supply of aggregates with the required properties. In a tunnel production, substantial variations in aggregate properties can be encountered along the tunnel route. Classifying and separating high-quality resources during tunnelling is both area- and time-demanding, but both time and space are limited resources at construction sites. As a result, the tunnel materials have often been used without separation of sections of higher quality and used for lower grade applications or deposited. Necessary high-quality aggregates would then have to be transported in from a quarry.

**TRANSPORT** Transport of aggregates is a main contributor to the CO<sub>2</sub> footprint of a construction project. A life cycle analysis for a Norwegian road tunnel constructed by drilling and blasting showed that the most important contributor to the climate change impacts was the loading and hauling process (L. Huang et al., 2015). The relative contribution from loading and hauling increases when the tunnel becomes bigger or longer. Regarding transport, aggregate suitability is a two-sided problem: If local aggregates cannot be used, surplus aggregates have to be transported out, while high-quality materials have to be transported in from a quarry.

**TOOLS FOR SUSTAINABILITY ASSESSMENT** In order to quantify and compare different solutions, significant resources have been spent on the development of life cycle assessment (LCA) tools. Environmental product declarations have been developed as a tool for each producer to declare the life cycle environmental impact of their specific products. CEEQUAL and BREEAM are two established general sustainability rating schemes for construction projects. Through the European Committee for Standardiza-

tion (CEN), a set of indicators for sustainability assessment of roads have been developed, but they have not yet been adapted to a standard (CWA 17089, 2016). A LCA tool geared specifically towards utilisation of aggregate resources was developed through the *Kortreist stein* project (Hov et al., 2019).

Design changes may often be necessary for a local aggregate resource to be used in construction, e.g. a weaker material can be used if the thickness of the construction is increased. However, these alterations are often not permitted by traditional quality requirements, and as a result, not all viable alternatives are analysed in the LCA.

**ECONOMY AS A DRIVING FORCE** Making extra considerations for material use and aggregate production will imply extra costs. A Norwegian calculation showed that the transport cost exceeds the cost of the aggregate itself when the transport distance by truck is longer than 30 km (Wolden, 2014). Hence, there is a great potential for increased cost efficiency due to improved logistics and reduced transport. By reducing the need for transport, additional funds can be spent on optimising aggregate production on site.

Ensuring that sustainability assessment methods include the economic considerations mentioned here will ease the introduction of new solutions for resource utilisation in construction projects.



## METHODS

---

The initial research method for this study was a survey investigating international practice for aggregate use (3.1). Next, a literature study of standards and specifications for aggregates was conducted (3.2). Two full-scale studies constitute the main research contributions to the thesis. The first full-scale study investigates the influence of jaw crusher parameters on the quality of large-size primary crushed aggregates (3.3). The other full-scale study is an accelerated pavement test, investigating the influence of gradation and groundwater levels on the performance of unbound aggregates (3.4). The choice of research methods is explained in this chapter. Details regarding the research methods are described in the respective research papers (Appendix A–F).

### 3.1 SURVEY OF PRACTICE FOR AGGREGATE USE

Answering the first research question (RQ) required collection of knowledge regarding international practice for aggregate use in road construction. To gather information about this subject, a survey with questions regarding pavement structures, quality requirements for aggregates and import/export of aggregates was prepared. The information regarding pavement design and aggregate requirements is mainly public information available in specifications and standards published by road authorities. However, the design varies according to traffic volume and local conditions, and design classes vary between countries. To ensure that comparable information could be gathered from a wide selection of countries, a simple questionnaire was designed, asking for information relevant for specific conditions. The involvement of local experts ensured that the most used design alternatives were highlighted, as many pavement design specifications allow for a choice between several design alternatives.

The participants were asked to outline a typical pavement structure in their region for a two-lane road with annual average daily traffic (AADT) of 10 000 vehicles, including normal layer thicknesses and aggregate sizes. The questionnaire also contained questions regarding the specific quality requirements regulating the choice of aggregates, as well as import and export of aggregates in each region.

The survey was sent to experts participating in World Road Association (PIARC), European Committee for Standardization (CEN) and Nordic Road Association (NRF), and the aim was to gather information that would illustrate a variety of pavement designs, aggregate sizes and quality requirements.

More details regarding the methodology and results are described in Paper A.

### 3.2 LITERATURE REVIEW OF STANDARDS AND QUALITY ASSESSMENT METHODS

Knowledge regarding the description, specification and quality assessment of large-size aggregates were needed to answer RQ2. To gather knowledge about which properties of unbound materials are considered important for road construction, a review of standards and research regarding aggregate quality assessment was conducted.

The existing European standards for pavement aggregates are limited to upper sieve size  $\leq 90$  mm (EN 13242, 2007; EN 13285, 2018). The use of larger aggregates must be specified by individual construction clients or in local regulations such as national requirements. At the same time as this PhD study was carried out, a new standard for large-size construction aggregates was developed by Standards Norway (NS 3468, 2019). The standard covers large-size aggregates, which are defined as products with an upper sieve size  $> 90$  mm. The aim of the new Norwegian standard is to simplify the process of describing, specifying and trading large-size aggregates and to ensure consistency for both producers and buyers. The objectives for the standard development coincided with the objectives for the PhD research regarding the challenges related to the characterisation of large-size aggregates. A central concern in the preparation of the standard has been to agree on practicable methods to enable efficient quality assessment of large-size materials.

Paper A showed that large-size aggregates are used for road construction in several countries besides Norway. From this, it may be assumed that more countries would find a standardisation of such materials useful. Hence, the new standard for large-size aggregates was included as a central part of the literature study.

The new Norwegian standard describes some new test methods, mainly adaptations of standardised test methods, made applicable for larger sample sizes. The non-standardised test methods include new or adapted methods for particle size distribution (PSD) analysis, and sampling and sample preparation for testing mechanical properties. The literature study allowed for an assessment of the requirements and test methods described in the new standard in light of international research.

As the new standard is only published in Norwegian, an additional aim became to give a description of the new requirements in English and introduce the standard to a broader audience.

The results from the literature study are presented in Paper B.

### 3.3 FULL-SCALE CRUSHING TEST

RQ3 asks how production methods affect the quality of large-size aggregates. When local aggregate resources are used at construction sites, the production often involves a mobile jaw crusher in a simple setup. A study of published literature on the subject revealed a knowledge gap regarding the quality of primary crushed aggregates. A full-scale crushing test was designed to

investigate the influence of crusher settings and feed gradation on the quality of large-size aggregates after primary crushing. The impact of feed and crusher settings were isolated by limiting the test to a single crusher and a single rock type. The full-scale crushing test aimed to replicate a setup for aggregate production from surplus materials at a construction site.

Considerations regarding the choice of research methods are described in the following sections. The full details of the testing are described in Paper C. Some results regarding the relations between particle shape and mechanical properties are reported separately in a master's thesis by Luke (2017).

### 3.3.1 *Full-scale test setup*

The following feed and jaw crusher parameters were identified as relevant for the full-scale test:

- Upper feed size
- Lower feed size
- Speed of the crusher
- Stroke of the crusher
- Crusher opening
- Feed rate

The focus of this study was the parameters that can be influenced in a production setting using the equipment available on site, and the study was limited to a single crusher. Hence, the geometry of the crusher cavity was excluded from the available jaw crusher parameters.

The full-scale test could either have been conducted in a controlled environment at Metso Minerals' test facility, or in an ongoing production in a quarry or a construction site. An advantage of conducting tests at a production site would be that the test conditions corresponded to actual conditions. However, a wide test programme would be time-consuming and costly, as the ongoing production would have to be stopped in order to conduct the tests. Furthermore, the power draw of the jaw crusher could be monitored continuously during crushing at the test facility. The test facility alternative was chosen due to the advantage of a controlled test environment and the lack of time limitations, ensuring the possibility to complete a comprehensive test programme.

One limitation introduced by the choice of the test facility was that continuous feeding of the crusher was not possible. Instead, individual test portions were loaded onto a vibratory feeder using a wheel loader. The size of each test portion (1500–2500 kg) was designed to be large enough to ensure a period of continuous and stable crushing where measurements and sampling could be conducted.

The crusher stroke is an adjustable parameter in machine design, but jaw crushers are usually constructed for a constant stroke. The crusher used in the tests did not have the possibility to adjust stroke. Feed rate is a parameter that is easy to adjust, but hard to quantify. In the tests, two feed levels were selected, a high feed rate that ensured the crushing chamber was full (choke feeding), and a low feed rate where the throughput of the crusher was reduced by about half. Hence, the available parameters for the study were upper and lower feed size, feed rate, closed side setting (CSS) and speed.

Table 3.1 shows the available settings of the parameters selected for the test, where feed size 100/400 mm, high feed rate, CSS 70 mm and high crusher speed were selected as the standard settings. Table 3.2 lists the 12 parameter combinations used to test all available settings. Each test (T4–T15) was conducted in minimum three parallels, in total 45 test crushings. The process flowchart in Figure 3.1 shows the setup of the full-scale crushing test, and where in the process samples were collected.

Table 3.1: Summary of available settings of the feed and crusher parameters.

PARAMETER	AVAILABLE SETTINGS
Lower feed material size	0, 100, 180 mm
Upper feed material size	300, 400 mm
Feed rate	High, low
Closed side setting	40, 70, 100 mm
Crusher speed	355, 284 rpm

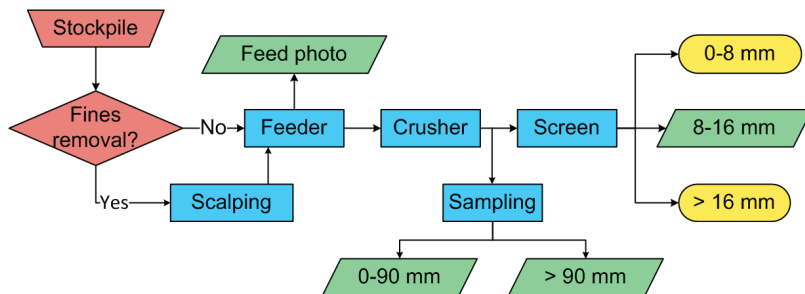


Figure 3.1: Process flowchart for the full-scale crushing test, including sampling.

### 3.3.2 Selection of test material

The feed material for the full-scale crushing test was produced in an open-pit quarry in Nokia, Finland, close to the test facility in Tampere. The selected test material was blasted rock, supplied in the size range 0–500 mm. The rock type was a coarse-grained granodiorite. The material was blasted as part of

Table 3.2: Parameter combinations used in full-scale crushing test.

TEST ID	FEED SIZE [mm]	FEED LEVEL	CLOSED SIDE SETTING [mm]	CRUSHER SPEED [rpm]
T4	100/400	High	70	355
T5	100/400	Low	70	355
T6	100/400	High	40	355
T7	100/400	High	100	355
T8	180/400	High	70	355
T9	0/300	High	40	355
T10	0/300	High	70	355
T11	100/300	Low	40	355
T12	100/300	High	40	355
T13	100/300	High	70	355
T14	0/400	High	70	284
T15	100/400	High	70	284

the ordinary quarry production, but was not crushed ahead of delivery to the test facility.

The selection criterion was that the material should fulfil requirements for use as subbase material given by Norwegian Public Roads Administration (2014), which was the valid specification at the time. The material was pre-assessed for resistance to fragmentation (Los Angeles test, (EN 1097-2, 2010)) and resistance to wear (micro-Deval test, (EN 1097-1, 2011)), and the declared values (Table 3.3) fulfilled the requirements.

Table 3.3: Declared values for mechanical properties.

TEST METHOD	TEST RESULT
Resistance to fragmentation (Los Angeles test)	LA = 28
Resistance to wear (micro-Deval test)	M <sub>DE</sub> = 9

### 3.3.3 Laboratory test programme

The following properties were selected to describe the quality of the crushed materials, based on current requirements for large-size aggregates:

- Particle size distribution
- Particle shape
- Mechanical properties

The properties were tested according to relevant European standards, with some adjustments for particle sizes exceeding the standards. Samples from each crushing test were gathered as illustrated by the green parallelograms in Figure 3.1.

Feed PSD was analysed from the feed photos using digital image processing (DIP). Two examples of the feed pictures are shown in Figure 3.2. The red spheres in the photos have a diameter of 250 mm and are used to scale the images in the DIP tool.



Figure 3.2: Examples of photos used in digital image processing of feed particle size distributions. Photo: Metso Minerals

The 0–90 mm and >90 mm samples from the crusher were used to analyse product PSD and particle shape. PSD was evaluated using sieve sizes from 1 to 200 mm. A total of 45 PSD samples were collected from the crusher, each weighing from 143 to 430 kg, on average 238 kg. The sampling was conducted by placing the wheel loader bucket at the end of the output conveyor from the crusher during a time where the crushing was continuous and stable. By registering the duration of sampling and the sample weight, the crusher throughput could be calculated. The size of the PSD samples was influenced both by the expected gradation and by the time needed to obtain a valid throughput calculation. To avoid segregation and ensure representativity, the full test portion from the wheel loader bucket was collected for analysis, as shown in Figure 3.3.

The PSD samples were split manually at the crushing plant, separating material >90 mm from the samples transported to the laboratory. The 0–90 mm sieve samples brought to the laboratory weighed on average 151 kg per sample. To reduce the sample size towards the required 80 kg, the samples weighing more than 160 kg were split in half using a riffle box.

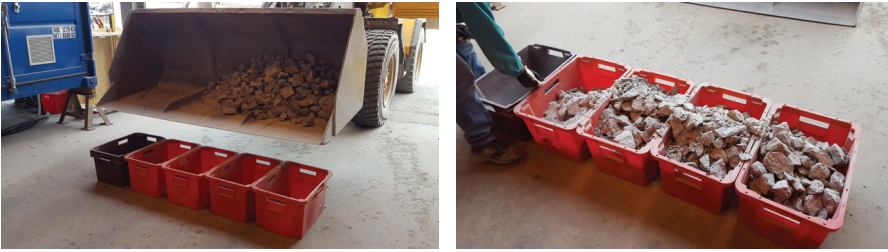


Figure 3.3: Method for collection of product samples from wheel loader bucket.

A few adjustments to standard laboratory procedure (EN 933-1, 2012) was made due to the large sample sizes:

- Smallest sieve size used was 1 mm.
- The test portions were not washed prior to sieving; the analysis followed the procedure for dry sieving.
- For some samples, material  $< 25$  mm was subsampled to minimum 6.3 kg using a riffle box before sieving continued.

As the focus of the present research is on large-size aggregates and variations in the larger particle sizes, variations in the sizes smaller than 1 mm was considered less important. For particle shape, the standard procedure does not consider material smaller than 4 mm (EN 933-3, 2012). By limiting the sieve size to  $\geq 1$  mm, washing of samples could be avoided without degrading the sieving result. As the samples had been stored indoors for several months prior to the analyses, the material was dry, and moisture was not a problem during sieving.

Mechanical properties were tested with the Los Angeles and micro-Deval tests in 10–14 mm test portions (EN 1097-2, 2010; EN 1097-1, 2011). For these test methods, the standard procedure allows for samples to be collected from larger aggregate sizes, and laboratory crushing can be used in sample preparation. As the literature review had shown that material properties are known to improve by crushing, the laboratory test programme was designed to test material prepared in two ways:

1. 10–14 mm material sieved from the jaw crusher product (8–16 mm samples)
2. 10–14 mm material produced by laboratory crushing 63–90 mm material from the jaw crusher product (PSD samples)

This approach aimed to quantify the variation in material properties due to sample preparation.

### 3.3.4 Statistical analysis

Regression analysis was used to correlate crusher operation and product quality to feed and crusher properties. To enable analysis of the combined effect of two or more variables, multiple linear regression analysis was performed using the statistics software Minitab 19 (Minitab, 2019). In these analyses, the measured properties describing crusher operation and product quality were defined as dependent variables. Parameters describing the feed size, feed rate and crusher settings were defined as possible explanatory variables.

To conduct a regression analysis without presumptions for which independent variables should be used, the Minitab function fit regression model using backwards elimination was used to decide which explanatory variables are valuable predictors for each dependent variable. The variables describing the size of the feed materials are to some extent correlated, so to avoid cross-correlation, only one such explanatory variable was allowed in the regression of each dependent variable.

The explanatory variables were either continuous or categorical/discrete. The discrete variables are input to Minitab as categorical predictors, or dummy variables, using the value with the highest number of observations as the reference level. Hence, high feed rate is coded as  $FR = 0$ , low feed rate as  $FR = 1$ ; normal speed as  $v = 0$  and reduced speed as  $v = 1$ . Similarly, 70 mm is chosen as the reference level for CSS, and CSS 40 mm and 100 mm are compared to CSS 70 mm separately.

An example from the analysis is shown in Figure 3.4, where capacity is the dependent variable, explained by the continuous variable lower feed size  $F_{10}$  and the discrete variable closed side setting CSS. The analysis is conducted so that the slope of the lines are decided by the continuous variable, while the discrete variables add a constant value to the regression line. A combined coefficient of determination ( $r^2$ ) is calculated for the regression depending on both  $F_{10}$  and CSS. In Figure 3.4, the data points are clearly separated by CSS, and the data for each CSS value fits regression lines of equal slope.

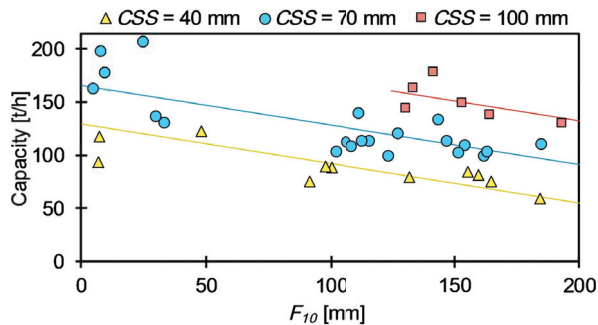


Figure 3.4: Multiple linear regression example from Paper C: Crusher capacity depending on lower feed size  $F_{10}$  and closed side setting CSS,  $r^2 = 0.77$ .

The regression analysis shows that the capacity of the crushing operation is dependent on both the feed size and the crusher setting – the capacity increases with increasing CSS and decreasing  $F_{10}$  size. In this example,  $r^2 = 0.77$ , meaning that 77% of the variation in capacity can be explained from the variation in  $F_{10}$  and CSS. Without separating the data points for CSS, the correlation between capacity and  $F_{10}$  would not be visible. Analysing each CSS individually would give less certainty in the conclusions because the number of samples in each analysis would be smaller.

The multiple linear regression analysis described here is used throughout Paper C.

### 3.4 ACCELERATED PAVEMENT TEST

RQ4 and RQ5 both concern the performance of large-size unbound aggregates. Uzan (1999) listed four reasons why the characterisation of unbound materials for pavement design is difficult:

1. The response of granular materials is strongly nonlinear
2. Stress paths applied in the laboratory are limited by the equipment and do not reproduce stress paths in the pavement structure under moving load
3. The maximum aggregate size for laboratory tests is 25–50 mm
4. No undisturbed samples can be obtained from the field

Reasons 2–4 are all related to the limitations of laboratory testing. In order to investigate the performance of pavement structures with large-size subbase aggregates in full scale, and avoid the limitations of laboratory methods, an accelerated pavement test (APT) was conducted using a heavy vehicle simulator (HVS). The HVS equipment replicates real traffic loads and can be used on both real road structures and constructed test sections.

Two instrumented structures were constructed side-by-side in a HVS test pit at the Swedish National Road and Transport Research Institute (VTI) full-scale pavement testing facility (Figure 3.5). Each structure was 5.0 m wide and 7.5 m long, and in depth, the pavement structures were constructed using full-scale layer thicknesses and aggregate sizes.

The difference between the two structures was the gradation of the subbase layers, relating the APT to RQ4. Three different groundwater levels were induced in order to change the moisture content in the structures and investigate RQ5. Considerations regarding the choice of research methods are described in the following sections. The full details of the testing are described in Papers D–F.

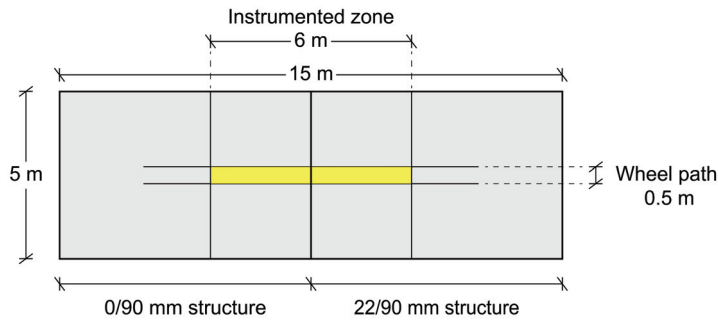


Figure 3.5: Outline of HVS test pit seen from above.

#### 3.4.1 Pavement design and selection of materials

Although the traffic is accelerated, an APT is a time-consuming test. To be able to plan and construct the structure, conduct accelerated traffic and the following data analysis during the time frame of the PhD study, the test was limited to a single test setup. However, by dividing the test pit in two and using two subbase gradations, two structures could be analysed in one test.

The pavement structures were designed to be comparable to previous tests conducted at VTI, with a total pavement thickness of about 60 cm. The design follows the typical flexible pavement design in Sweden and Norway, with relatively thin asphalt concrete (AC) layers over unbound base and subbase layers constructed from crushed rock. From the bottom of the subbase layers and down to the bottom of the concrete test pit, the subgrade consisted of silty sand.

To investigate the influence of gradation on pavement performance, the APT was designed using one well-graded subbase material with controlled fines content, and one open-graded subbase material not containing fines. The two types of subbase material are both described in specifications from Norwegian Public Roads Administration (2018), and considered equivalent alternatives in the Norwegian pavement design system. The starting point for the test design was a 22/125 mm subbase material, which was supplied from a road construction site in Norway. This material originated from drill and blast tunnelling at the construction site, and was produced by mobile crushing and screening equipment on-site. Due to the allowances for over- and undersize in aggregate gradations, the material fit the specification for both 22/90 mm and 22/125 mm subbase.

Direct access to the aggregate production process at the construction site was not possible, so 22/125 mm material was collected from stockpile and 0/125 mm material was not available. To create a well-graded alternative material, the 22/125 mm material was mixed with 0/32 mm material from the same source using a wheel loader. The 22/125 and 0/32 mm mix ratio was decided by the fines content in the finished product, which was limited by the product specification (Norwegian Public Roads Administration, 2018).

With a 1:1 weight ratio, the grading requirements, including maximum fines content, for 0/90 mm subbase was fulfilled. The mixed material did not contain enough 125 mm material to be classified 0/125 mm. For consistency, the original 22/125 mm material was reclassified as 22/90 mm, so that the two subbase materials used in the APT was an open-graded 22/90 mm and a well-graded 0/90 mm.

Figure 3.6 displays the detailed outlines of the final pavement structures, with layer thicknesses specified in mm. Differences in layer thicknesses between the two structures are due to practical adjustments in the construction process, such as differences in compaction.

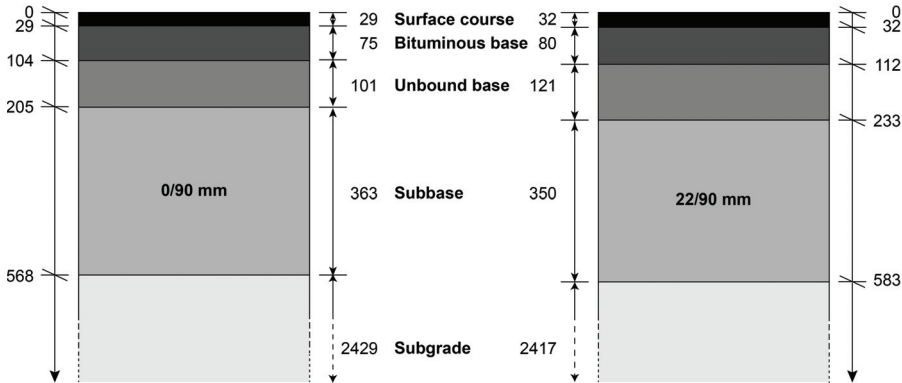


Figure 3.6: Outline of pavement structures in APT. Depth and layer thicknesses measured in mm. AC – asphalt concrete; UB – unbound base; Sb – subbase; Sg – subgrade.

#### 3.4.2 Instrumentation of pavement structures

Both pavement structures were instrumented to enable measurements of stress, strain, moisture and temperature during testing. At the bottom of the bituminous layers, longitudinal and transversal strain were measured by asphalt strain gauges (ASGs). Vertical strain was measured by strain measuring units ( $\epsilon$ MUs) in both bituminous and unbound layers, extending to about 30 cm into the subgrade. Vertical stress was measured by soil pressure cells (SPCs) at three levels in the subbase layers. Moisture sensors were placed in all unbound layers. Both structures were instrumented identically, with a vertical distribution of sensors as shown in Figure 3.7.

To ensure that the HVS kept constant speed over all sensors, all instrumentation was placed in the middle 6 m of the test pit (Figure 3.5).

#### 3.4.3 Accelerated traffic

The APT was conducted using dual-wheel loading, with 60 kN dual-wheel load, corresponding to 120 kN axle load. The tyre pressure was 800 kPa. The

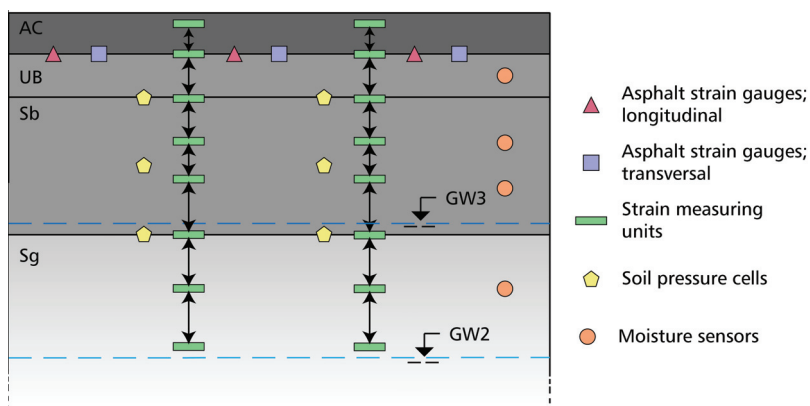


Figure 3.7: Instrumentation of pavement structures in APT. Size of symbols and horizontal distance between sensors not to scale.

loading was bidirectional, at a constant speed of 12 km/h. The accelerated traffic was initially planned to 1 000 000 load repetitions or until the rut depth reached 20 mm. The load repetitions are applied following a normal distribution curve to simulate lateral wander in a distance of  $\pm 25$  cm from the centre position. As the structures showed a slower rut development than expected, the accelerated traffic was extended to 1 233 000 load repetitions.

#### 3.4.4 Climatic conditions

To ensure constant test conditions, a climate chamber was installed around the HVS, and the temperature was held constant at 10 °C.

In the first phase of the test, w1, the materials in both structures were moist, but no groundwater table (GWT) was present in the test pit. This phase had a planned duration of at least 500 000 load repetitions, or up to 700 000 load repetitions, until the rut depth exceeded 8 mm. The rut development in both structures was lower than expected, as the rut development levelled off after about 450 000 load repetitions. Phase w1 was ended after 550 000 load repetitions, at a rut depth of 5–6 mm.

In phase w2, water was added to the test pit so that a constant GWT was located at a depth of 30 cm below the formation level (Figure 3.7). Based on previous research presented by Saevarsdottir and Erlingsson (2013a), the introduction of a GWT in the subgrade below the pavement structures was expected to accelerate the degradation of the structures so that a rut depth of 20 mm would be reached within 300 000 load repetitions. However, after 385 000 load repetitions on groundwater level w2 (935 000 load repetitions in total), the rut depth was only about 12 mm. This gave the opportunity to add a third groundwater phase (w3) to the test, where GWT was raised to about 5 cm into the subbase layers. Almost 300 000 load repetitions were added in this phase, until both structures reached a rut depth of 20 mm after 1 233 000 load repetitions.

### 3.4.5 *Measurements*

**FALLING WEIGHT DEFLECTOMETER** During the APT, falling weight deflectometer (FWD) measurements were conducted on each groundwater level. The tests were conducted using a KUAB FWD with a 300 mm diameter load plate at three load levels; 30 kN, 50 kN and 65 kN. FWD testing was conducted both during the APT and at each groundwater level after the APT was finished. As the climate chamber had to be removed in order to move the HVS and give room for the FWD, the temperature was not 10 °C during these measurements.

Stiffness moduli for subgrade, subbase and base layers were back-calculated from the FWD results using multi-layer elastic theory (MLET). Calculations were made in an iterative process using the ERAPAVE software (Erlingsson and Ahmed, 2013). During back-calculation, subgrade stiffness was assumed equal for both structures, while the stiffness for the other unbound layers varied between the structures due to material differences and differences in moisture content. AC stiffness was adjusted for according to pavement temperature measured at the time of FWD testing, and assumed equal for both structures.

**LASER RUT DEPTH MEASUREMENTS** The rut profile was measured at regular intervals throughout the test using a laser and straight edge setup. Three profiles for each structure were measured, on average once per 24 000 load repetitions. The laser registered the surface profile at 1 cm intervals over a width of 2.5 m.

**RESPONSE MEASUREMENTS** The pavement response was measured nine times during the APT. The most extensive response measurements were conducted at the start of the APT, after an initial pre-loading phase of 20 000 load repetitions with reduced dual-wheel load (30 kN/700 kPa). This response programme included measurements with variation in wheel configuration (single and dual), wheel load (30, 40, 50, 60 and 80 kN) and tyre inflation pressure (600, 800, 900 kPa). At the start of the two next groundwater phases, a similar response testing programme was conducted, but limited to dual-wheel configuration and tyre pressures 600 and 800 kPa. The remaining six response measurements were conducted with dual-wheel configuration and constant tyre pressure 800 kPa, while the dual-wheel load was varied.

The response measurements were conducted with the wheel configuration in the centre position (sensors located between loading wheels) and in position -15 cm (one wheel located directly above the sensors). Once per groundwater phase, a limited amount of measurements were conducted with the wheel configuration varying between all wheel positions included in the lateral wander.

### 3.4.6 Modelling of pavement response and performance

All modelling was focussed on the unbound materials. Simplifications were made for the AC layers, as they are not part of the scope for this thesis. Previous research has shown that at the temperature used in the APT, 10 °C, the accumulation of permanent deformations in AC materials is negligible compared to the deformation in the unbound layers (Saevarsdottir and Erlingsson, 2013b; Ahmed and Erlingsson, 2015).

#### 3.4.6.1 Response models

Two different approaches were applied to model the pavement response behaviour:

- a linear elastic (LE) procedure based on FWD measurements
- a non-linear elastic (NLE) procedure based on measured vertical strain throughout the structures

The response models were used to calculate traffic-induced stresses, strains and displacements in the pavement structures. Both the LE and NLE behaviour were calculated with MLET using the ERAPAVE software.

For the LE approach, all materials were treated as linear elastic, with stiffness calculated from Eq. 2.4. FWD results were back-calculated based on layer thicknesses, moisture content and measured deflection.

In the NLE approach, unbound base and subbase were treated as stress-dependent with stiffness following Eq. 2.5, while AC and subgrade were treated as LE materials with stiffness following Eq. 2.4.

All unbound materials studied in this thesis are considered coarse-grained with  $k_3 = 0$ , simplifying Eq. 2.5 to Eq. 3.1.

$$M_R = k_1 p_\alpha \left( \frac{\theta}{p_\alpha} \right)^{k_2} \quad (3.1)$$

Coefficient  $k_1$  and  $k_2$  in Eq. 3.1 should not be back-calculated simultaneously (Li and Baus, 2005). Coefficient  $k_2$  is known to be less or insignificantly affected by moisture (Rada and Witczak, 1981; Kolisoja, 1997; Rahman and Erlingsson, 2016). To isolate the effect of changing moisture levels on  $M_R$ , coefficient  $k_2$  was kept constant at 0.6 for all materials and moisture levels, while coefficient  $k_1$  was varied to fit the measured vertical strain.

#### 3.4.6.2 Permanent deformation modelling

Permanent deformations were calculated using two different models, the established mechanistic-empirical pavement design guide (MEPDG) model (ARA Inc., 2004) and a new model developed by Rahman and Erlingsson (2019). Both models calculate permanent deformations based on elastic strain.

The subgrade was treated as equal for both structures, except for the vertical strain which varied due to the properties of the layers above. In the calculations, the subbases were divided into three sublayers, and the subgrade was divided into six sublayers. The layer subdivision corresponded to the distance between  $\epsilon_{\text{MU}}$  coils for the instrumented part of the structures, including two 15 cm layers in the top part of the subgrade. The uninstrumented subgrade (depth about 87 cm – 3 m) was divided into four layers of equal thickness. The vertical resilient strain at the midpoint of each sublayer was calculated from the response model.

**MEPDG MODEL** In the MEPDG model, accumulated permanent strain  $\hat{\epsilon}_p$  can be calculated from vertical resilient strain  $\epsilon_v$  and number of load repetitions  $N$  using Eq. 3.2 (ARA Inc., 2004).  $\frac{\epsilon_0}{\epsilon_r}$ ,  $\rho$  and  $\beta$  are material parameters calculated from the moisture content.  $\beta_1$  is a layer-specific calibration factor. The vertical resilient strain normally denoted  $\epsilon_r$  is here denoted  $\epsilon_v$ , to avoid confusion with the  $\frac{\epsilon_0}{\epsilon_r}$  constant.

$$\hat{\epsilon}_p = \beta_1 \left( \frac{\epsilon_0}{\epsilon_r} \right) e^{-\left(\frac{\rho}{N}\right)^\beta} \epsilon_v \quad (3.2)$$

**RE MODEL** The model proposed by Rahman and Erlingsson (2019) (RE model) is a further development of a stress-based model published in Rahman and Erlingsson (2015), now adapted for calculation from strain. In the RE model, accumulated permanent strain  $\hat{\epsilon}_p$  can be calculated from vertical resilient strain  $\epsilon_r$  and number of load repetitions  $N$  using Eq. 3.3. The factors  $a$  and  $b$  are regression-based material parameters.

$$\hat{\epsilon}_p(N) = a\epsilon_r N^b \epsilon_r \quad (3.3)$$

In the original stress-based model,  $a$  was found to be moisture dependent (Rahman and Erlingsson, 2016). A task for the current research was to find whether this was true also for the strain-based version of the model.

**INCORPORATION OF LATERAL WANDER AND CHANGING MOISTURE CONDITIONS** The time-hardening approach (Figure 2.13) was used to account for the varying strain conditions due to the wheel wandering and the changing moisture conditions.  $N_i^{eq}$  is calculated from Eq. 3.4 for the MEPDG model and Eq. 3.5 for the RE model, where  $i$  refers to the current load level, and  $i - 1$  refers to the previous load level.

$$N_i^{eq} = \rho \left( -\ln \left( \frac{\hat{\epsilon}_{p_{i-1}}}{\beta_1 \frac{\epsilon_0}{\epsilon_r} \epsilon_{v_i}} \right) \right)^{-\frac{1}{\beta}} \quad (3.4)$$

$$N_i^{eq} = \left( \frac{\hat{\epsilon} p_{i-1}}{a \epsilon_{r_i}} \right)^{\frac{1}{b \epsilon_{r_i}}} \quad (3.5)$$

For each load level  $i$ , accumulated permanent strain is calculated for  $N = \Delta N_i + N_i^{eq}$  load cycles using Eq. 3.2 and Eq. 3.3.

The incorporation of lateral wander and calculation of rut profiles followed the approach by Saevarsdottir and Erlingsson (2015). The normal-distributed lateral wander of the dual-wheel load was incorporated in increments of 500 load repetitions. The rut development is calculated for every 5 cm over a 2 m wide profile, incorporating the wander of the dual-wheel load relative to the calculation position.

## KEY FINDINGS – SUMMARY AND DISCUSSION

---

The key findings from each research paper are summarised and discussed in this chapter. Key findings from Paper A and B in section 4.1, Paper C in section 4.2, and Paper D, E and F in section 4.3. Some general findings are discussed in section 4.4. The papers provide more detailed discussions on methods and results.

### 4.1 USE OF LARGE-SIZE AGGREGATES IN PAVEMENT STRUCTURES

#### 4.1.1 *Paper A*

The purpose of the survey described in section 3.1 was to gain knowledge regarding the different practices for aggregate use and pavement design in various countries. This knowledge would enable a better interpretation of the relevance of international research for large-size aggregates. The results presented in Paper A have shown that there are large variations in practice for aggregate use internationally.

The 17 respondents to the survey represented 18 regions in Europe, Asia and North America. As 13 of the 17 respondents represented European countries, the results are mainly relevant for European conditions. However, the selection of countries was judged sufficient to illustrate a variety of pavement designs, aggregate sizes and quality requirements.

Pavement thicknesses vary among the surveyed countries, as Figure 4.1 shows. There are variations within countries due to variation in subgrade conditions, frost and climatic conditions, and drainage conditions. Variations between countries are mainly due to different pavement design systems and differences in quality and availability of construction materials.

The variation in aggregate sizes is most evident in the subbase materials, shown in Figure 4.2. The pavement thickness affects the size of the aggregates used, as the allowed particle sizes in many requirements are related to the thickness of each layer. Thus, the countries having the thickest pavements also use the largest aggregates. Comparing full pavement thickness and maximum aggregate size allowed in subbase, we see that the four regions allowing the thickest pavements are also among the five countries that allow the coarsest unbound materials.

The results from the survey show that the use of traditional quality assessment methods is still dominating. None of the countries represented in the survey mentioned performance-based quality requirements specifically, and all countries that provided specific information on quality requirements still used traditional tests like particle shape, amount of crushed and broken

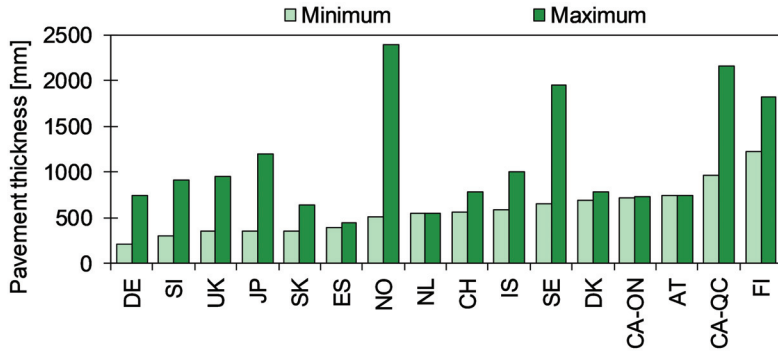


Figure 4.1: Minimum and maximum pavement thicknesses for annual average daily traffic (AADT)  $\approx$  10 000.

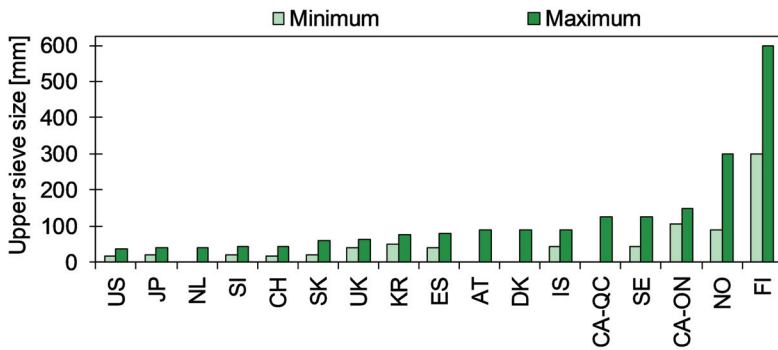


Figure 4.2: Upper sieve size limits for subbase materials.

surfaces, and resistance to fragmentation. However, the survey did not specifically ask for information regarding performance-based testing.

International aggregate trade is widespread and necessary, and several countries use imported aggregates to reduce transportation. In this sense, the varying quality demands for aggregates can be viewed as an opportunity for aggregate utilization. International trade of aggregates is aided by common sets of specifications for aggregates – such as the European standards – but that is lacking for the large-size aggregates.

The information and analysis in Paper A enabled comparison of how aggregate use and pavement design varies between countries. Large-size aggregates are mainly used in northern countries such as Norway, Sweden, Finland and Canada, which may be related both to the need for frost protection and the availability of aggregates. Many countries are reliant on import of aggregates and have adapted their pavement designs to use less aggregates. In northern countries, pavement structures are thicker due to the need for frost protection, which in turn allows for larger particle sizes.

Despite divergent practice for aggregate use, quality requirements in the studied countries meet equivalent standards. The use of international

standards for product specifications and quality tests aids the international aggregate market.

#### 4.1.2 Paper B

In Norway, large-size aggregates ( $D \geq 90$  mm) are the most common products used in subbase and frost protection layers, the layers which constitute the largest part of the pavement structures. Paper A showed that such aggregates are used for road construction in other countries as well. The background for both Paper B and the new Norwegian standard NS 3468 (2019) was the lack of standard specifications and test methods for large-size aggregates. Without standards, the specification of such products is the responsibility of each construction client. Without proper specifications, the aggregate producers have to meet different product specifications from different customers. Furthermore, it is difficult for the customer to verify the quality of the ordered products when specifications cannot be related to relevant quality assessment methods.

The discussion in Paper B underlines the main concern: the difficulties regarding the quality assessment of large-size aggregates. There is a lack of test methods for the full range of particle sizes, even for the most basic descriptor, which is the particle size distribution (PSD).

NS 3468 introduces a differentiation between sievable and non-sievable aggregates, where aggregates  $< 180$  mm are classified as sievable. However, the limit for sievability should not be viewed as constant. On the contrary, it is dependant on the available sieving equipment. Most available laboratory equipment for sieving large-size particles is only suitable for manual sieving. If automated equipment for sieving samples up to 180 mm is not available, the boundary for sievability should be lowered, e.g. to 90 mm. Choosing 90 mm as the limit for sievability would also simplify the specifications; aggregates specified by EN 13242 (2007) or EN 13285 (2018) are sievable, aggregates specified by NS 3468 (2019) are non-sievable. Hence, the alternative methods for classifying PSD described in NS 3468 would be available for all aggregates specified using the standard for large-size aggregates.

The currently available digital image processing (DIP) tools give a two-dimensional area-based analysis of particle sizes, while sieving is a three-dimensional weight-based analysis. Literature on the connection between particle shape and size classification shows that the two analysis methods may result in different distributions. Because existing requirements for PSD are defined for weight-based analysis, a methodology for relating area-based distributions from DIP to weight-based distributions should be described.

NS 3468 sets a constant requirement for sample size, i.e. number of visible particles, for DIP at minimum 400 particles. For the traditional sieving analysis, the required sample weight increases with increasing particle sizes to ensure a representative amount of particles of all sizes. The requirements for minimum number of particles for DIP should be differentiated according to particle sizes and gradation. Wide gradations, especially all-in aggregates (e.g. 0/300 mm),

require a higher number of particles in the analysis than aggregates in a narrower size range (e.g. 22/125 mm).

NS 3468 specifies testing of 10–14 mm samples for quantifying the mechanical properties for aggregates of all sizes. Several research efforts have shown that sample preparation can improve the measured physical properties of an aggregate product. These facts introduce errors in the quality assessment for large-size aggregates where the material must be laboratory crushed in order to obtain the required particle sizes for testing. Further research is needed to verify whether laboratory prepared samples are representative for aggregates more than ten times their size.

All challenges are not solved by implementing the new Norwegian standard for large-size aggregates. Experience from the first edition of the standard should be combined with new research in the further development of specifications for large-size aggregates. The following improvements to NS 3468 are suggested in Paper B:

- Lower the limit for sievability from 180 mm to 90 mm.
- Describe a method for relating PSD from DIP to PSD from sieving.
- Differentiate the requirement for number of particles present in PSD analysis by DIP according to particle sizes.

The identified challenges related to large-size aggregates are not of a specific Norwegian nature, but also relevant when such materials are used in other countries.

#### 4.1.3 *Joint discussion for papers A–B*

Large-size aggregates are more commonly used in Norway than in many other countries, but their use is not limited to Norway alone. As more focus is laid on sustainable sourcing of construction materials, the use of locally produced large-size materials from tunnels and road cuts can become relevant in several regions. When high-quality resources are available at or close to construction sites, mobile production of large-size aggregates is an affordable solution compared to transporting material from quarries.

The specification of aggregates is regulated by European standards. As the standards specify categories related to each test method, requirements are allowed to vary among countries. However, clear specifications rely on suitable test methods for each of the material properties, and this is what is lacking for the large-size aggregates. There are few available laboratory tests for large particle sizes. Large particles require large sample sizes to ensure representative sampling, which complicates the quality assessment. Difficulties in sampling and testing may result in the quality assessment not being conducted correctly. Instead of risking faulty or lacking quality assessment, practical adaptations of the test methods such as those suggested by NS 3468 should be applied, even if they involve larger error margins.

The challenges related to specification and quality assessment of large-size aggregates is not only a Norwegian issue, hence, the aggregate and construction business in several countries would benefit from an international adaptation of the new Norwegian standard for large-size construction aggregates.

#### 4.2 PRODUCTION METHODS AFFECTING AGGREGATE QUALITY

The output from primary jaw crushers has seldom been considered finished products, even though such products are used in substantial volumes in pavement structures. Little emphasis has traditionally been given to the quality of these products, as research has focussed on the products from later crushing stages.

The declared mechanical properties in Table 3.3 show that the raw material used in the crushing tests was well within the requirements for use in road construction. If this resource was found in a construction project, mobile production equipment could be set up in a single-stage crushing process in order to utilise the available rock material for construction aggregates.

A specific aim of the full-scale crushing test was to verify whether relations known from research into finer aggregates produced using more than one crushing stage are valid also for large-size aggregates produced from primary crushing. For several parameters, the jaw crusher results corresponded well to known relations from research on other crusher types and smaller aggregate sizes:

- A reduced feed rate results in a steeper PSD curve and increased flakiness for lower sizes.
- Reduced speed results in a steeper PSD curve and increased specific energy consumption (SEC) (Figure 4.3).
- Including fines in the feed significantly improves particle shape.
- Single-graded feed produced poor particle shape.
- Mechanical tests show a clear improvement from sample preparation by laboratory crushing (Figure 4.4).

Figure 4.3 shows how the SEC increases when the lower size of the feed material ( $F_{10}$ ) increases. Likewise, lower closed side setting (CSS) leads to higher SEC. The crushing of coarser material requires a larger reduction rate, as does crushing with lower CSS. The relation between SEC and  $F_{10}$  at a set CSS is linear. When the crusher speed is reduced, the energy consumption during crushing increases.

Luke (2017) examined the relation between particle shape and mechanical properties for a subset of the samples from the jaw crusher tests. Luke measured flakiness index (FI) and shape index (SI) of both primary crushed and laboratory crushed 10–16 mm samples ahead of mechanical testing, and

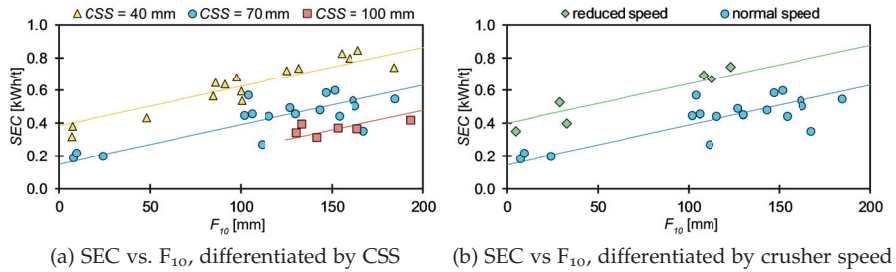


Figure 4.3: Specific energy consumption vs. lower size of feed material ( $F_{10}$ ), differentiated by CSS and crusher speed. Regression analysis combining SEC,  $F_{10}$ , CSS and speed:  $r^2 = 0.83$ .

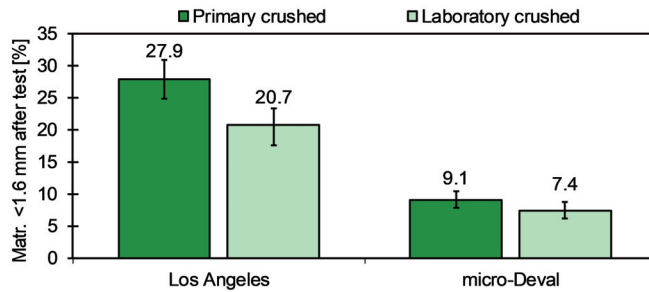


Figure 4.4: The impact of sample preparation by laboratory crushing on measured mechanical properties (average values). The error bars indicate maximum and minimum values for each data set ( $N = 38$  for each column).

found that differences in particle shape could be a possible explanation of the improved mechanical results for the laboratory crushed samples. The FI of primary crushed samples were 39 %, compared to 10 % for laboratory crushed samples, while SI changed from 55 % to 9 %. Los Angeles value was 29 % lower for laboratory crushed samples, and the micro-Deval value was reduced by 19 %, similar as in Figure 4.4. However, the analyses in Paper C showed that differences in FI for the primary crushed samples did not affect the two mechanical properties (Figure 4.5). These results imply that the improvement in mechanical properties after laboratory crushing happens because the crushing breaks the particles along internal flaws, which leaves more solid rock particles in the crushed product. To summarise, laboratory crushing leads to both improved particle shape and improved mechanical properties, but the improvement in mechanical properties is not caused by the shape improvement. These findings show that the measured mechanical properties are not purely intrinsic, but are affected by the production methods.

Some have argued that setting requirements for both Los Angeles and micro-Deval tests are redundant. No correlation was found between Los Angeles and micro-Deval test results in Paper C, showing that the two tests

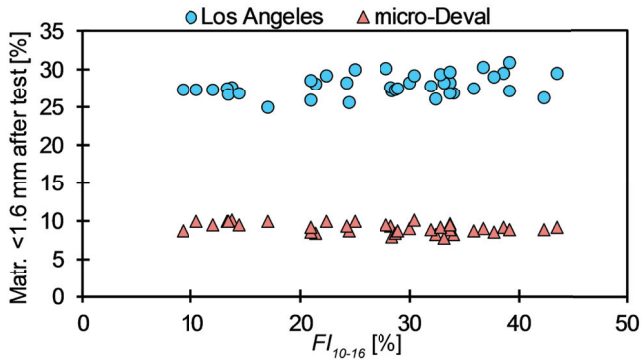


Figure 4.5: Mechanical properties vs. flakiness index for particles in the size range used in mechanical testing.

analyse separate properties. These considerations are, however, limited by the fact that only one rock type was analysed.

Particle shape measured as FI was the characteristic most affected by the changing feed and crusher parameters. Figure 4.6 shows how the flakiness of individual particle size fractions vary according to crusher setting, feed gradation, feed rate and crusher speed. Flakiness was found to have a maximum value in the 12.5–16 mm size range, and decrease with increasing particle size > 16 mm. This tendency was the same for all three CSS sizes. In this regard, the results are slightly different from previous research where an optimum particle shape has been found for particle sizes close to the CSS size. Particle shape varies greatly within the product gradation, and it is necessary to analyse individual size fractions to quantify the effects of changing feed and crusher parameters. The standard weighted-average FI calculation hides shape variations in the smaller particle sizes. Including fines in the feed significantly improved particle shape, and resulted in almost constant flakiness independent of particle size. Removing material < 100 mm from the feed resulted in a doubling of average FI for materials below the CSS size ( $FI_{<CSS}$ ). Removing all material below 180 mm increased  $FI_{<CSS}$  by a factor 3. The poor particle shape produced using low feed level and single-graded feed (180/400 mm) confirmed that inter-particle crushing is a prerequisite for cubical shape.

The efficiency of the crushing process was quantified as energy consumption per tonne of produced material, or specific energy consumption (SEC). The lowest SEC was found with high crusher speed, high CSS and a small lower feed size ( $F_{10}$ ). High CSS and small  $F_{10}$  involves a low reduction ratio, hence, less energy was needed for the crushing.

In road construction, a wide variety of gradations are allowed as long as general requirements for fines content and over- and undersize are fulfilled. The gradation will vary if the feed material to the crushing process varies, as Paper C showed. Due to the requirements for maximum fines content, a screening process must always be included in the production setup to ensure

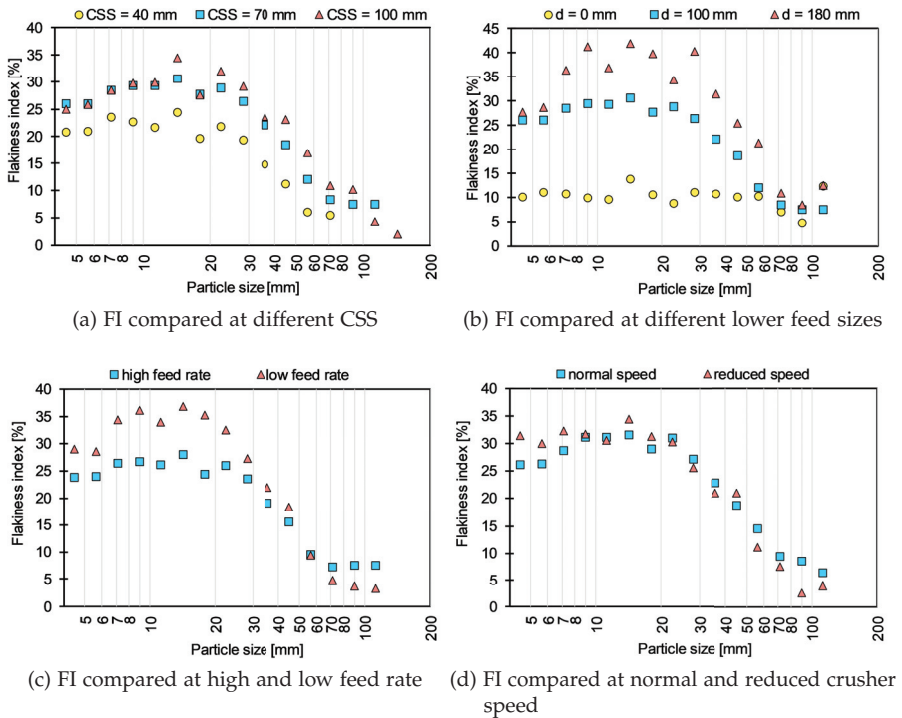


Figure 4.6: Particle shape measured as FI for individual particle size fractions.

a consistent product gradation. The main opportunity for quality optimisation from primary crushing is to ensure cubical particle shape by including fines in the crushing and ensuring continuous choke feeding. Because of the subsequent screening process, a higher fines content in the crushed product due to provisions to improve shape can be accepted. However, the fines removed by screening will in many cases be classified as waste. To ensure optimal utilisation of the available resources, a balance must be found between particle shape and fines content in the crushed product.

The multiple linear regression analysis proved to be a valuable tool for analysing the impact of feed and crusher parameters. Combining the analysis of several parameters at once increased the number of samples in each analysis, hence increasing the certainty of the regression analysis compared to if each parameter should be analysed separately.

A limitation of the research was that the tests were limited to a single rock type. The understanding of the relation between particle shape and mechanical properties would have been aided by the inclusion of more rock types with varying properties. Particle shape was consistently most flaky in the 12.5–16 mm size fraction. This size may be related to the mineral or crystal size in the tested rock type, and would possibly have varied if several rock types were tested.

The aim for the parameter study was to investigate whether previous research results regarding crusher operation and aggregate quality are valid also for a simple single-stage jaw crusher operation on large-size aggregates. The results show that crushing efficiency in terms of SEC and product quality in terms of particle shape and PSD can be controlled. The quality of construction aggregates can be optimised by adjustments to the production process, even for a single-stage crushing process. In order to improve mechanical properties, several crushing steps are needed.

#### 4.3 INFLUENCE OF GRADATION AND MOISTURE ON PAVEMENT PERFORMANCE

Papers D–F all investigated the influence of moisture and gradation on pavement response and performance from accelerated pavement test (APT) results. The common basis for all three papers was the three groundwater phases (w<sub>1</sub>–w<sub>3</sub>) and the resulting moisture variations in the pavement structures.

The moisture sensor registrations in Figure 4.7 show how the moisture transport through the structures differed due to the subbase gradation. In the open-graded 22/90 mm subbase structure, less moisture was stored in the subbase layer, and the transportation of water to the unbound base layer was much slower than through the 0/90 mm subbase. The subgrade beneath the structures reacted very promptly to the introduction of a groundwater table (GWT) in the transition between phase w<sub>1</sub> and w<sub>2</sub>. The subgrade sensor was located 15 cm above the w<sub>2</sub> GWT. Since there was only a very small increase in subgrade water content from phase w<sub>2</sub> to w<sub>3</sub>, the subgrade at this depth was almost fully saturated already in phase w<sub>2</sub>.

Key findings from each paper are summarised in the following sections. Paper D presents some selected measurements, while the full analysis and modelling of the APT data are gathered in Paper E and Paper F. A joint discussion of the implications of the results from all three papers can be found in section 4.3.4.

##### 4.3.1 *Paper D*

Paper D presents measurements conducted during the APT:

- Back-calculated falling weight deflectometer (FWD) measurements from the end of each groundwater phase
- Development of stress and strain in the subbase materials throughout APT
- Surface rut development

The raised GWT was clearly affecting the FWD measurements (Figure 4.8), because the deflection increased from phase to phase, expressing a weakening of the structures. The weakening was seen for both structures, although

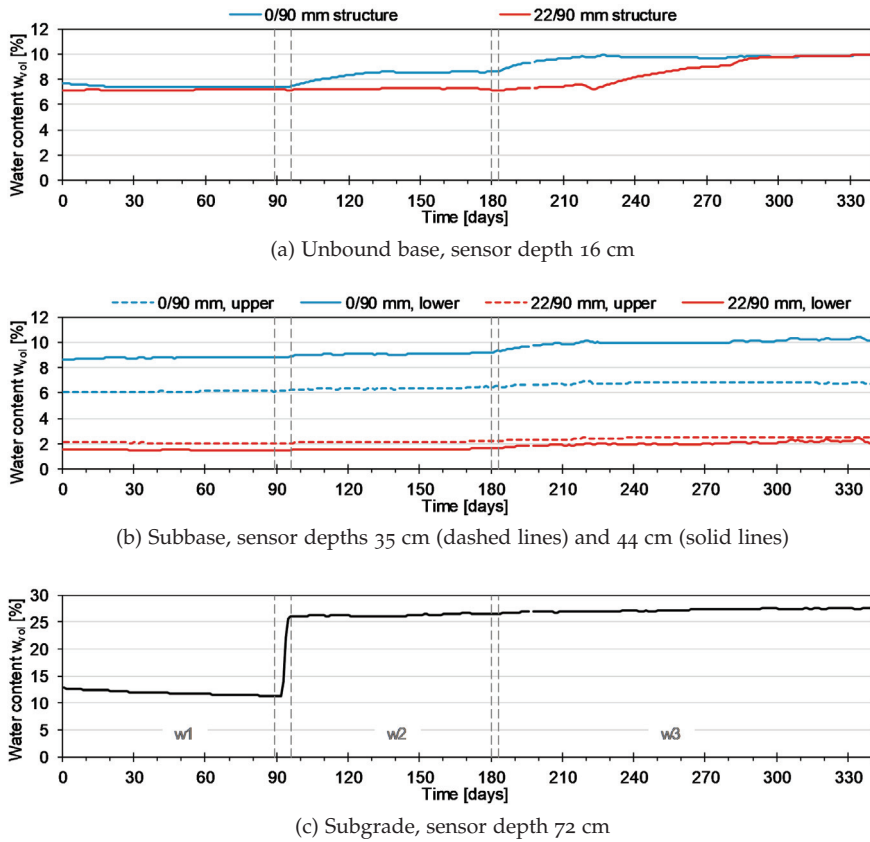


Figure 4.7: Registered volumetric water content from sensors in unbound base, subbase and subgrade during APT. Start and end of groundwater adjustment periods indicated by vertical dashed lines.

the reaction was more pronounced for the 0/90 mm structure. The back-calculation of material stiffness for unbound layers was related to water content at the time of FWD measurements. The 22/90 mm structure showed less increase in water content compared to the 0/90 mm structure, and showed less reduction in stiffness from phase to phase.

Figure 4.9 displays the development of induced vertical stress and strain as a function of load repetitions at three levels in the subbase layers. Vertical stress was registered by soil pressure cells (SPCs), while strain measuring units ( $\epsilon$ MUs) registered vertical strain. The initial measurements were made at 20 000 load repetitions, after the initial pre-loading phase. The stress level (Figure 4.9a) increased gradually as more load repetitions were added, while it decreased at each GWT raise. The gradual increase can be explained as a stiffening of the subbase materials due to compaction from traffic. The immediate stress decreases as GWT was raised indicated that the materials were weakened by the introduction of water into the test pit.

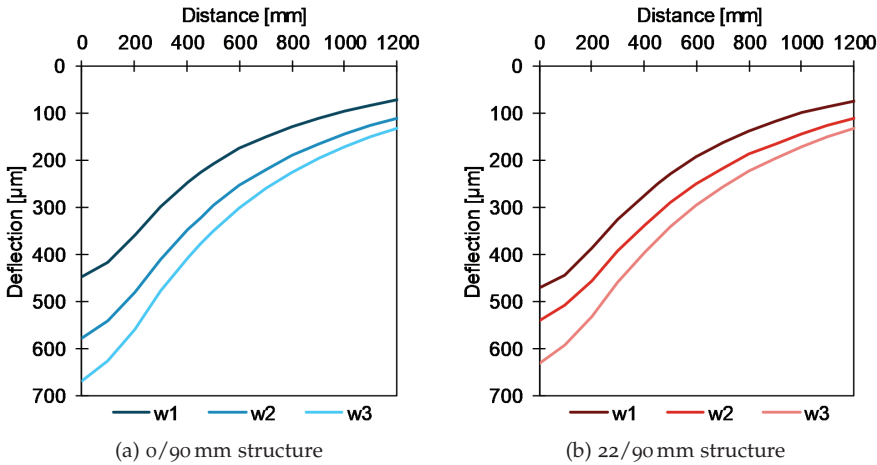


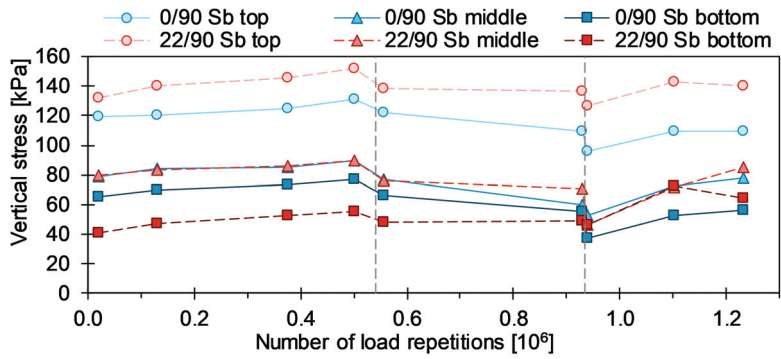
Figure 4.8: Back-calculated deflection from FWD, adjusted to 10 °C.

The strain development in the subbase layers is shown in Figure 4.9b, and follows similar trends as the stress development.  $\epsilon$ MUs registered an increase in strain as traffic load was applied, indicating a gradual weakening of the structures at the same time as the stress sensors showed gradually increased stress indicating strengthening. The immediate decrease in strain as GWT was raised was not expected. It indicates a stiffening of the structures, which disagrees with both the stress registrations and the FWD results. No explanation was found for these conflicting results in Paper D. Comparing the registered strain signals from the start of each GWT phase, there is no difference between phase w1 and w2, while the strain increases by 60–70 % in phase w3. The analysis was somewhat inhibited by the lack of data from phase w2, where stress and strain were registered only at the beginning and end of the phase, and the development between the endpoints is unknown.

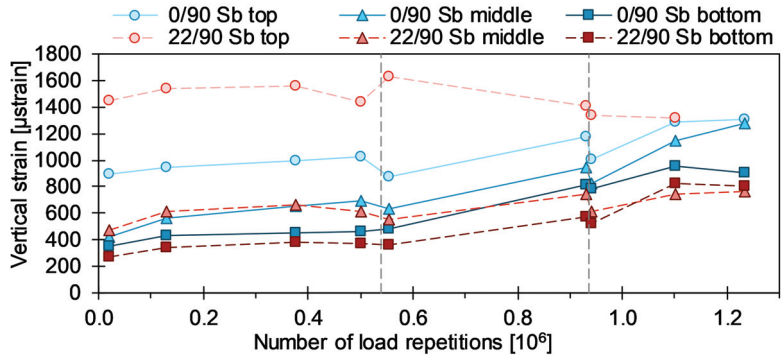
Figure 4.10 shows the surface rut development as a function of load repetitions. A post-compaction tendency can be seen in the initial phase, while the later rut development fits linear trends. The rutting accelerates considerably as GWT is introduced to the upper part of the structure. Even though the structures responded differently to the GWT increases, both reached a maximum rut rate of about 2.7 mm per 100 000 load repetitions in phase w3, and similar rut depth ( $\approx 19$  mm) when the test was finished after 1 233 000 load repetitions.

#### 4.3.2 Paper E

In Paper E, the response behaviour of the pavement structures was modelled based on FWD measurements and stress and strain registrations. Three specific hypotheses were formulated for Paper E:



(a) Vertical stress measured by SPCs



(b) Vertical strain measured by εMUs

Figure 4.9: Development of induced vertical stress and strain at three levels in the two subbase layers during APT. Vertical dashed lines indicate GWT raises.

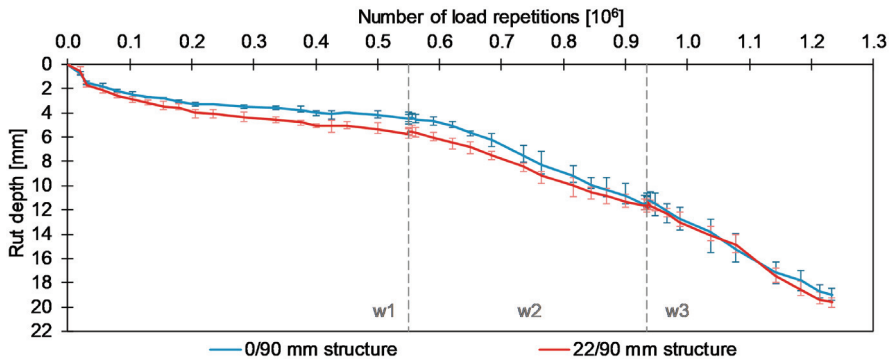


Figure 4.10: Rut development during APT. Each line represents the average of three laser profiles; error bars show max/min measurements. Dashed vertical lines indicate GWT phase transitions.

1. The choice between open-graded and well-graded subbase material has no significance for the long-term pavement performance as long as material properties fulfil set requirements
2. An open-graded subbase material is less affected by moisture changes than a well-graded subbase material
3. Existing models fit better to well-graded materials than open-graded large-size materials

Paper D showed conflicting results regarding the development of stress and strain immediately as GWT was raised. To avoid these concerns, the response modelling was based on the measured stress and strain at the end of each GWT phase. At the end of the phases, the structures had received post-compaction from traffic, and the measurements were assumed not to be affected by any transition effects due to the GWT change. Furthermore, using data from the end of the phases ensured that the water content had reached a stable level.

The stress and strain data from Paper D were supplemented by vertical strain registrations from unbound base and subgrade, and measurements of longitudinal and transversal strain at the bottom of asphalt concrete (AC) layers. For the 0/90 mm structure, the vertical strain for all sensors increased with increasing GWT. For the 22/90 mm structure, on the other hand, the strain increased in the subgrade and lower levels of the subbase, while it decreases in the unbound base and top of the subbase. This may indicate that for the 22/90 mm structure, the lower layers were weakened by the increased GWT, while the upper layers were more affected by the post-compacting effect from traffic. This was an effect of the reduced water transporting ability of the open-graded material. In the subgrade, the strain levels increased from  $w_1$  to  $w_2$ , but were similar for phase  $w_2$  and  $w_3$ .

Two alternative response models were developed:

- A linear elastic (LE) model based on FWD
- A non-linear elastic (NLE) model based on vertical strain registrations from  $\epsilon_{MU}$

Vertical stress and vertical and tensile strain calculated from the response models were compared to sensor registrations. Figure 4.11 shows the fit of the two response models to measured vertical strain as a function of depth, while Figure 4.12 shows corresponding results for vertical stress. The NLE model was built on the vertical strain measurements, so naturally, the modelled strain fitted very well to the measured strain. The LE model underestimated both vertical strain, tensile strain and vertical stress, where the underestimation was highest for the vertical strain. The LE model did, however, provide a better fit to the stress distribution in the 22/90 mm subbase than the NLE model. The poor fit of the LE model shows that the unbound materials should be considered stress sensitive. The NLE model overestimated the tensile strain at the bottom of the AC layers, both longitudinal and transversal, while

the vertical stress in the subbases was underestimated. There were large variations in the tensile strain registrations, making the models' fit hard to interpret. Both models calculated a decrease in stress for both structures as GWT was raised, and both models showed a larger decrease for the 0/90 mm structure than the 22/90 mm structure. The measured stress did not support such clear trends, especially for the 22/90 mm structure where the lowest stress at all subbase levels was found in phase w2.

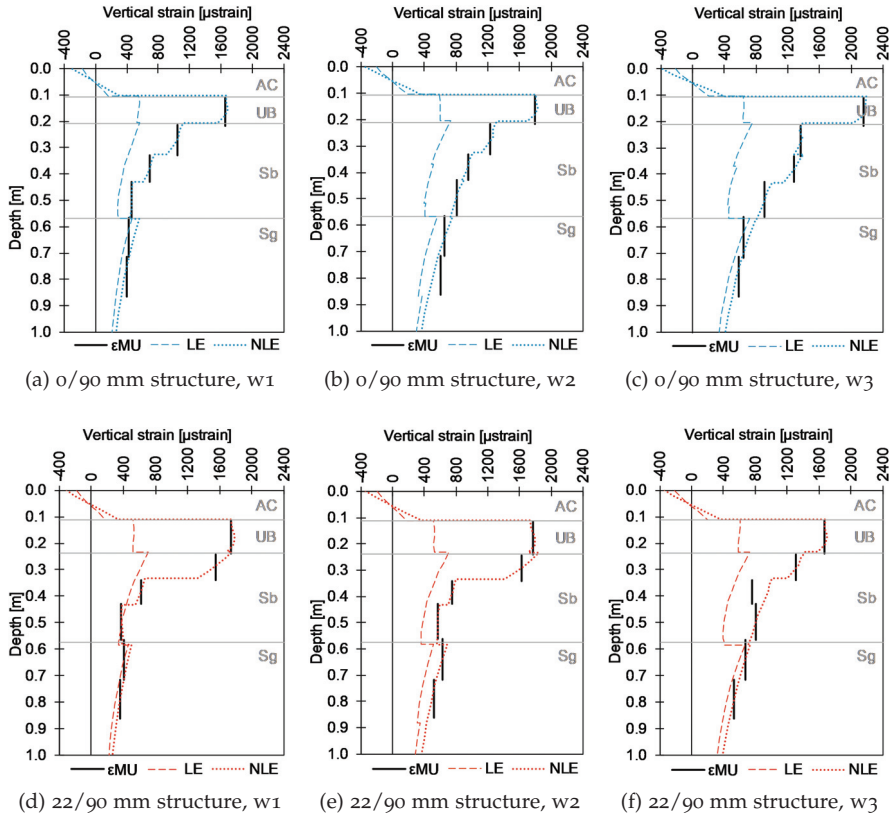


Figure 4.11: Comparison between measured and modelled induced vertical elastic strain as a function of depth at the end of each groundwater phase. w1 – 500 000 load repetitions; w2 – 930 000; w3 – 1 233 000. Horizontal lines indicate layer boundaries.

Vertical strain was measured through all unbound layers including subgrade, while vertical stress was only measured in the subbase. Hence, the strain registrations in Figure 4.11 gave a more reliable comparison between modelled and measured values as a function of depth.

The APT results showed that the influence of moisture was far superior to the influence of the difference in gradation between the two structures. Both structures proved to be durable, and neither structure showed any sign of breakdown due to the traffic or flooding. On this general level, the

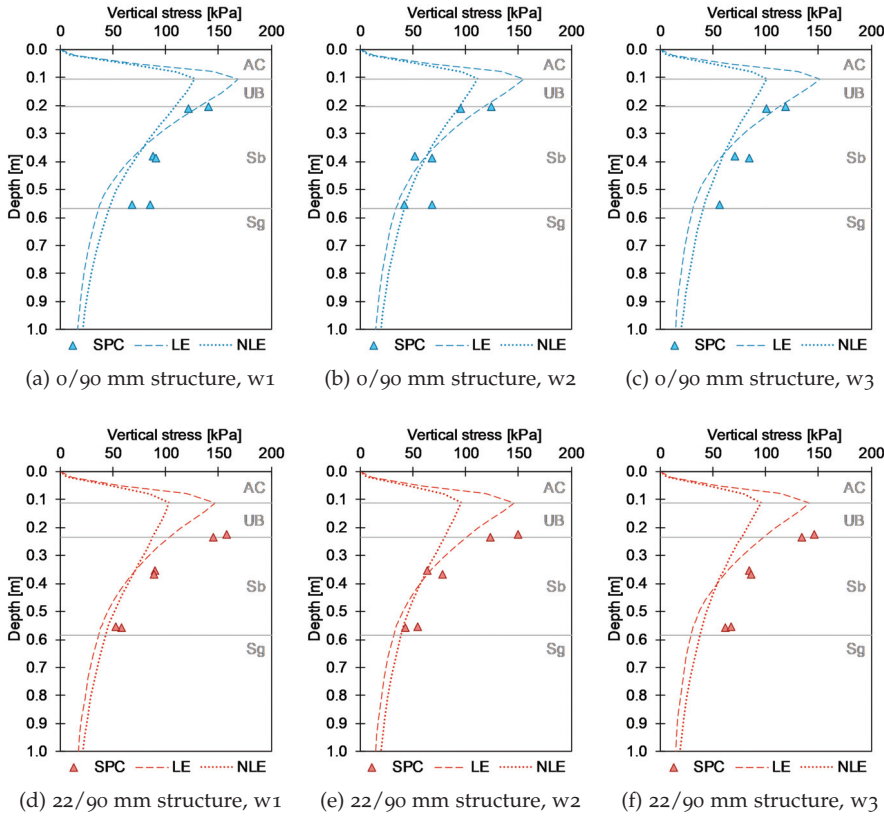


Figure 4.12: Comparison between measured and modelled induced vertical stress as a function of depth at the end of each groundwater phase. w1 – 500 000 load repetitions; w2 – 930 000; w3 – 1 233 000. Horizontal lines indicate layer boundaries.

first hypothesis is confirmed, in that as long as the pavement structure is constructed of strong materials with a controlled fines content and compacted well, the difference in gradation has little impact on the long-term pavement performance.

The APT analysis identified clear differences in the response of the two pavement structures, most notably in their response to the raising GWT. The increase in water content is both lower and slower in the open-graded structure. Both vertical strain and longitudinal tensile strain increases more in the well-graded structure as GWT is raised to the highest level. These findings confirm hypothesis 2, although the effect on the overall structure through accumulated permanent deformations is similar between the structures.

Hypothesis 3 was evaluated based on the models’ fit to the response behaviour of the two structures. The effect is most evident for the modelling of stress, where both LE and NLE models provide a reasonable fit for the 0/90 mm structure, while both models underestimate the stress level in the

22/90 mm structure. For vertical and tensile strain, the differences between models are more clear than the difference between the models' fit to each structure. Hence, no clear conclusion can be drawn regarding hypothesis 3.

#### 4.3.3 Paper F

In Paper F, the permanent deformation behaviour of the tested structures was modelled as a function of load repetitions and moisture conditions. The accumulation of permanent deformations under different moisture conditions was calculated by two models and compared to measured surface rutting. As both permanent deformation models selected for Paper F calculated permanent strain from resilient strain in each layer, a reliable estimation for resilient strain as a function of depth was required. The NLE response model from Paper E was chosen, as this model was based on the measured traffic-induced strain, and replicated the resilient strain very well.

Data for permanent deformations in each layer was collected by static  $\epsilon_{MU}$  registrations. Figure 4.13 shows how the modelled permanent deformation for each layer fits to the measured permanent deformation. The black  $\Sigma$  lines represent the sum of the UB, Sb and Sg lines in each figure. The time-hardening approach proved successful in implementing changing moisture conditions, as both permanent deformation models identified the acceleration of permanent deformations as GWT was raised.

Figure 4.14 compares the total permanent deformations from both models to the measured rut depth at the pavement surface of both structures. Here, modelling of the uninstrumented subgrade is included in addition to the data from Figure 4.13. Neither model was able to replicate the linear rut development measured on the surface for phase w2 and w3. For the 22/90 mm structure, both models overestimated the rut development in phase w2, which lead to a general overestimation of the rut depth also in phase w3 for the MEPDG model.

Cross-sections of the rut profile is shown in Figure 4.15, where the modelled profiles are compared to the measured surface rut profiles at the end of each groundwater phase. The RE model provides a very good fit to the overall shape of the rut profile, calculating a narrower rut profile than the MEPDG model.

The analysis in Paper F proved that the RE model (Equation 3.3) could be adjusted for moisture variations using a linear water content relationship. The RE model generally provided a simpler moisture dependency calculation compared to the MEPDG model. For the MEPDG model, the calculation of moisture dependency suggested by ARA Inc. (2004) was not sufficient to cover the acceleration in permanent deformation between GWT phases. However, a moisture dependency relationship for the open-graded subbase material could not be established for the RE model.

The subgrade deformation constituted a significant part of the total rut depth, showing that knowledge of the subgrade soil is essential to achieve a reliable modelling result. The MEPDG model required significant adjustments

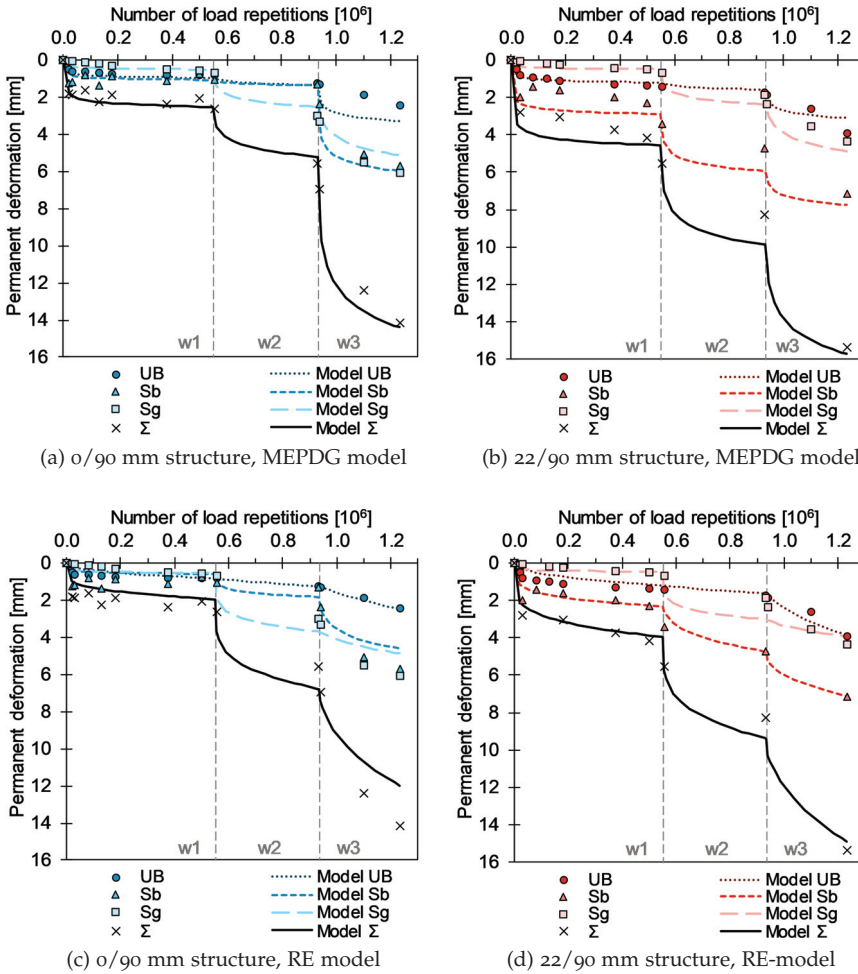


Figure 4.13: Modelled and measured permanent deformations for unbound base (UB), subbase (Sb) and upper 15 cm of subgrade (Sg). Dashed vertical lines indicate GWT phase transitions.

in order to obtain reasonable deformation values for the uninstrumented subgrade. Without reduction of the calibration factor  $\beta_1$ , the MEPDG model calculated deformation values of the same magnitude as the surface rut (20 mm) from the uninstrumented subgrade alone. The RE model calculated a reasonable estimation of the subgrade deformations using only the established water content relations without need for adjustments to fit the surface rut profile.

Paper F clearly showed how increased moisture impacted the pavement performance. Increasing GWT accelerated the accumulation of permanent deformations in all unbound layers. The fact that both structures showed similar rut development throughout the test showed that gradation was of

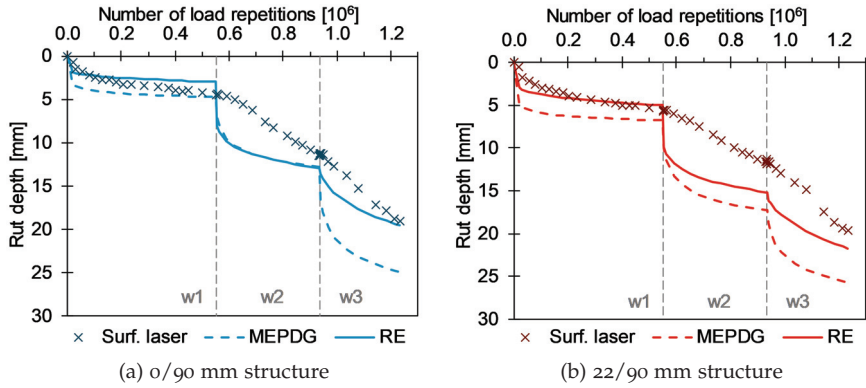


Figure 4.14: Modelled rut development compared to surface laser measurements. Dashed vertical lines indicate GWT phase transitions.

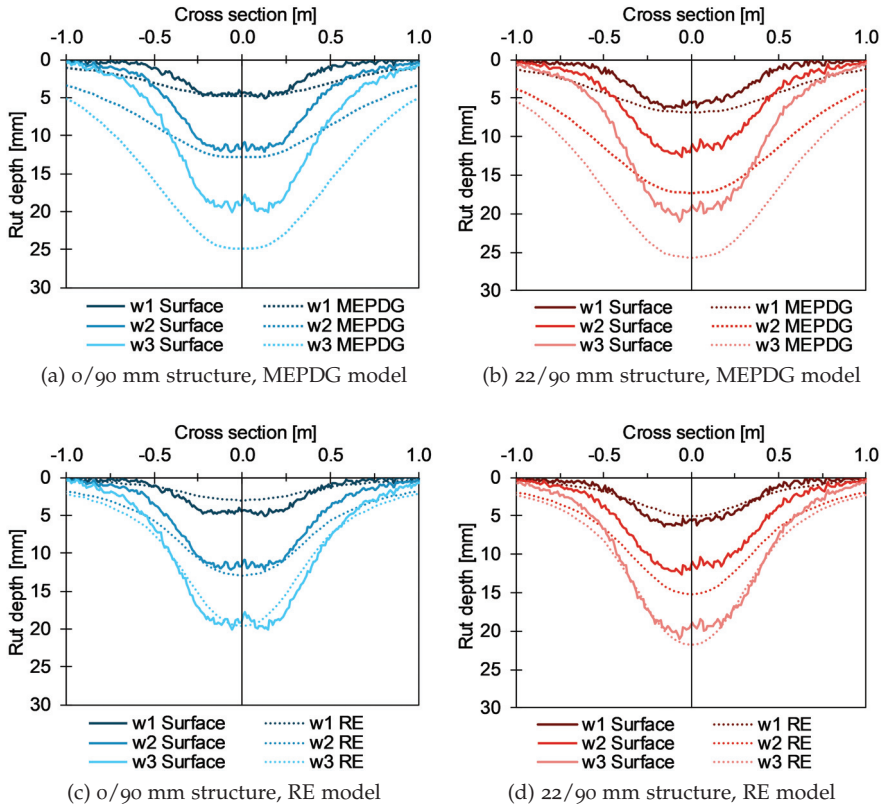


Figure 4.15: Modelled and measured rut profiles at the end of each groundwater phase (550 000, 935 000 and 1 233 000 load repetitions).

less importance for the overall pavement performance. These results were likely governed by the high degree of compaction of the unbound materials achieved during construction.

The new RE model was very well suited for cross-sectional calculation of rut development from full-scale testing, and the RE model was also easily and reliably adapted to changing moisture conditions.

#### 4.3.4 *Joint discussion for papers D–F*

The APT provided a solid basis for analysing the influence of gradation and moisture on pavement response and performance. The accelerated traffic corresponded to an AADT of 3000 vehicles over a design lifetime of 20 years, assuming 10 % heavy vehicles. For this amount of traffic, the observed rut depth of up to 20 mm is small, proving both structures durable. The results should not be directly compared to a pavement structure in regular operation, as major degrading factors such as temperature variations, frost and studded tyres are missing. The moisture levels were adjusted in the APT, but a road in operation experiences much more rapid moisture fluctuations.

The GWT levels employed in the APT represented three possible moisture states experienced by a pavement structure in operation:

- w1: A moist condition with the GWT far below the pavement surface.
- w2: A wet condition where the pavement drainage system keeps the GWT at the maximum designed level.
- w3: A flooded condition where the pavement drainage system is unable to keep GWT away from the pavement structure, and some pavement materials become saturated.

By applying an APT instead of laboratory methods, the water content in the pavement structures could not be controlled directly. Instead, the water content in all unbound materials changed as an effect of the increased groundwater levels. This provided the opportunity to analyse the moisture behaviour of the complete pavement structures instead of the individual pavement materials. By using the same subgrade and unbound base materials in both structures, the influence of subbase gradation was clearly visible.

Stress measurements showed an immediate decrease in stress as GWT was raised, which could be explained as a weakening caused by lubrication of particle contact points. However, both vertical and tensile strain sensors showed a decrease in strain at the same time as stress decreased, indicating a structural strengthening which does not fit the lubrication explanation. The moisture registrations did not support the immediate changes in stresses and strains, particularly in the transition between w2 and w3, where no changes in water content were seen by the time of the first response measurement in phase w3.

A drawback in the analyses was the lack of response data from phase w2, where at least two intermediate response measurements were planned, but

unfortunately not conducted due to misunderstandings. More data from this phase could possibly have helped interpret the conflicting stress and strain development. Furthermore, additional data from phase w2 could have improved the permanent deformation modelling, where the models overestimated the rut development from that phase.

The time-hardening approach succeeded in implementing both lateral wander and changing moisture conditions for both permanent deformation models. The new RE model was very well suited for cross-sectional calculation of rut development from full-scale testing, and easily adaptable to changing moisture conditions.

For the tested pavement structures, the influence of moisture had more effect than gradation on pavement response and performance. The raised GWT from w1 to w3 caused the rutting rate to increase by factor 5 for the open-graded structure, and factor 6 for the well-graded structure. Both subbase materials complied with requirements for pavement materials which are designed to ensure that the materials are not moisture susceptible. For more extreme variation in gradation, i.e. higher fines content for the well-graded material, the influence of gradation would likely have been more pronounced as moisture increased.

#### 4.4 GENERAL FINDINGS

In the research presented here, production methods and pavement performance were mainly related through the considerations regarding gradation of subbase materials. In the production of 0/90 mm material for the APT, the 22/90 mm material had to be mixed with 0/32 mm material at a 1:1 weight ratio. The weight ratio shows how much high-quality aggregate material potentially is wasted by using 22/D as the most common material instead of 0/D. There is great potential for increased utilisation of aggregate resources within the current requirements for pavement materials. As long as the fines content is controlled, using all-in materials such as 0/90 mm does not diminish pavement performance.

In the standard for unbound aggregates, LA results are divided into categories in increments of 5 points (EN 13242, 2007). Thus, an improvement in LA value from 27.9 to 20.7 due to sample preparation as found in Paper C would classify the material a category higher. A change of this magnitude would have impact on which applications the material would be allowed for. Such changes could have large impact on materials which are close to a limit for quality requirements.

For optimal utilisation of aggregate resources, it is vital that material choices are compared on equal basis, that is, with equal sample preparation. By using several crushing steps, the mechanical properties can to some extent be enhanced, but this is governed by the intrinsic properties of the rock material. Regardless of material properties, a durable pavement structure relies on construction procedures that ensure homogeneity and proper compaction.

Although pavement structures may be designed with a load distribution that allows weaker materials to be used in lower layers, all materials must still be strong enough to withstand the construction process. For weaker materials, abrasion and fragmentation during transport, handling and construction traffic may lead to increased fines content. Degradation during the construction period can be a limiting factor for utilisation of weaker materials.

A local aggregate resource classified at the wrong side of the required specification can have large impact on the mass balance and sustainability of a construction project. Pavement design methods should allow for adaptation of the design to local materials if that would increase the sustainability of the construction projects. To enable such adaptations, a transition from empirical to analytical pavement design systems is needed.

The development of analytical pavement design systems are challenging, not least because of the extensive efforts needed for calibration. Analytical methods are still at the mechanistic-empirical stage, and not purely mechanistic. Field and laboratory testing is required to obtain reliable calibration data for the response and distress models. Extensive test programmes for large-size aggregates are very demanding, because the particle size requires large samples and there are few suitable test methods.

Although the research presented in the papers are related to international literature and methods, there is no doubt that the topic of this thesis is more relevant in Norway than in other countries. Road construction in scarcely populated areas, with easier access to tunnels and road cuts than established quarries is a hallmark of the Norwegian road construction industry. In this kind of local engineering issues, we cannot lean on the international research community to fill our knowledge gaps. That does, however, not mean that the findings are not relevant also for the international research community.

Increased concern for sustainability and environmental issues related to construction has resulted in great interest in the utilisation of local aggregate resources. These issues could advocate for increased research interest for pavement materials and particularly the implications of using poorer qualities than the traditional requirements permit.



## CONCLUSIONS AND FURTHER WORK

---

This chapter summarises the conclusions from the research in section 5.1, suggests continuation in section 5.2, and outlines possibilities and needs for further research in section 5.3 .

### 5.1 CONCLUSIONS

High-quality aggregate resources are limited and non-renewable, and using the right quality for the right purpose is the first step to optimal utilisation. A bottom-up perspective where a construction project is planned based on available local resources should be employed. Instead of designing a pavement structure first and then finding suitable materials, the structures should be designed to utilise the local resources. To achieve this, a change from empirical to analytical pavement design systems is needed. The bottom-up perspective can reduce both aggregate transport and waste generation from construction sites. Utilising local aggregate resources limit the need for new quarried materials and contribute to a more sustainable construction sector.

The novelty value of this thesis lies in the improved understanding of large-size aggregates. To enable the development of an analytical pavement design system for Norway, the performance of typical road materials under realistic loading conditions must be understood. The results in this thesis provide inputs for the development of a new pavement design system, where material models must be calibrated to Norwegian conditions, including typical Norwegian pavement materials. The transition from empirical to analytical pavement design requires extensive field and laboratory testing to obtain reliable calibration data. The research presented in this thesis are examples of such data collection.

Conclusions related to each research question (RQ) are highlighted in the following:

**RQ1** How does the Norwegian practice for aggregate use, with large-size unbound aggregates in subbase and frost protection layers, differ from other countries?

The survey and literature study presented in Paper A and B showed that the construction practice of using large-size aggregates is uncommon outside the Nordic countries (mainly Norway, Sweden, Finland). The use of thin hot mix asphalt (HMA) layers implies that a substantial part of the bearing capacity is provided from unbound layers. The use of large-size aggregates is related to the availability of aggregate resources

and the massive pavement structures required for frost protection reasons.

- RQ2 How are large-size unbound aggregates currently described, specified, and quality assessed?

Large-size unbound aggregates are currently outside the scope of international standards, as Paper B shows. Because of this, the use of large-size aggregates must be specified by national requirements or individual construction clients.

Several standard quality assessment methods are not available or practically feasible for large-size aggregates. Some adapted test methods are described in the Norwegian standard for large-size aggregates. Paper A shows that aggregates are products in wide international trade, which suggests that an international standard for large-size aggregates is needed.

- RQ3 How do production methods affect the quality of large-size unbound aggregates?

The view of primary crushed aggregates as products has been missing from previous research on aggregate production. Particle shape is the property most affected by changes in the production method. The poor particle shape produced using low feed level and single-graded feed (180/400 mm) shows that inter-particle crushing is a prerequisite for cubical shape. Choke feeding is necessary to obtain inter-particle crushing and cubical particle shape.

Investigation of individual particle size fractions is necessary to understand the relation between crushing and particle shape. The standard weighted-average calculation of flakiness index (FI) for full gradations hides variation in shape for smaller particles.

Mechanical properties are not improved by improving particle shape, but laboratory crushing improved both particle shape and mechanical properties by breakage along flaws in the particles. Several crushing stages are needed to optimise mechanical properties.

The optimisation of the crushing process is a balance between particle shape, gradation (fines content) and specific energy consumption.

- RQ4 How does variation in characteristics of large-size unbound aggregates affect pavement performance?

Gradation was chosen as the main characteristic for this thesis, as the choice of gradation has large impact on resource utilisation. The analyses in Papers D–F all show that an open-graded subbase material (22/90 mm) is less affected by moisture changes than a well-graded subbase material (0/90 mm).

More effort is needed to obtain proper compaction of the open-graded material, hence, a higher rut development was observed for the 22/90 mm structure at the beginning of the accelerated pavement test (APT). As long as the design properties for pavement materials are fulfilled, e.g. fines content and stiffness following compaction, the two subbase materials tested in this thesis prove similar properties during loading. For well-compacted large-size pavement materials, gradation was of less importance for the accumulation of permanent deformations.

RQ5 How do changing moisture conditions affect the performance of large-size unbound aggregates?

Increased moisture levels in the pavement structures reduce the stiffness of the large-size aggregates, and accelerate the degradation of the pavement structures. In the comparison of two well-compacted pavement structures, the influence of moisture was far superior to the influence of the difference in gradation between the two structures. Introducing a groundwater table (GWT) in the subgrade 30 cm below the pavement structure accelerated permanent deformations in both pavement structures.

The accumulation of permanent deformations was modelled using two strain-based models. The influence of changing moisture conditions can be implemented in both models by using a time-hardening approach. Changing moisture conditions were most reliably implemented in the RE model.

The understanding of the consequences of climate changes for pavement structures is improved from the results presented in Paper E and Paper F.

Overall, the research has shown that the utilisation of aggregate resources in pavement structures have a clear potential for increase without compromising long-term pavement performance. There is room for optimisation of aggregate utilisation even within current quality requirements.

By changing the Norwegian road construction practice from using subbase materials such as 22/125 mm to all-in materials such as 0/90 or 0/125, more high-quality material will be utilised in pavement structures instead of being classified as waste. Utilising more of the available local resources can reduce the amount of aggregate transport, contributing to a reduced CO<sub>2</sub> footprint of the construction projects. All-in aggregates are already specified in the pavement design manual (Norwegian Public Roads Administration, 2018), so these effects can be gained without changes to the present requirements.

Adapting pavement structures to future climate changes leads to more reliable and resilient infrastructure. Making efforts for optimal utilisation of available aggregate resources will reduce the consumption of non-renewable resources. By using more local resources, the aggregate transport can be reduced, which will reduce the carbon footprint of the construction projects.

Combined, these effects will help ensure a more sustainable infrastructure development.

## 5.2 POSSIBILITIES FOR CONTINUATION OF THE RESEARCH

During both full-scale tests, more material or data was obtained than was possible to analyse within the scope and time frame of this thesis. The material and data described below are collected, stored and available for analysis, and should be utilised in further research.

- The full-scale crushing test
  - 31.5–63 mm material from all crushing tests, originally intended to evaluate the development of a new coarse Los Angeles test.
  - Jaw crusher feed, product and operation data presented in Paper C can be used to model jaw crusher performance.
- The accelerated pavement test
  - Response data from tests with varying wheel load.
  - Response data from tests with varying tyre pressure.
  - Response data from tests covering the full lateral wander of the loading wheel.

This material and data can be prepared for continued research in new students' theses in cooperation with the original authors.

## 5.3 FUTURE RESEARCH NEEDS

During the research design phase, many research methods were considered to answer the RQs. The use of laboratory methods instead of full-scale testing could have enabled more extensive testing, e.g. more than one material for each test. However, no laboratory tests were available which would not require some down-scaling of the test material. As the focus of this thesis was specifically on large-size aggregates, full-scale tests were preferred.

Research is needed to develop a test method for mechanical properties for large-size aggregates, especially resistance to fragmentation. Existing test methods are not suited for quality assessment of aggregate products where the product gradation does not include 10–14 mm particles.

To enable implementation of the requirements for digital image processing (DIP) suggested in NS 3468 (2019), a consistent method for relating area-based particle size distribution (PSD) from DIP to weight-based PSD from sieving must be established. Within this development, the processing tools for DIP must be able to analyse pictures from stockpiles where particles are overlapping and parts of particles can be hidden from view.

The present research gained general knowledge regarding the performance of large-size aggregates with two gradations under three moisture conditions.

To develop an analytical pavement design system, material data from diverse aggregate qualities and gradations are needed. Further testing with heavy vehicle simulator (HVS), falling weight deflectometer (FWD) and multi-stage repeated load triaxial (MSRLT) is needed to obtain this data.

Although the pavement structures in the APT was tested under three different moisture conditions, the test does not replicate the fluctuating moisture conditions experienced by a pavement structure in operation. Future research should involve instrumented field tests to measure pavement response under realistic moisture fluctuations.

The research in this thesis has not involved freezing and thawing. The choice between an open-graded and a well-graded aggregate will influence the frost properties of the pavement structure. The knowledge regarding the influence of gradation and moisture conditions must be related to research on frost properties of large-size aggregates to find combinations of moisture and frost related properties that will ensure long service life for pavements affected by seasonal frost.

Another issue not covered by the present research is the impact of increased axle loads and tyre pressure. Data was gathered for some variations and can be analysed in the future. A future analytical pavement design system must be able to implement all combinations of traffic loads, moisture conditions and material properties.



## BIBLIOGRAPHY

---

- Ahlvin, R. G. (1991). *Origin of developments for structural design of pavements*. US Army Corps of Engineers. Retrieved from <https://apps.dtic.mil/dtic/tr/fulltext/u2/a245673.pdf>
- Ahmed, A. W. (2014). *Mechanistic-Empirical Modelling of Flexible Pavement Performance - Verifications Using APT Measurements* (Doctoral dissertation, Royal Institute of Technology, Stockholm, Sweden). Retrieved from <http://urn.kb.se/resolve?urn=urn:nbn:se:vti:diva-6950>
- Ahmed, A. W., & Erlingsson, S. (2015). Evaluation of a permanent deformation model for asphalt concrete mixtures using extra-large wheel-tracking and heavy vehicle simulator tests. *Road Materials and Pavement Design*, 16(1), 154–171. doi:10.1080/14680629.2014.987311
- Amorim, S. I., Pais, J. C., Vale, A. C., & Minhoto, M. J. (2015). A model for equivalent axle load factors. *International Journal of Pavement Engineering*, 16(10), 881–893. doi:10.1080/10298436.2014.968570
- ARA Inc. (2004). *Guide for the Mechanistic-Empirical Design of New and Rehabilitated Pavement Structures, Final report, NCHRP 1-37A*. Transportation Research Board of the National Academies. Washington DC, USA. Retrieved from <http://onlinepubs.trb.org/onlinepubs/archive/mepdg/guide.htm>
- Bengtsson, M. (2009). *Quality-Driven Production of Aggregates in Crushing Plants* (PhD thesis, Chalmers University of Technology).
- Bhadani, K., Asbjörnsson, G., Hulthén, E., & Evertsson, C. M. (2020). Development and implementation of key performance indicators for aggregate production using dynamic simulation. *Minerals Engineering*, 145, 106065. doi:10.1016/j.mineng.2019.106065
- Briggs, C., & Evertsson, C. M. (1998). Shape potential of rock. *Minerals Engineering*, 11(2), 125–132. doi:10.1016/S0892-6875(97)00145-3
- Cary, C. E., & Zapata, C. E. (2011). Resilient Modulus for Unsaturated Unbound Materials. *Road Materials and Pavement Design*, 12(3), 615–638. doi:10.1080/14680629.2011.9695263
- Charlier, R., Horny, P., Sršen, M., Hermansson, Å., Bjarnason, G., Erlingsson, S., & Pavšič, P. (2009). Water Influence on Bearing Capacity and Pavement Performance: Field Observations. In A. R. Dawson (Ed.), *Water in road structures* (pp. 175–192). doi:10.1007/978-1-4020-8562-8\_8
- Cleary, P., Sinnott, M., Morrison, R., Cummins, S., & Delaney, G. (2017). Analysis of cone crusher performance with changes in material properties and operating conditions using DEM. *Minerals Engineering*, 100, 49–70. doi:10.1016/j.mineng.2016.10.005
- Cook, C. S., Tanyu, B. F., & Yavuz, A. B. (2017). Effect of Particle Shape on Durability and Performance of Unbound Aggregate Base. *Journal of Materials in Civil Engineering*, 29(2), 04016221. doi:10.1061/(ASCE)MT.1943-5533.0001752
- CWA 17089. (2016). *Indicators for the sustainability assessment for roads CWA 17089:2016*. Brussels, Belgium: European Committee for Standardization.
- Danielsen, S. W., & Kuznetsova, E. (2015). Environmental Impact and Sustainability in Aggregate Production and Use. In G. Lollino, A. Manconi, F. Guzzetti, M.

- Culshaw, P. Bobrowsky, & F. Luino (Eds.), *Engineering geology for society and territory - volume 5* (Vol. 5, pp. 41–44). doi:10.1007/978-3-319-09048-1\_7
- Dawson, A. R. (2008). Rut Accumulation and Power Law Models for Low-Volume Pavements under Mixed Traffic. *Transportation Research Record: Journal of the Transportation Research Board*, 2068(1), 78–86. doi:10.3141/2068-09
- Dawson, A. R., & Mundy, M. (1999). Construction with Unbound Road Aggregates in Europe (COURAGE) - Final report. European Commission. Retrieved from <https://trimis.ec.europa.eu/sites/default/files/project/documents/couragefrep.pdf>
- Directorate of Mining. (2019). *Harde fakta om mineralnæringen - mineralstatistikk 2018*. Direktoratet for mineralforvaltning med Bergmesteren for Svalbard (DMF). Retrieved from <https://www.dirmin.no/harde-fakta-om-mineralnaeringen-mineralstatistikk-2018>
- Ekblad, J., & Isacsson, U. (2006). Influence of Water on Resilient Properties of Coarse Granular Materials. *Road Materials and Pavement Design*, 7(3), 369–404. doi:10.1080/14680629.2006.9690043
- Ekblad, J., & Isacsson, U. (2008). Influence of water and mica content on resilient properties of coarse granular materials. *International Journal of Pavement Engineering*, 9(3), 215–227. doi:10.1080/10298430701551193
- Eloranta, J. (1995). *Influence of crushing process variables on the product quality of crushed rock* (Doctoral dissertation, Tampere University of Technology, Tampere, Finland).
- Eloranta, J. (Ed.). (2009). *Crushing and Screening Handbook* (4th ed.). Tampere: Metso Minerals.
- EN 1097-1. (2011). *Tests for mechanical and physical properties of aggregates - Part 1: Determination of the resistance to wear (micro-Deval) EN 1097-1:2011*. Brussels, Belgium: European Committee for Standardization.
- EN 1097-2. (2010). *Tests for mechanical and physical properties of aggregates - Part 2: Methods for the determination of resistance to fragmentation EN 1097-2:2010*. Brussels, Belgium: European Committee for Standardization.
- EN 13242. (2007). *Aggregates for unbound and hydraulically bound materials for use in civil engineering work and road construction EN 13242:2002+A1:2007*. Brussels, Belgium: European Committee for Standardization.
- EN 13285. (2018). *Unbound mixtures - Specifications EN 13285:2018*. Brussels, Belgium: European Committee for Standardization.
- EN 933-1. (2012). *Tests for geometrical properties of aggregates - Part 1: Determination of particle size distribution - Sieving method EN 933-1:2012*. Brussels, Belgium: European Committee for Standardization.
- EN 933-3. (2012). *Tests for geometrical properties of aggregates - Part 3: Determination of particle shape - Flakiness index EN 933-3:2012*. Brussels, Belgium: European Committee for Standardization.
- EN 933-4. (2008). *Tests for geometrical properties of aggregates - Part 4: Determination of particle shape - Shape index EN 933-4:2008*. Brussels, Belgium: European Committee for Standardization.
- Erlingsson, S. (2012). Rutting development in a flexible pavement structure. *Road Materials and Pavement Design*, 13(2), 218–234. doi:10.1080/14680629.2012.682383
- Erlingsson, S., & Ahmed, A. W. (2013). Fast layered elastic response program for the analysis of flexible pavement structures. *Road Materials and Pavement Design*, 14(1), 196–210. doi:10.1080/14680629.2012.757558

- Erlingsson, S., & Rahman, M. S. (2013). Evaluation of Permanent Deformation Characteristics of Unbound Granular Materials by Means of Multistage Repeated-Load Triaxial Tests. *Transportation Research Record: Journal of the Transportation Research Board*, 2369(1), 11–19. doi:10.3141/2369-02
- European Aggregates Association. (2020). *Annual review 2018-2019*. Union Européenne des Producteurs de Granulats (UEPG). Brussels, Belgium. Retrieved from <http://www.uepg.eu/uploads/Modules/Publications/uepg-annual-review-2018-2019.pdf>
- Evertsson, C. M. (2000). *Cone crusher performance* (Doctoral dissertation, Chalmers University of Technology).
- Gidel, G., Hornych, P., Breyse, D., & Denis, A. (2001). A new approach for investigating the permanent deformation behaviour of unbound granular material using the repeated loading triaxial apparatus. *Bulletin des laboratoires des Ponts et Chaussées*, (233).
- Grønhaug, A. (1967). *Evaluation and influence of aggregate particle shape and forms*. Oslo.
- Gupta, A., & Yan, D. S. (2016). *Mineral processing design and operations: an introduction* (2nd ed.). Elsevier.
- Hansson, J., & Svensson, P. (2001). Stress distribution in unbound aggregate of road structure: influence of surface roughness and particle shape. *Bulletin of Engineering Geology and the Environment*, 60(3), 223–226. doi:10.1007/s100640100103
- Hicks, R. G., & Monismith, C. L. (1971). Factors influencing the resilient response of granular materials. *Highway research record*, (345). Retrieved from <http://onlinepubs.trb.org/Onlinepubs/hrr/1971/345/345-002.pdf>
- Hov, H. I., Kaas, C. G., Ødegaard, G. P., & Galaaen, J. S. (2019). *LCA-verktøy Kortreist stein (SteinLCA)*. Multiconsult. Retrieved from <https://www.sintef.no/globalassets/project/kortreist-stein/018-notat-beskrivelse-steinlca-endig.pdf>
- Huang, L., Bohne, R. A., Bruland, A., Jakobsen, P. D., & Lohne, J. (2015). Environmental impact of drill and blast tunnelling: life cycle assessment. *Journal of Cleaner Production*, 86, 110–117. doi:10.1016/j.jclepro.2014.08.083
- Huang, Y. H. (2012). *Pavement Analysis and Design* (2nd ed.). Pearson Education Inc.
- Jern, M. (2004). *The geological conditions for aggregate production, with special focus on blasting and fines production* (Doctoral dissertation, Chalmers University of Technology, Göteborg, Sweden).
- Johansson, M., Bengtsson, M., Evertsson, C. M., & Hulthén, E. (2017). A fundamental model of an industrial-scale jaw crusher. *Minerals Engineering*, 105, 69–78. doi:10.1016/j.mineng.2017.01.012
- Kim, D., Salgado, R., & Altschaeffl, A. G. (2005). Effects of Supersingle Tire Loadings on Pavements. *Journal of Transportation Engineering*, 131(10), 732–743. doi:10.1061/(ASCE)0733-947X(2005)131:10(732)
- Kolisoja, P. (1997). *Resilient deformation characteristics of granular materials* (Doctoral dissertation, Tampere University of Technology, Tampere).
- Korkiala-Tanttu, L. (2005). A new material model for permanent deformations in pavements. In *Proceedings of the international conferences on the bearing capacity of roads, railways and airfields*.
- Langer, W., Drew, L., & Sachs, J. (2004). *Aggregate and the Environment*. American Geological Institute. Retrieved from <http://agris.fao.org/agris-search/search.do?recordID=US201300100395>
- Lees, G. (1964). The Measurement of Particle Shape and Its Influence in Engineering Materials. *British Granite and Whinstone Federation Journal*, 4(2), 17–38.

- Legendre, D., & Zevenhoven, R. (2014). Assessing the energy efficiency of a jaw crusher. *Energy*, 74, 119–130. doi:10.1016/j.energy.2014.04.036
- Lekarp, F., & Dawson, A. R. (1998). Modelling permanent deformation behaviour of unbound granular materials. *Construction and Building Materials*, 12(1), 9–18. doi:10.1016/S0950-0618(97)00078-0
- Lekarp, F., Isacsson, U., & Dawson, A. R. (2000a). State of the Art. I: Resilient Response of Unbound Aggregates. *Journal of Transportation Engineering*, 126(1), 66–75. doi:10.1061/(ASCE)0733-947X(2000)126:1(66)
- Lekarp, F., Isacsson, U., & Dawson, A. R. (2000b). State of the Art. II: Permanent Strain Response of Unbound Aggregates. *Journal of Transportation Engineering*, 126(1), 76–83. doi:10.1061/(ASCE)0733-947X(2000)126:1(76)
- Li, T., & Baus, R. L. (2005). Nonlinear Parameters for Granular Base Materials from Plate Tests. *Journal of Geotechnical and Geoenvironmental Engineering*, 131(7), 907–913. doi:10.1061/(ASCE)1090-0241(2005)131:7(907)
- Lindholm, R. (2012). *A practical approach to sedimentology*. Springer Science & Business Media.
- Lindqvist, M., & Evertsson, C. M. (2003). Liner wear in jaw crushers. *Minerals Engineering*, 16(1), 1–12. doi:10.1016/S0892-6875(02)00179-6
- Luke, N. A. F. (2017). *Kornform og mekaniske egenskaper for et granodiorittmateriale etter testknusing og laboratorieknusing [Particle shape and mechanical properties for a granodiorite material after test crushing and laboratory crushing]* (Masters thesis, Norwegian University of Science and Technology, Trondheim, Norway). Retrieved from <http://hdl.handle.net/11250/2486074>
- Lytton, R. L., Uzan, J., Fernando, E., Roque, R., Hiltunen, D., & Stoffels, S. M. (1993). *Development and validation of performance prediction models and specifications for asphalt binders and paving mixes*. Washington DC, USA: Strategic Highway Research Program. Retrieved from <http://onlinepubs.trb.org/onlinepubs/shrp/SHRP-A-357.pdf>
- Mamlouk, M. (2006). Design of flexible pavements. In T. Fwa (Ed.), *The handbook of highway engineering* (pp. 8–1–8–35). CRC Press.
- Mineral Products Association. (2016). *The Mineral Products Industry at a Glance - 2016 edition*. London: Mineral Products Association. Retrieved from [https://mineralproducts.org/documents/Mineral%7B%5C\\_%7DProducts%7B%5C\\_%7DIndustry%7B%5C\\_%7DA%7B%5C\\_%7DA%7B%5C\\_%7DGlance%7B%5C\\_%7D2016.pdf](https://mineralproducts.org/documents/Mineral%7B%5C_%7DProducts%7B%5C_%7DIndustry%7B%5C_%7DA%7B%5C_%7DA%7B%5C_%7DGlance%7B%5C_%7D2016.pdf)
- Minitab. (2019). Minitab 19 Statistical software. Minitab LLC.
- Morrison, R., & Cleary, P. (2008). Towards a virtual comminution machine. *Minerals Engineering*, 21(11), 770–781. doi:10.1016/j.mineng.2008.06.005
- Norwegian Public Roads Administration. (2014). *Håndbok N200 Vegbygging [Manual N200 Road construction]*. Oslo, Norway: Statens vegvesen Vegdirektoratet. Retrieved from <http://hdl.handle.net/11250/2505119>
- Norwegian Public Roads Administration. (2018). *Håndbok N200 Vegbygging [Manual N200 Road construction]*. Oslo, Norway: Statens vegvesen Vegdirektoratet. Retrieved from [https://www.vegvesen.no/%7B%5C\\_%7Dattachment/2364236/binary/1269980](https://www.vegvesen.no/%7B%5C_%7Dattachment/2364236/binary/1269980)
- Norwegian Public Roads Administration. (2019). *Håndbok N100 Veg- og gateutforming [Manual N100 Road and street design]*. Statens vegvesen Vegdirektoratet. Retrieved from [https://www.vegvesen.no/%7B%5C\\_%7Dattachment/61414](https://www.vegvesen.no/%7B%5C_%7Dattachment/61414)
- NS 3468. (2019). *Coarse materials of stone for use in civil engineering works - Specification NS 3468:2019*. Lysaker, Norway: Standards Norway.

- Quist, J., & Evertsson, C. M. (2016). Cone crusher modelling and simulation using DEM. *Minerals Engineering*, 85, 92–105. doi:10.1016/j.mineng.2015.11.004
- Rada, G., & Witczak, M. W. (1981). *Comprehensive evaluation of laboratory resilient moduli results for granular material*. Retrieved from <http://onlinepubs.trb.org/Onlinepubs/trr/1981/810/810-004.pdf>
- Rahman, M. S. (2015). *Characterising the Deformation Behaviour of Unbound Granular Materials in Pavement Structures* (Doctoral dissertation, KTH Royal Institute of Technology, Stockholm, Sweden). Retrieved from <http://urn.kb.se/resolve?urn=urn:nbn:se:kth:diva-162277>
- Rahman, M. S., & Erlingsson, S. (2015). A model for predicting permanent deformation of unbound granular materials. *Road Materials and Pavement Design*, 16(3), 653–673. doi:10.1080/14680629.2015.1026382
- Rahman, M. S., & Erlingsson, S. (2016). Moisture influence on the resilient deformation behaviour of unbound granular materials. *International Journal of Pavement Engineering*, 17(9), 763–775. doi:10.1080/10298436.2015.1019497
- Rahman, M. S., & Erlingsson, S. (2019). Modelling permanent deformation behaviour of unbound granular materials. *Unpublished manuscript*.
- Räisänen, M., & Mertamo, M. (2004). An evaluation of the procedure and results of laboratory crushing in quality assessment of rock aggregate raw materials. *Bulletin of Engineering Geology and the Environment*, 63(1), 33–39. doi:10.1007/s10064-003-0218-1
- Rothery, K., & Mellor, S. (2007). *Crushing and screening*. Nottingham: The Institute of Quarrying.
- Ruuskanen, J. (2006). *Influence of rock properties on compressive crusher performance* (Doctoral dissertation, Tampere University of Technology).
- Saevarsdottir, T., & Erlingsson, S. (2013a). Effect of moisture content on pavement behaviour in a heavy vehicle simulator test. *Road Materials and Pavement Design*, 14(sup1), 274–286. doi:10.1080/14680629.2013.774762
- Saevarsdottir, T., & Erlingsson, S. (2013b). Water impact on the behaviour of flexible pavement structures in an accelerated test. *Road Materials and Pavement Design*, 14(2), 256–277. doi:10.1080/14680629.2013.779308
- Saevarsdottir, T., & Erlingsson, S. (2015). Modelling of responses and rutting profile of a flexible pavement structure in a heavy vehicle simulator test. *Road Materials and Pavement Design*, 16(1), 1–18. doi:10.1080/14680629.2014.939698
- Seneviratne, S., Nicholls, N., Easterling, D., Goodess, C., Kanae, S., Kossin, J., ... Zhang, X. (2012). Changes in climate extremes and their impacts on the natural physical environment. In C. Field, V. Barros, T. Stocker, D. Qin, D. Dokken, K. Ebi, ... P. Midgley (Eds.), *Managing the risk of extreme events and disasters to advance climate change adaptation. a special report of working groups i and ii of the intergovernmental panel on climatechange (ipcc)* (pp. 109–230). Cambridge, UK, Cambridge University Press. Retrieved from [https://www.ipcc.ch/site/assets/uploads/2018/03/SREX-Chap3%7B%5C\\_%7DFINAL-1.pdf](https://www.ipcc.ch/site/assets/uploads/2018/03/SREX-Chap3%7B%5C_%7DFINAL-1.pdf)
- Shergold, F. A. (1959). A study of the granulators used in the production of roadmaking aggregates.
- Sweere, G. T. (1990). *Unbound Granular Bases for Roads* (Doctoral dissertation, Technische Universiteit Delft, Delft). Retrieved from <http://resolver.tudelft.nl/uuid:1cc1c86a-7a2d-4bdc-8903-c665594f11eb>
- Szczelina, P. (2000). *Auslegung von Backenbrechern durch Modellierung des Körnerverhaltens* (Doctoral dissertation, Technische Universität Bergakademie Freiberg).
- Thom, N. (2008). *Principles of Pavement Engineering*. doi:10.1680/pope.34808

- Tseng, K.-H., & Lytton, R. L. (1989). Prediction of Permanent Deformation in Flexible Pavement Materials. In *Implication of aggregates in the design, construction, and performance of flexible pavements* (pp. 154–172). doi:10.1520/STP24562S
- United Nations. (2015). *Transforming our world: The 2030 agenda for sustainable development*. Retrieved from <https://sustainabledevelopment.un.org/post2015/transformingourworld>
- Uthus, L. (2007). *Deformation Properties of Unbound Granular Aggregate*. Trondheim: Norwegian University of Science et al. Retrieved from <http://hdl.handle.net/11250/231354>
- Uzan, J. (1985). Characterization of granular material. *Transportation research record*, 1022(1), 52–59. Retrieved from <http://onlinepubs.trb.org/Onlinepubs/trr/1985/1022/1022-007.pdf>
- Uzan, J. (1999). Granular Material Characterization for Mechanistic Pavement Design. *Journal of Transportation Engineering*, 125(2), 108–113. doi:10.1061/(ASCE)0733-947X(1999)125:2(108)
- Werkmeister, S. (2003). *Permanent deformation behaviour of unbound granular materials in pavement constructions* (Doctoral dissertation, Technischen Universität Dresden). Retrieved from <https://nbn-resolving.org/urn:nbn:de:swb:14-105224444109-42674>
- Werkmeister, S., Dawson, A. R., & Wellner, F. (2004). Pavement Design Model for Unbound Granular Materials. *Journal of Transportation Engineering*, 130(5), 665–674. doi:10.1061/(ASCE)0733-947X(2004)130:5(665)
- Werkmeister, S., Dawson, A. R., & Wellner, F. (2001). Permanent deformation behavior of granular materials and the shakedown concept. *Transportation Research Record*, 1757(1), 75–81.
- Wills, B. A., & Finch, J. (2015). *Wills' mineral processing technology: an introduction to the practical aspects of ore treatment and mineral recovery* (8th ed.). Butterworth-Heinemann.
- Wiman, L. G. (2001). *Accelerated load testing of pavements HVS-NORDIC tests in Sweden 1999*. Swedish National Road and Research Institute. Linköping, Sweden. Retrieved from <http://vti.diva-portal.org/smash/get/diva2:675215/FULLTEXT01.pdf>
- Witczak, M. W., Houston, W. N., & Andrei, D. (2000). Resilient Modulus as Function of Soil Moisture—A Study of the Expected Changes in Resilient Modulus of the Unbound Layers with Changes in Moisture for 10 LTPP Sites. Development of the 2002 Guide DD-3.35 for the Development of New and Rehabilitated Pavements. *Report No. NCHRP*, 1–37.
- Wolden, K. (2014). *Grunnlagsmateriale for regional plan for masseforvaltning i Akershus fylke*. Geological Survey of Norway. Trondheim: Norges geologiske undersøkelse. Retrieved from [http://www.ngu.no/upload/Publikasjoner/Rapporter/2014/2014%7B%5C\\_%7Do18.pdf](http://www.ngu.no/upload/Publikasjoner/Rapporter/2014/2014%7B%5C_%7Do18.pdf)
- Xiao, Y., & Tutumluer, E. (2012). *Best Value Granular Material for Road Foundations*. University of Illinois at Urbana-Champaign; Minnesota Department of Transportation. St. Paul, MN. Retrieved from <http://www.dot.state.mn.us/research/TS/2012/2012-01.pdf> <http://www.lrrb.org/pdf/201201.pdf>
- Yoder, E. J., & Witczak, M. W. (1975). *Principles of Pavement Design*. doi:10.1002/9780470172919
- Zhou, F., Fernando, E., & Scullion, T. (2010). *Development, calibration, and validation of performance prediction models for the Texas ME flexible pavement design system*.

- Texas Transportation Institute. Retrieved from <https://static.tti.tamu.edu/tti.tamu.edu/documents/o-5798-2.pdf>
- Zingg, T. (1935). *Beitrag zur Schotteranalyse* (Doctoral thesis, ETH Zürich). doi:10.3929/ethz-a-000103455



Part II  
APPENDIXES



## Comparison of practice for aggregate use in road construction – results from an international survey

Marit Fladvad, Joralf Aurstad & Børge Johannes Wigum

Fladvad, M., Aurstad, J. & Wigum, B.J. (2017) Comparison of practice for aggregate use in road construction – results from an international survey. In Loizos, A., Al-Qadi, I., Scarpas, T. (eds.) *Bearing Capacity of Roads, Railways and Airfields* (pp. 563–570). CRC Press. doi: 10.1201/9781315100333-74

This paper is not included due to copyright

## Large-size aggregates for road construction – a review of standard specifications and test methods

Marit Fladvad & Arnhild Ulvik

Fladvad, M. & Ulvik, A. (2019). Large-size aggregates for road construction – a review of standard specifications and test methods. *Bulletin of Engineering Geology and the Environment*. doi: 10.1007/s10064-019-01683-z

This paper is not included due to copyright



## **Influence of jaw crusher parameters on the quality of primary crushed aggregates**

Marit Fladvad & Tero Onnela

Fladvad, M. & Onnela, T. (2020). Influence of jaw crusher parameters on the quality of primary crushed aggregates. *Minerals Engineering* 151(2020)106338. doi: 10.1016/j.mineng.2020.106338





Contents lists available at ScienceDirect

Minerals Engineering

journal homepage: [www.elsevier.com/locate/mineng](http://www.elsevier.com/locate/mineng)

# Influence of jaw crusher parameters on the quality of primary crushed aggregates

Marit Fladvad<sup>a,b,\*</sup>, Tero Onnela<sup>c</sup><sup>a</sup> Department of Geoscience and Petroleum, NTNU – Norwegian University of Science and Technology, S.P. Andersens veg 15a, 7031 Trondheim, Norway<sup>b</sup> Norwegian Public Roads Administration, Abels gate 5, 7030 Trondheim, Norway<sup>c</sup> Metso Minerals, Lokomonkatu 3, 33100 Tampere, Finland

## ARTICLE INFO

### Keywords:

Construction aggregates  
Jaw crusher  
Parameter study  
Aggregate quality  
Crusher operation

## ABSTRACT

A parameter study using a jaw crusher is designed to investigate the influence of feed gradation, crusher setting and crusher speed on the crusher operation and the quality of the produced aggregates. The study is focused on the production of all-in large-size (top size  $\geq 90$  mm) aggregates, suitable for use in subbase and frost protection layers in a pavement structure. Aggregate quality is measured in terms of product gradation, particle shape and mechanical properties.

Feed gradation, crusher setting and crusher speed affects the specific energy consumption during crushing. Particle shape is affected by all parameters; feed gradation, feed rate, crusher setting and crusher speed. Mechanical properties are least affected by the jaw crusher parameters, but sample preparation using laboratory crushing clearly affect mechanical properties.

The results from this study provide valuable knowledge for the optimisation of single-stage crushing regarding crusher operation and aggregate quality. By adapting the crushing process to the available feed material and desired product, the quality of the crushed product can be optimised along with the crusher operation.

## 1. Introduction

In road construction, local aggregate resources can be utilised through aggregate production on the construction site. The aggregate production process, where construction aggregates are produced from bedrock, often involves several crushing steps. The output is normally considered a product after two or more crushing stages. However, primary, or single-stage, crushed aggregate materials can be used as products in road construction, in e.g. unbound subbase and frost protection layers. Such productions usually involve a simple setup with mobile crushing equipment. Research into aggregate production and quality have traditionally been focused on products from subsequent crushing stages, not products from primary crushing. There is a knowledge gap regarding the influence of the crushing process on the quality of primary crushed aggregates.

Compared to many other countries, the Norwegian practice for aggregate use, with particle sizes up towards 300 mm in the pavement structure is uncommon. In a survey, Fladvad et al. (2017) found that 12 of 17 surveyed countries restrict material sizes for unbound aggregates to 100 mm or smaller, including the US, UK, Austria, Denmark and

Iceland. This is profoundly different from the Norwegian design guidelines (Norwegian Public Roads Administration, 2018), which specifies the gradings 22/125 mm and 22/180 mm as common subbase materials.

The European standards for aggregates (EN 13242, 2007; EN 13285, 2018) are only valid for materials with an upper sieve size of 90 mm or smaller. This size limitation to the standards introduces challenges for producers and costumers because local specifications for aggregate products must be created. One such local specification is the new Norwegian standard for large-size construction aggregates, which defines common methods for description and quality assessment for large-size aggregates (NS 3468, 2019).

Quality assessment of aggregates is mainly ruled by tests regarding mechanical strength for the rock type in question. These tests are related to the rock deposit, and test results are regarded as representative for all aggregate gradings produced from the source rock. The current requirements for mechanical aggregate properties are based on laboratory testing of crushed material in standardised fractions. When the materials used in the pavement structure are of a coarser size fraction than what is required for the laboratory tests, the material tested has to

\* Corresponding author at: Department of Geoscience and Petroleum, NTNU – Norwegian University of Science and Technology, S.P. Andersens veg 15a, 7031 Trondheim, Norway.

E-mail address: [marit.fladvad@ntnu.no](mailto:marit.fladvad@ntnu.no) (M. Fladvad).

<https://doi.org/10.1016/j.mineng.2020.106338>

Received 19 July 2019; Received in revised form 30 November 2019; Accepted 9 March 2020

0892-6875/© 2020 The Authors. Published by Elsevier Ltd. This is an open access article under the CC BY license

(<http://creativecommons.org/licenses/by/4.0/>).

be crushed down to the appropriate size in the laboratory. This practice implies the assumption that aggregate properties are predominantly determined by the geological origin of the resource (i.e. mineralogy, petrology), and only negligibly influenced by the production, e.g. blasting and crushing.

A growing focus on the utilisation of local aggregate resources at construction sites has increased the interest in the quality of primary crushed aggregates in Norway. The construction of long tunnels has created a surplus of hard rock resources in several road and railway construction projects. Large volumes of blasted rock are available at tunnel construction sites, and the production of primary crushed aggregates provides an affordable construction material with low CO<sub>2</sub> emissions from transport. Blasted rock is no longer allowed used in the pavement structure without further processing. The production of local aggregates is conducted by mobile crushing and screening equipment, which both due to economical and space restrictions require a simple setup.

The part of aggregate processing investigated in this paper is the crushing, specifically primary crushing using a jaw crusher. Coarse aggregates for unbound use are often produced using a single crushing stage in a jaw crusher, as opposed to concrete or asphalt aggregates, where at least two and often three or four crushing stages are used, employing several crusher types. Most published literature is focused on the use of cone crushers and several types of impact crushers. There is a gap of knowledge regarding the quality of large-size aggregates, especially coarse aggregates produced in a single-stage crushing plant.

To close this knowledge gap, a jaw crusher parameter test is designed based on previous research into crushing and aggregate production, presented in the following:

As a general rule, the strength of rock increases with decreasing mineral grain diameter (Brace, 1961; Brattli, 1992). Although some rock types are considered more suitable for aggregate production than others, mechanical properties for aggregates cannot be inferred directly from rock type. Erichsen et al. (2008) presented an overview of mechanical tests from a Norwegian aggregate database and concluded that the variation in mechanical properties can be as great within specific rock types as between different rock types. Miskovsky et al. (2004) showed that mineral content influence the mechanical properties, but also that micro-cracks influence the same properties, and hence, incautious production can cause considerable deterioration of the rock material.

Räisänen and Mertamo (2004) found that laboratory crushers can provide aggregates with too good shape properties, leading to over-estimation of the aggregate quality, and stated that correlation between laboratory and industrial multi-stage crushing plants cannot be made.

Eloranta (1995) investigated the crushing process with emphasis on particle shape (cubicity) of the produced material, and found that the most important properties are the feed gradation and crusher stroke. These findings were based on full-scale tests with gyratory and cone crushers. Based on these tests, Eloranta (1995) presented guidelines for crushing when the goal is to produce cubical aggregates. These guidelines differentiate on whether the feed material contains fines.

Briggs and Evertsson (1998) also focused on product shape, and after testing materials in the size range 16–40 mm, found that the operation of the crusher to a large degree influences aggregate shape. They found that multi-point loading creates better-shaped products than single-point loading, and further that efficient size reduction and improvement of shape are two mutually excluding objectives.

The subject for Bengtsson (2009) was product quality with focus on particle shape, after secondary and tertiary crushing. Among his findings were empirical models showing that crusher setting, feed size, crusher speed and throw affects particle shape in products from cone crushers. Increased average feed size increases flakiness index, likewise does decreased crusher speed. Further, Bengtsson states that in full-scale crushing, there is no evidence that feed shape affects product shape.

Bouquety et al. (2007) investigated the influence of crusher setting and feed grading on the shape of products from tertiary crushing, and found that shape varies within the product gradation with increasing flakiness for decreasing particle size. Consequently, they conclude that increased product size results in better shape.

Johansson et al. (2017) presented a fundamental model of a industrial-scale jaw crusher based on previous studies of cone crushers. The model predicts capacity and power draw for various speeds and crusher settings.

When testing several materials from one deposit, Andersson and Öjertorn (2014) found that the particle shape (flakiness) of a material affects its resistance to fragmentation measured by the Los Angeles abrasion test. Benediktsson (2015) artificially varied the amount of flaky particles in samples for mechanical testing, and found that flakiness affects the results from mechanical testing. In addition to material broken down to 1.6 mm or smaller as described in the test specification, Benediktsson also measured the amount of material left in the original test size after testing. The general trend found was that the mechanical results are improved by reduced flakiness in the sample.

Guimaraes et al. (2007) found that energy consumption during crushing increases with increasing fines generation, because the energy required is proportional to the amount of new surface created.

Lee (2012) researched compressive crushing with a goal of optimising the product yield (amount of valuable product compared to by-products) and energy consumption, with focus on cone crushers. Among her findings was that to optimise product yield, interparticle crushing should be held at a minimum. Particle shape was not considered in Lees studies.

Cook et al. (2017) investigated aggregate mixtures from four different rock types, and found that particle shape affects the packing density of unbound aggregates, especially for open-graded mixes. Further, they found that micro-Deval value is mainly decided by mineralogy, but that particle shape can also affect the value. Increasing flatness led to increasing micro-Deval value. Erichsen et al. (2011) describes differences and similarities between the mechanical tests for aggregates, and highlights their empirical nature. Furthermore, in Erichsen (2015), a new method for presenting the results from the mechanical tests is proposed. Coronado et al. (2011) conducted an experimental study on unbound granular pavement materials, aiming to develop a material ranking based on mechanical behaviour rather than empirical tests such as the Los Angeles and micro-Deval tests. They found that the ranking provided by empirical tests on samples of a set particle size range does not match the performance of the same aggregates when the full gradation is tested in a triaxial test.

None of the presented research had focus on products from primary crushing. For applications where large-size aggregates are used, such as unbound aggregates for road structures, single-stage crushing can be applied. The interest of the current research is to conduct full-scale tests with jaw crushers in the primary crushing stage, to gain knowledge about how a single crushing stage after blasting can affect the quality of the produced aggregate. The aim is to verify whether relations known from research into finer aggregates produced using more than one crushing stage are valid also for large-size aggregates produced from primary crushing. The hypothesis used in the research design is: Crushing efficiency and product quality can be optimised by adjustments to crusher and feed parameters. Crushing efficiency can be measured as capacity and energy consumption. Product quality is measured in terms of particle shape and mechanical properties. The crusher and feed parameters used are closed side setting (CSS), speed, feed rate and feed gradation.

This paper presents a parameter study investigating the effect of feed and jaw crusher parameters on the quality of aggregates produced from single-stage crushing. The parameter study is evaluated using mechanical and geometrical tests for aggregate properties. In order to keep the focus on the gradation and crusher parameters, the study is limited to one rock type. The aggregates produced during the study are

in the size range 0–125 mm.

## 2. Materials and methods

### 2.1. Test material

To correlate the production parameters with the resulting aggregate properties, the geological properties were held constant while the crusher properties were changed. The test was therefore restricted to a single rock type. The material tested was a granodiorite, a coarse-grained intrusive igneous rock from Nokia, Finland. The test material was supplied from an open-pit quarry in regular operation.

The test material was pre-assessed through testing of its resistance to fragmentation (Los Angeles test, EN 1097-2 (2010)) and resistance to wear (micro-Deval test, EN 1097-1 (2011)), and found to be suitable for unbound use in road construction following Norwegian requirements (Norwegian Public Roads Administration, 2014). The declared values for mechanical strength are given in Table 1.

The blasted rock material supplied to the test plant was in the 0/500 mm<sup>1</sup> size range, the maximum particle size ( $D_{max}$ ) stretching to 630 mm. The material was produced by drilling and blasting and had not been crushed previously. The blasting was conducted using a borehole diameter of 83 mm, borehole spacing of 3 m, and burden of 2.3 m. In the quarry, a hydraulic hammer had been used to split oversize rocks down to the desired top size. To avoid jamming the crusher, the input material was also assessed visually at the test plant, and oversized particles were removed manually before the material was fed to the crusher.

To create variations in minimum and maximum size of the feed material, the materials were scalped at the test plant before being fed to the jaw crusher. The scalper had elongated openings with slot widths 100 mm and 225 mm. The oversize removal and scalping process enabled the production of five particle size fractions ( $d/D$ ):

- 0/400 mm
- 100/400 mm
- 180/400 mm
- 0/300 mm
- 100/300 mm

The particle size distributions for the five feed sizes are shown in Fig. 1. Due to the allowance for over- and undersize in the naming of particle size fractions, the sizes  $d$  and  $D$  are not identical to the scalper slot widths.

Although each test was run in minimum three parallels with identical test portion preparation, there is variation in the sizes for every feed material. To account for these variations, the sizes  $F_{10}$  and  $F_{90}$  will be used instead of the theoretical  $d$  and  $D$  in the presentation of individual results.  $F_{10}$  and  $F_{90}$  are the sizes which 10% and 90% of the feed materials passes, respectively. These sizes are easily recognised from the PSD curves as the sizes at which the curve passes the 10% or 90% lines.

### 2.2. Methods

#### 2.2.1. Full-scale crushing test

The test setup followed the process flow sheet in Fig. 2. Blue rectangles illustrate processes; green parallelograms illustrate outputs used for further analysis, while yellow ellipses are products not further

<sup>1</sup> Throughout this paper, aggregate sizes are described as following the notation from EN 13242 (2007):  $d/D$  denotes an aggregate particle size distribution where up to 20% over- and undersize particles are present, while  $d-D$  signifies a distribution where all particles are in the size range from  $d$  to  $D$ , with no under- or oversize.  $d$  = lower sieve size;  $D$  = upper sieve size.

**Table 1**

Declared values for mechanical properties of test material.

Test method	Test result
Resistance to fragmentation (Los Angeles), EN 1097-2	$LA = 28$
Resistance to wear (micro-Deval), EN 1097-1	$M_{DE} = 9$

analysed.

The tests were conducted using a Nordberg C80 jaw crusher. The crusher has an opening of 800 x 500 mm; the recommended maximum material size for this crusher is specified to 410 mm. The crusher was fed by a vibrating feeder with adjustable feed rate.

The stroke of the crusher was constant at 30 mm, while three CSS were used: 40 mm, 70 mm, and 100 mm. The normal speed for the crusher was 355 rpm. A reduced speed of 284 rpm was also tested, corresponding to a 25% reduction.

Two feed levels were used, defined as high and low feed rate. At the high feed rate, the crusher was choke fed, ensuring the crusher could run at maximum capacity. The low feed rate allowed the crusher to run empty during the crushing; hence involving a lower density of material in the crusher and reduced throughput. The feed rates were not fixed, but manually adjusted by the crusher operator.

A summary of the parameters can be seen in Table 2, while Table 3 shows the full test matrix with the individual parameter combinations. Each of the 12 main tests T4 – T15 in Table 3 was conducted in minimum three parallels.

In each test, a minimum of 1500 kg of blasted rock was crushed. Depending on the feed gradation and the setting of the crusher, the amount of material crushed varied from 1500 kg to 2500 kg.

During testing, the crusher was monitored, and data for power draw was extracted from the monitoring system.

To measure the throughput of the crushing operation, a sample was taken from the output flow from the crusher using a wheel loader during the middle of the test when the crusher was running steadily. This way, the effects of lower quality crushing during starting and stopping of the crushing operation was eliminated from the sampled material. The duration of the sampling was registered, the amount of material was weighed, and from this data, the throughput [tonnes/hour] of the crushing operation was calculated.

#### 2.2.2. Sampling

Photos for image analysis was taken after the material was loaded onto the feeder, before the feeder was started. The feed gradation curves are calculated using the digital image processing (DIP) software Split-Desktop 4.0, based on one photo from each test feed. The images were scaled by two 250 mm spheres included in the image with the feed material. Consistency in the DIP was ensured by analysing a share of the images separately by two different analysts, and the results were compared with compliant results.

Material samples for particle size distribution analysis were taken from each crushing test by extracting material directly from the output conveyor from the crusher using a wheel loader. The amount of material in these samples varied from 130 kg to 430 kg, depending on the expected gradation. To avoid segregation and ensure representativity, the full test portion from the wheel loader bucket was collected.

The remaining material after a finished test was then screened to extract 8–16 mm material for mechanical testing. Samples of minimum 50 kg 8–16 mm were collected from each test product.

#### 2.2.3. Laboratory testing

##### Particle size distribution.

The particle size distribution for the product from each test was measured combining manual sieving for the material > 90 mm, and mechanical sieving for the material < 90 mm.

Following NS 3468 (2019), the samples were sieved manually with

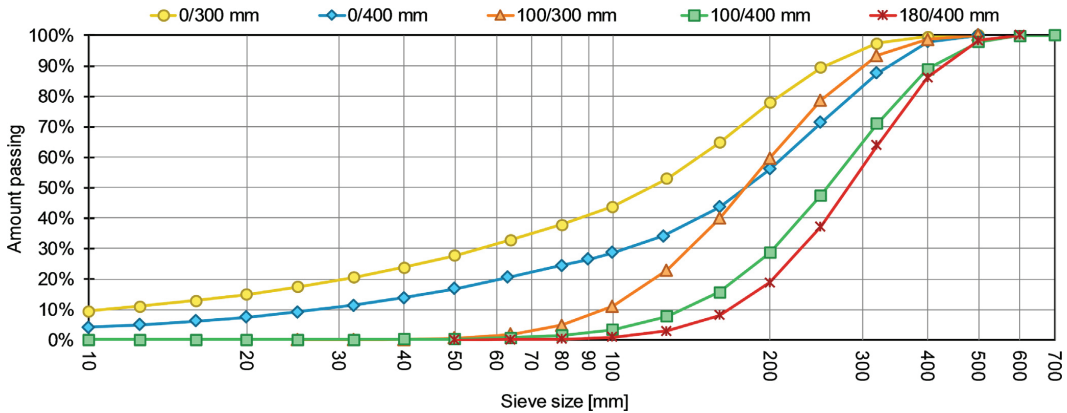


Fig. 1. Feed material particle size distributions from image analysis. Each line represents average values from all tested materials of each size fraction.

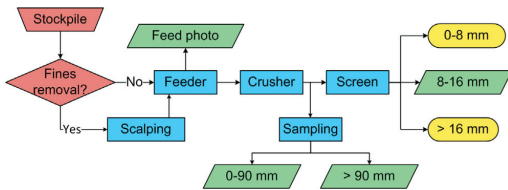


Fig. 2. Process flow sheet for the crushing tests, including sampling for laboratory testing.

Table 2  
Summary of available settings of the feed and crusher parameters.

Parameter	Available settings
Lower feed material size ( <i>d</i> )	0, 100, 180 mm
Upper feed material size ( <i>D</i> )	300, 400 mm
Feed level	High, low
Closed side setting (CSS)	40, 70, 100 mm
Crusher speed	355, 284 rpm

Table 3  
Parameter combinations used during testing.

Test ID	Feed material size [mm]	Feed level	Closed side setting [mm]	Crusher speed [rpm]
T4	100/400	High	70	355
T5	100/400	Low	70	355
T6	100/400	High	40	355
T7	100/400	High	100	355
T8	180/400	High	70	355
T9	0/300	High	40	355
T10	0/300	High	70	355
T11	100/300	Low	40	355
T12	100/300	High	40	355
T13	100/300	High	70	355
T14	0/400	High	70	284
T15	100/400	High	70	284

a 90 mm field sieve at the crushing site, and all material smaller than 90 mm was brought to the laboratory for further testing. Material larger than 90 mm was sieved manually at the crushing site with sieves of sizes 100, 125, 160 and 200 mm. This method was chosen in order to reduce the sample sizes brought to the laboratory. After the 90 mm split, the resulting size of the samples brought to the laboratory varied

from 90 to 270 kg. In the laboratory, large samples were divided and reduced using a riffle box, always keeping a sample of minimum 80 kg for the PSD analysis.

The mechanical sieving method was based on standard EN 933-1 (EN 933-1, 2012), with the following adjustments:

- Smallest sieve size used: 1 mm
- The test portions were not washed prior to sieving; the analysis followed the procedure for dry sieving
- For some samples, material < 25 mm was subsampled to minimum 6.3 kg using a riffle box before sieving continued

Table 4 contains an overview of the sieves used. The minimum sieve size of 1 mm was chosen because this research is mainly concerned with the coarse part of the particle size distribution curve. By using these sieve sizes, washing and drying of the samples could be avoided. The samples were stored indoors for several months prior to sieving; hence, moisture was not a problem during sieving.

Particle shape. The particle shape of the product material was measured using the flakiness index method (EN 933-3, 2012), which is valid

Table 4  
Particle size fractions and related sieve sizes used for the laboratory analyses. Square sieves are used for analysis of particle size distributions, bar sieves are used for analysis of flakiness.

Particle size fraction	Aperture size, square sieve	Slot width, bar sieve
> 200 mm	200.0 mm	125.00 mm
160–200 mm	160.0 mm	100.00 mm
125–160 mm	125.0 mm	80.00 mm
100–125 mm	100.0 mm	63.00 mm
90–100 mm	90.0 mm	50.00 mm
80–90 mm	80.0 mm	40.00 mm
63–80 mm	63.0 mm	40.00 mm
50–63 mm	50.0 mm	31.50 mm
40–50 mm	40.0 mm	25.00 mm
31.5–40 mm	31.5 mm	20.00 mm
25–31.5 mm	25.0 mm	16.00 mm
20–25 mm	20.0 mm	12.50 mm
16–20 mm	16.0 mm	10.00 mm
12.5–16 mm	12.5 mm	8.00 mm
10–12.5 mm	10.0 mm	6.30 mm
8–10 mm	8.0 mm	5.00 mm
6.3–8 mm	6.3 mm	4.00 mm
5–6.3 mm	5.0 mm	3.15 mm
4–5 mm	4.0 mm	2.50 mm
2–4 mm	2.0 mm	–
1–2 mm	1.0 mm	–

for material in the size range 4–100 mm. The samples were analysed using standard laboratory sieves for the 0–90 mm product samples brought to the laboratory. In addition, the material > 90 mm which were sieved manually for size distribution at the test site was also manually sieved for particle shape analysis using custom-made bar sieves with slot widths of 50, 63, 80, 100, and 125 mm. The individual particle fractions used are shown in Table 4, starting with 4–5 mm as the smallest fraction.

$$FI = 100 \frac{M_2}{M_1} \tag{1}$$

According to the standard, the flakiness index is calculated from Eq. 1, where

$M_1$  is the sum of the masses of the particles in each of the particle size fractions  $d_i$ – $D_i$  in grams

$M_2$  is the sum of the masses of the particles in each particle size fraction passing the corresponding bar sieve of slot width  $0.5D_i$  in grams.

**Mechanical properties.** Resistance to wear was measured using the micro-Deval test (EN 1097-1, 2011), and resistance to fragmentation was measured using the Los Angeles test (EN 1097-2, 2010). Both tests require 10–14 mm test material. Each test was done twice for each product sample: First, the test portions were prepared by sieving 8–16 mm material from the primary crushing. Next, 63–90 mm material from the primary crushing was laboratory crushed to obtain the 10–14 mm test size. In addition to recording the mass retained on the 1.6 mm sieve after testing as the standards specify, mass retained on the 10 mm sieve was also recorded for both test methods. This was chosen in order to quantify how much of the test portion is left in the original test fraction after testing.

The laboratory crushing followed the method description from Norwegian Public Roads Administration (2016). The sample is crushed twice, using a laboratory jaw crusher with setting 11 mm. In the first crushing stage, 63–90 mm rock particles are crushed individually. In the second crushing stage, the product from the first crushing stage is loaded into the crusher in a single batch. The amount of material used in laboratory crushing is minimum 30 kg. The crusher was tested at several settings, and 11 mm was chosen because this was the setting which generated the most material in the 10–14 mm size range.

### 3. Results

#### 3.1. Crusher operation

When the crusher is fed at the high feed rate, the measured throughput can be characterised as the capacity of the crushing operation. This capacity varied from 77.8 t/h to 194.3 t/h. The highest capacity is registered for the tests including fines in the feed material. Reducing the feed rate resulted in a 50–56% reduction of the throughput.

The capacity of the crushing operation can be modelled using regression analysis combining categorical and continuous predictors. Regression analysis for capacity using CSS and the lower size of the feed material ( $F_{10}$ ) results in a coefficient of determination  $r^2 = 0.77$ . The relation is displayed in Fig. 3. The highest capacity is achieved with large CSS and low  $F_{10}$  size.

Specific energy consumption (SEC), consumed energy per tonne of crushed material, is a measure of the efficiency of the crushing process. SEC is calculated from the gross power draw and throughput using Eq. 2:

$$SEC = \frac{\text{Power draw}}{\text{Throughput}} \tag{2}$$

The energy demand varied from 0.20 to 0.78 kWh/t. SEC can be

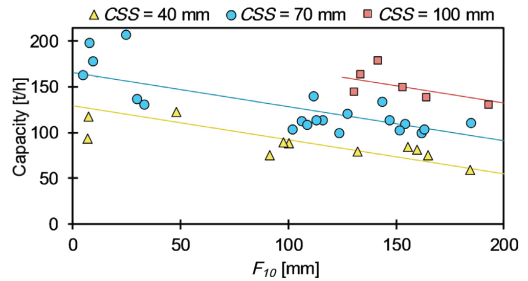
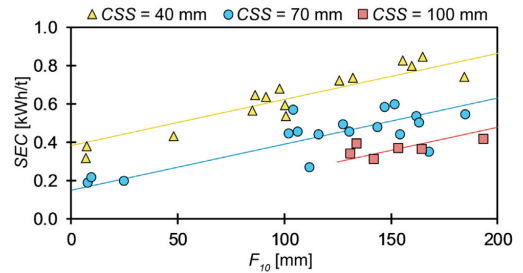
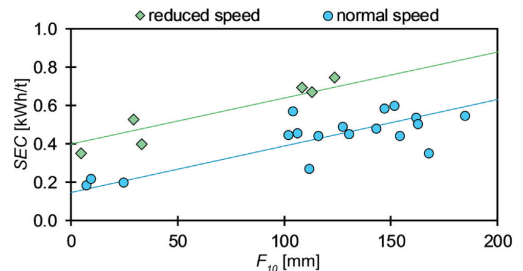


Fig. 3. Capacity vs  $F_{10}$ , differentiated by CSS. Combined regression analysis:  $r^2 = 0.77$ .



(a) SEC vs  $F_{10}$ , differentiated by CSS



(b) SEC vs  $F_{10}$ , differentiated by crusher speed

Fig. 4. Specific energy consumption vs  $F_{10}$ . Regression analysis combining SEC,  $F_{10}$ , CSS and speed:  $r^2 = 0.83$ .

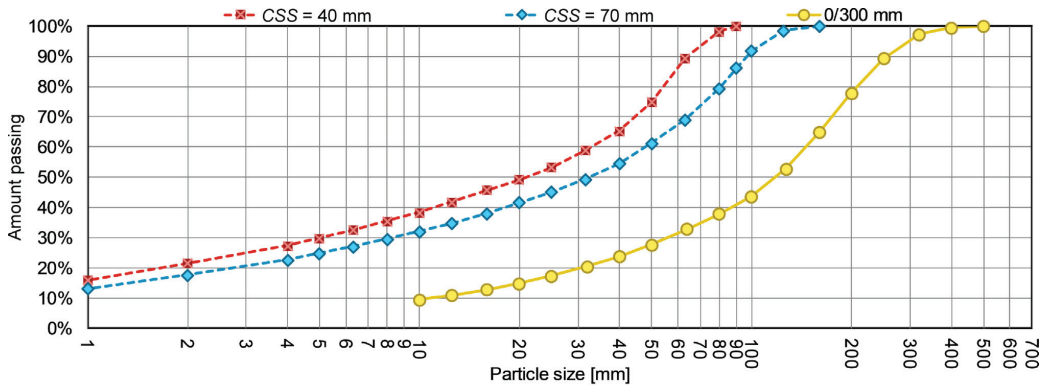
modelled in a similar way as capacity, accounting for crusher speed in addition to CSS and  $F_{10}$ . The relation is shown in Fig. 4, with a combined  $r^2 = 0.83$ .

Reducing the speed of the crusher results in increased energy consumption per tonne of crushed material. The increase is about 0.25 kWh/t, independent of  $F_{10}$ . The lowest energy consumption per tonne is found with high crusher speed, high CSS and low  $F_{10}$  size.

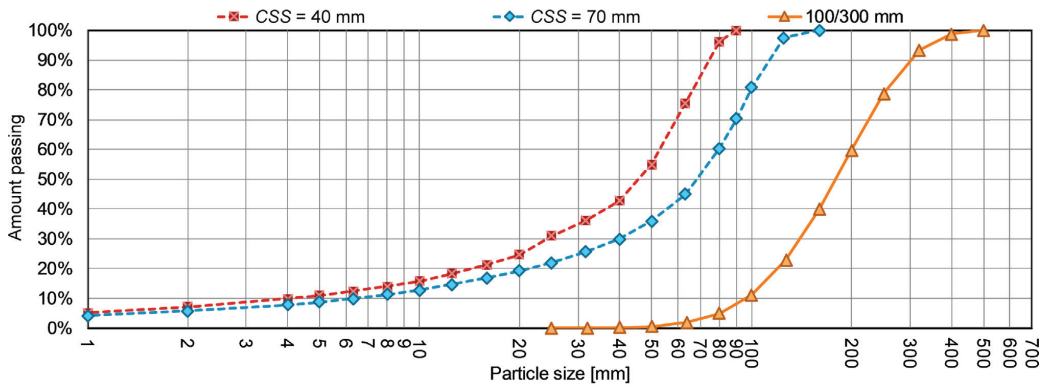
The test setup did not combine CSS = 100 mm with feed materials including fines; hence, the  $F_{10}$  range for the CSS = 100 line is limited for both capacity (Fig. 3) and SEC (Fig. 4a). Reduced crusher speed was only tested for CSS = 70 mm; hence, the data points for normal speed in Fig. 4b is also limited to samples where CSS = 70 mm.

#### 3.2. Particle size distributions

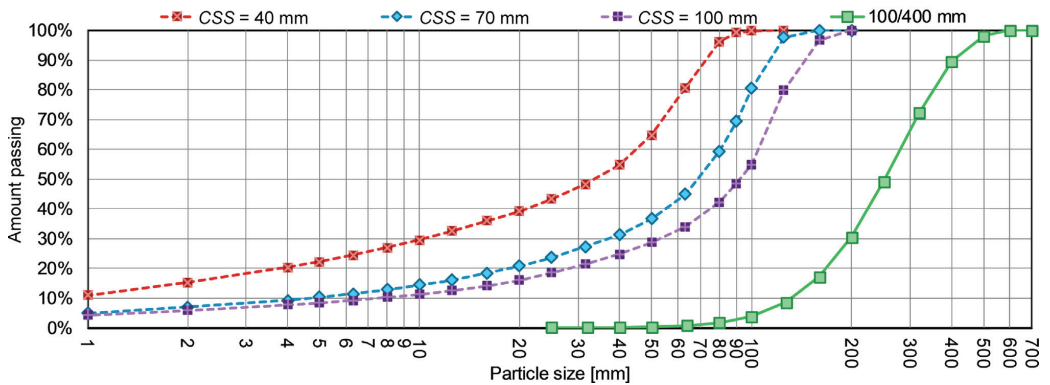
The effect of changing crusher openings on PSD for feed materials crushed at several CSS is shown in Fig. 5. For the tests where the feed did not contain fines, 43–55% of the product material is smaller than



(a) Feed material size 0/300 mm; products from CSS 40 and 70 mm.



(b) Feed material size 100/300 mm; products from CSS 40 and 70 mm



(c) Feed material size 100/400 mm; products from CSS 40, 70 and 100 mm

Fig. 5. Particle size distributions for feed and product materials for feed sizes 0/300 mm, 100/300 mm and 100/400 mm. Feed material distributions drawn in solid lines, product distributions in dashed lines. Each line represents the average of minimum 3 parallel tests.

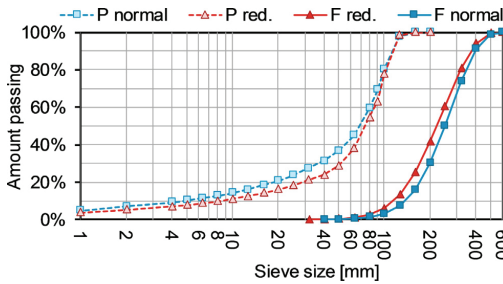
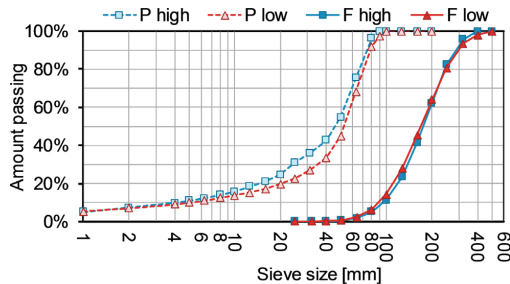


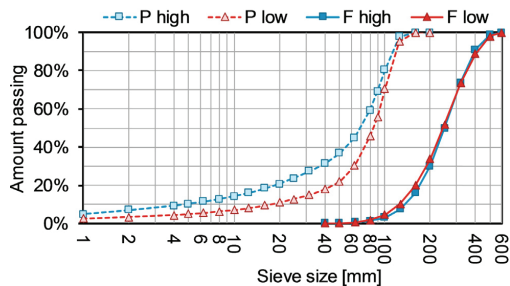
Fig. 6. Feed (F) and product (P) particle size distribution curves for 100/400 mm samples tested at normal and reduced speed. Each line represents the average of minimum 3 parallel tests.

CSS. For the feed material containing fines, the increase in material smaller than CSS in the product is about 40 percentage points. More than 96% of the product is smaller than 2-CSS, except for T11 where 92% is smaller than 2-CSS.

The effect of reduced crusher speed on PSD is seen in Fig. 6. When the crusher speed is reduced, the endpoints of the PSD curve – the top size and the amount of material smaller than 1 mm – is not affected. On the other hand, the PSD curve is steeper, and there is less material smaller than CSS. Although the feed material for the reduced speed test had a somewhat finer distribution with approximately 10 percentage points more material passing 160 mm compared to the feed material for the normal speed test, the product curves have the inverse relationship, where the product from the reduced speed test is coarser. 0/400 mm feed was only tested at the reduced speed, so no comparisons to normal speed can be made for this feed material.



(a) Feed size 100/300 mm



(b) Feed size 100/400 mm

Fig. 7. Feed (F) and product (P) particle size distribution curves for samples tested at high and low feed rate. Each line represents the average of minimum 3 parallel tests.

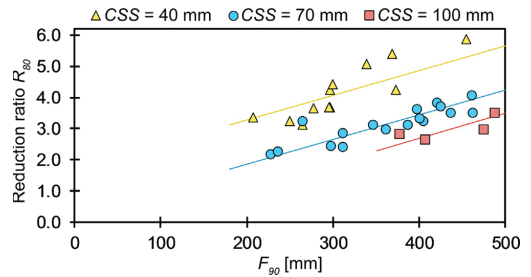


Fig. 8. Reduction ratio  $R_{80}$  vs. the upper size for the feed material  $F_{90}$ , differentiated by closed side setting CSS. Regression analysis combining  $R_{80}$ ,  $F_{90}$  and CSS;  $r^2 = 0.808$ .

The effect of reduced feed rate on the PSD is seen in Fig. 7. The reduced feed rate results in a 25% reduction in the amount of material smaller than CSS. The reduction is significant at the 99% confidence level. Reducing the feed rate does not affect the top size of the product.

3.3. Reduction ratio

The reduction ratio for each test is calculated as the ratio between the respective screen sizes through which 80% of the feed and product distribution passes (Eq. 3):

$$R_{80} = \frac{F_{80}}{P_{80}} \tag{3}$$

The test setup resulted in a span of reduction ratios for each CSS, as seen in Fig. 8. Among all tests,  $R_{80}$  ranged from a minimum of 2.2 to a maximum of 5.9.

$R_{80}$  can be reliably predicted from the ratio between  $F_{90}$  and CSS using Eq. 4 with  $r^2 = 0.842$ . The relation is shown in Fig. 9, with the symbols from Fig. 8 kept for comparison.

$$R_{80} = 0.997 + 0.4155 \frac{F_{90}}{CSS} \tag{4}$$

When the speed of the crusher was reduced by 25% from 355 to 284 rpm,  $R_{80}$  was reduced by about 0.5. This difference is statistically significant at the 95% confidence level.

The samples crushed at reduced feed rate had a somewhat reduced  $R_{80}$ , but the difference is too small to be statistically significant with the low number of samples (6 tests for reduced feed rate).

3.4. Particle shape

As seen in Section 3.2, the top size of the product from each test is related to CSS ( $P_{96} \approx 2CSS$ ). To enable comparison of the particle shape

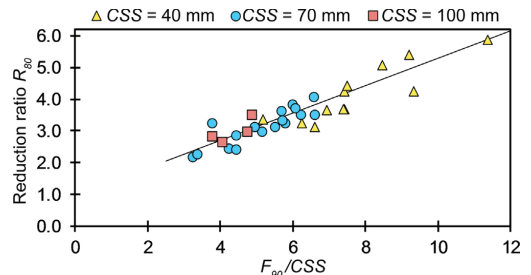
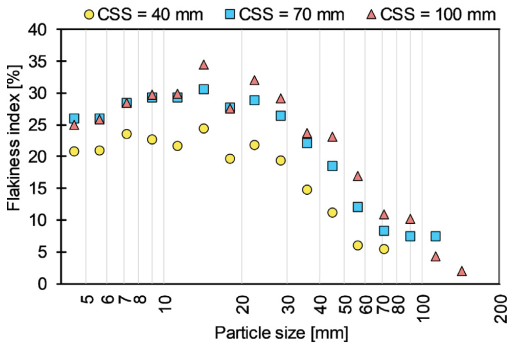
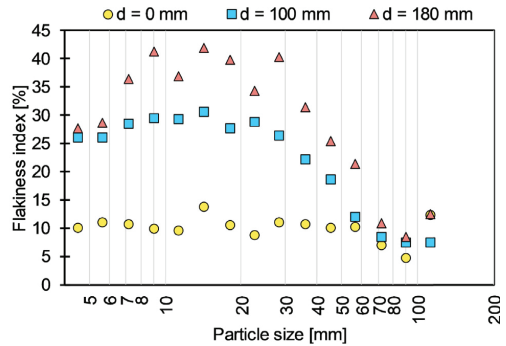


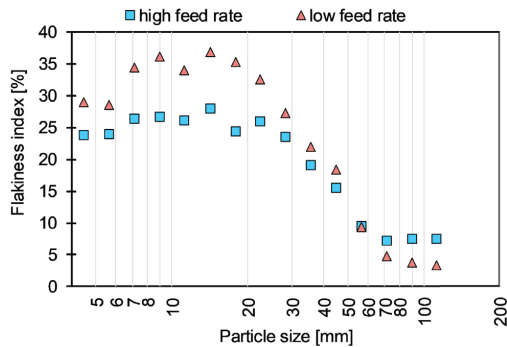
Fig. 9. Reduction ratio  $R_{80}$  as a function of the ratio between the upper size for the feed material  $F_{90}$  and the crusher setting CSS;  $r^2 = 0.842$ .



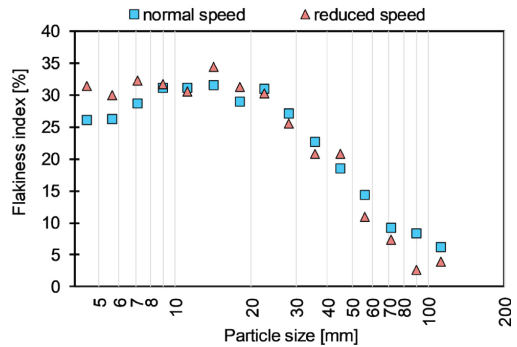
(a) *FI* compared at different *CSS*



(b) *FI* compared at different lower feed size *d*



(c) *FI* compared at high and low feed rate



(d) *FI* compared at normal and reduced crusher speed

Fig. 10. Particle shape measured as flakiness index for individual particle size fractions. The x-axis displays the middle size of each particle size fraction.

for the full product gradations, the results will be presented for the size range 4 mm–2*CSS* ( $FI_{<2CSS}$ ), rather than the standard calculation for 4–100 mm ( $FI_{4-100}$ ).

The average  $FI_{<2CSS}$  for all tests is 11.8, but the *FI* of the product is considerably different for material above and below *CSS*.  $FI_{<CSS}$  varies from 8 to 33 with an average value of 20.3, while  $FI_{>CSS}$  varies between 0 and 15 with an average value of 6.7. Products above *CSS* are less flaky and there is less variation in particle shape than below *CSS*.

The general trend for *FI* vs particle size can be seen in Fig. 10a; *FI* is lower for larger particles, and increases with decreasing particle size until a maximum is reached for the 12.5–16 mm size fraction. Below this size, the *FI* is stable (*CSS* = 40 mm) or somewhat decreasing (*CSS* = 70 and 100 mm). The maximum *FI* is found at the same particle size independent of *CSS*.

Another general tendency in Fig. 10a is that for a specific size fraction, *FI* is lower for products produced at lower *CSS*. In contrast,  $FI_{<2CSS}$  is not affected by *CSS* changing between 40, 70 and 100 mm, as the value is 12.7 with a variation of only  $\pm 0.3$  between the three settings. The results for *FI* vs *CSS* are however somewhat ambiguous, as the difference between *CSS* 40 mm and *CSS* 70 mm in Fig. 10a is clear for all particle sizes, while the difference between *FI* for *CSS* 70 mm and *CSS* 100 mm for the smaller sizes is minimal.

Including fines in the feed material results in a decreased flakiness index for the product, as seen in Fig. 10b. This effect is consistent for all product sizes from 4–5 mm to 80–100 mm. For the tests where fines were included in the feed, there are only minor differences in *FI* for different particle sizes. *FI* varies between 4.8 and 13.8 for *d* = 0, while the variation is much greater for *d* = 100 (7.5–30.6) and *d* = 180 mm

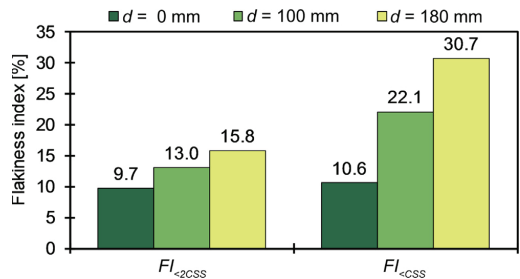


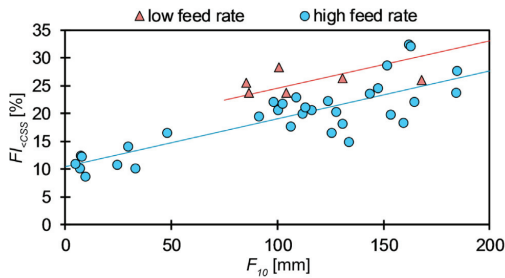
Fig. 11. Global *FI* ( $FI_{<2CSS}$ ) and *FI* for product smaller than *CSS* ( $FI_{<CSS}$ ) depending on lower feed size *d*.

(8.4–41.8).

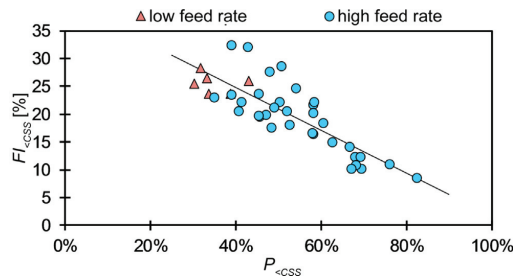
Fig. 11, where  $FI_{<2CSS}$  and  $FI_{<CSS}$  is compared, shows that the increase is most evident for  $FI_{<CSS}$ , which doubles when *d* is increased from 0 to 100 mm, and almost triples when *d* is increased from 0 to 180 mm.

The data show good correlation between  $FI_{<CSS}$  and  $F_{10}$  when feed rate is accounted for ( $r^2 = 0.713$ ), as seen in Fig. 12a;  $FI_{<CSS}$  is reduced when smaller material is present in the feed. Although the relationship is weaker than for  $F_{10}$ ,  $FI_{<CSS}$  is also increasing when the  $F_{90}$  size increases, showing the general trend that a coarser feed material results in a more flaky product.

Equal correlation is also found between  $FI_{<CSS}$  and the amount of



(a)  $FI_{<CSS>}$  vs  $F_{10}$ , differentiated by feed rate. Regression analysis combining  $FI_{<CSS>}$ ,  $F_{10}$  and feed rate:  $r^2 = 0.713$



(b)  $FI_{<CSS>}$  vs amount of product smaller than CSS ( $P_{<CSS>}$ ),  $r^2 = 0.680$

Fig. 12.  $FI$  for product smaller than CSS ( $FI_{<CSS>}$ ) related to feed or product gradation.

material smaller than CSS in the product gradation ( $r^2 = 0.680$ ) in Fig. 12b; increased amount of material smaller than CSS in the product gives a reduced  $FI_{<CSS>}$ . In this plot, the low feed rate samples fit to the same regression line as the high feed rate samples. The coarser product gradation resulting from the reduced feed rate found Fig. 7 is also visible in Fig. 12b.

Although few samples represent the low feed rate, a trend of increased  $FI$  for reduced feed rate is seen in Fig. 12a. When the feed rate is lowered,  $FI_{<2CSS>}$  decreases by 13% from 12.8 to 11.1.  $FI_{<CSS>}$ , on the other hand, increases by 20% from 21.3 to 25.6. The explanation for this is found in Fig. 10c, which shows that when the feed rate is low,  $FI$  increases for particles smaller than 50 mm and decreases for particles larger than 63 mm. The increase in  $FI$  is between 16 and 45% for all individual size fractions below 50 mm.

When the crusher speed is reduced,  $FI_{<2CSS>}$  decreases by 32% from 13.4 to 9.1, while  $FI_{<CSS>}$  remains almost unchanged with 23.5 for normal speed and 22.1 for reduced speed.  $FI$  results for all particle sizes are displayed in Fig. 10d. The results are not consistent, but there are indications of a shift of particle shape distribution when speed is reduced;  $FI$ s are reduced for large particles and increased for small particles.

No correlation is found between  $R_{80}$  and flakiness, neither for  $FI_{<2CSS>}$ ,  $FI_{<CSS>}$  or any of the individual size ranges.

3.5. Mechanical tests

Overall average results from mechanical testing of primary crushed material and laboratory crushed material are displayed in Fig. 13. The tests on primary crushed material have an average  $LA$  of 27.9, while the laboratory crushed material had an average value of 20.7, corresponding to a 26% reduction.  $M_{DE}$  is reduced from on average 9.1 for primary crushed to 7.4 for laboratory crushed material, a reduction by 19%. These results are calculated from 38 individual tests for each property, and variations in the measurements are shown by error bars

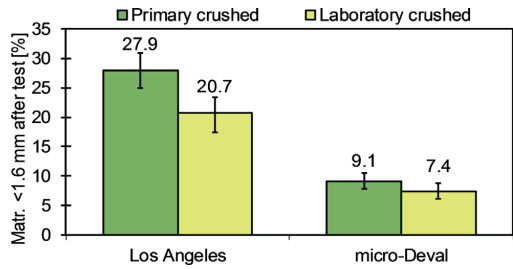


Fig. 13. Mechanical properties measured before and after laboratory crushing (average values). The error bars indicate maximum and minimum values for each data set ( $N = 38$  for each column).

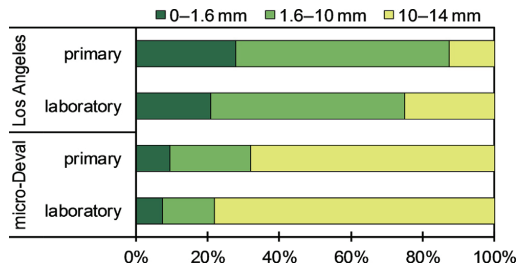


Fig. 14. Size distribution of material after testing by Los Angeles ( $N = 29$ ) and micro-Deval ( $N = 25$ ) methods for primary crushed material and laboratory crushed material.

for maximum and minimum in Fig. 13.

Fig. 14 shows the resulting size distribution for the test portion after the Los Angeles and micro-Deval methods, and how the distribution differs for primary crushed and laboratory crushed samples. The 0–1.6 mm bars represent the standard  $LA$  and  $M_{DE}$  values, while the 10–14 mm bars represent the  $LA_X$  and  $M_{DE_X}$  values. As sample preparation by laboratory crushing causes the  $LA$  value to decrease by 7 percentage points,  $LA_X$  increases by 12 percentage points. This shows that the impact of laboratory crushing is largest in terms of the amount of material remaining in the original test size 10–14 mm. This tendency is even clearer for micro-Deval, where laboratory crushing improves  $M_{DE}$  from 9.3 to 7.5, while  $M_{DE_X}$  is increased from 68 to 78.

No correlation is found between results for laboratory crushed vs primary crushed material neither for  $LA$  nor  $M_{DE}$ , as Fig. 16 illustrates. The improvement caused by laboratory crushing has shown to be consistent, as all points are gathered on or below the  $y = x$  line.

The two measures for mechanical properties are compared in Fig. 15. There is no correlation between Los Angeles abrasion and

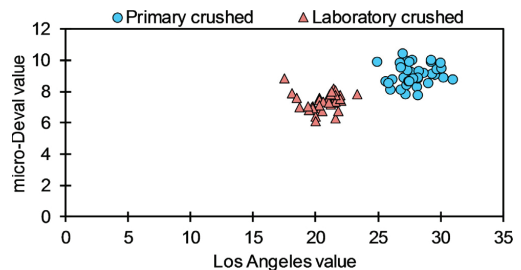


Fig. 15. Micro-Deval vs. Los Angeles test results, for primary and laboratory crushed material.

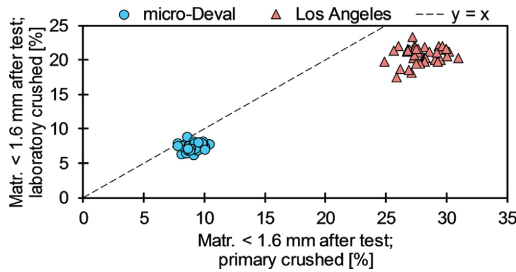


Fig. 16. Test results for laboratory crushed materials vs. primary crushed materials, for micro-Deval and Los Angeles tests.

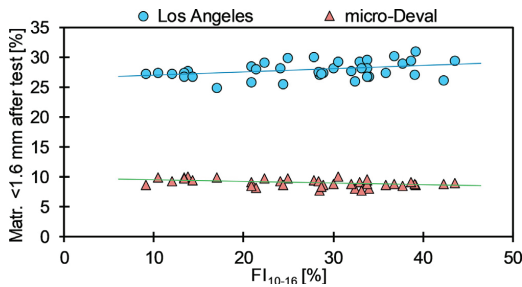


Fig. 17. Mechanical properties vs. flakiness index for particles in the size range used in mechanical testing (10–14 mm). Los Angeles:  $r^2 = 0.127$ , micro-Deval:  $r^2 = 0.188$ .

micro-Deval wear, neither for primary crushed nor laboratory crushed aggregates.

In the size range used for mechanical testing (10–16 mm), the test setup provoked variations in  $FI$  from 9.1 to 43.5. The mechanical properties for the primary crushed aggregates are compared to  $FI$  for 10–16 mm particles in Fig. 17. Even though the span in  $FI$  is large, there is no correlation to variation in either  $LA$  or  $M_{DE}$ .

The standard  $LA$  value does not correlate with any of the other parameters in the dataset. However, the amount of material left in the original test fraction after the  $LA$  test,  $LA_X$ , gives indications of relation both to the amount of product material smaller than  $CSS$  (Fig. 18a,  $r^2 = 0.539$ ) and the flakiness index for material smaller than  $CSS$  (Fig. 18b,  $r^2 = 0.475$ ).  $LA_X$  increases when the amount of product smaller than  $CSS$  increases. On the other hand,  $LA_X$  decreases when  $FI_{< CSS}$  increases.

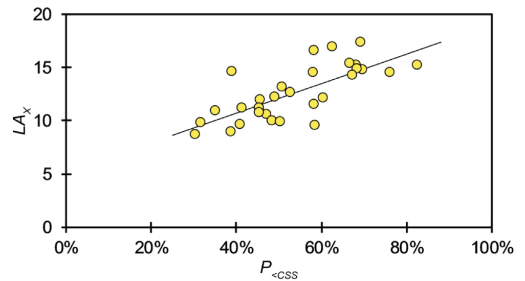
The closest predictor of  $M_{DE}$  found is  $F_{10}$ , which can explain 47% of the variation in  $M_{DE}$ . Although the variation in  $M_{DE}$  is small, the relation between  $M_{DE}$  and  $F_{10}$  is statistically significant at the 99% confidence level. For higher  $F_{10}$  sizes, the measured  $M_{DE}$  value is reduced, as seen in Fig. 19.

4. Discussion

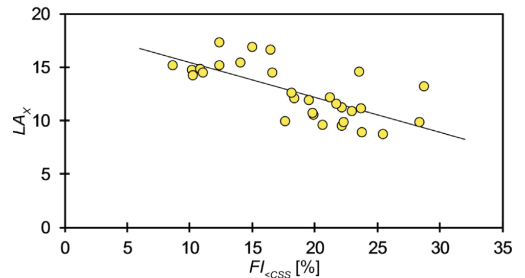
4.1. Test material

The average  $LA$  of granodiorite from Norwegian quarries is about 30, with variation from 17 to 48 for 19 surveyed deposits (Erichsen et al., 2008). The Finnish granodiorite used in the present research had a declared  $LA$  of 28; thus, the chosen test material is well within the normal quality range for this rock type.

The scalping process successfully enabled the separation of five different feed gradations from the original material provided from the quarry, as seen in Fig. 1. The variation between  $d = 0$  and  $d = 100$  mm



(a)  $LA_X$  vs amount of product smaller than  $CSS$  ( $P_{<CSS}$ );  $r^2 = 0.539$



(b)  $LA_X$  vs  $FI_{<CSS}$ ;  $r^2 = 0.496$

Fig. 18. Possible correlating factors for amount of material left in original test size after  $LA$  test ( $LA_X$ ).

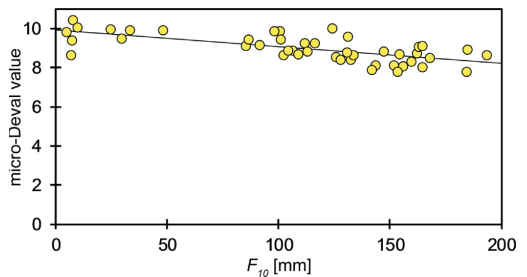


Fig. 19. Micro-Deval value  $M_{DE}$  depending on  $F_{10}$ ;  $r^2 = 0.468$ .

is used to analyse the effect of keeping fines present in the feed, while  $d = 180$  mm can illustrate the effect of segregation in the feed flow, resulting in periods of more uniformly graded feed material.

Due to the lack of suitable laboratory equipment for sieving of large-size materials, PSD for the feed materials are found using digital image processing (DIP). There are few specifications available regarding capturing of images for DIP for full gradation aggregate samples. A standard focused on large-sized aggregates (NS 3468, 2019), published after the tests presented in this paper were conducted, requires a minimum of 400 particles for each analysis. Especially for the coarse samples (e.g. 180–400 mm feed), the conditions are not optimal for DIP due to the limited number of particles visible in each image. For the feed samples containing fines, the number of particles was not a problem.

To obtain valid PSD results for the feed materials from sieving, the whole test portion of 1500–2500 kg should be analysed due to the large particle sizes. The reliability of the results would have improved had the feed samples been sieved, but due to the large particle sizes and

sample weights, this was not feasible. The method of taking photos of the feed material when it was loaded onto the feeder limited the number of particles in the analysis. On the other hand, this method ensured that the particles analysed in DIP were the exact same particles present in each crushing test. Capturing images from the stockpile would enable more particles to be present in each image, but would involve a risk of not uncovering differences in gradation between parallel tests due to segregation. In a production setup with continuous feeding, images could be provided from a conveyor belt feeding the crusher, allowing for the combined analysis of several images to obtain a valid number of particles.

DIP using images from the feeder enabled individual analyses of each feed sample, and the PSD curves in Fig. 1 show that the method was sufficiently accurate to display clear differences between the five chosen feed gradations.

#### 4.2. Setting/reduction ratio

As would be expected, a higher CSS increases the capacity of the crushing operation, because a larger opening of the crusher requires less size reduction before the material can be released from the crusher. However, when capacity is differentiated by CSS as in Fig. 3, a clear relation is also found between capacity and  $F_{10}$ . When smaller particle sizes are present in the feed, more voids between larger particles are filled with smaller particles - the material density in the crusher is increased - and the degree of interparticle crushing increases. At the same time, smaller particles require fewer crushing events before their size is reduced enough to be released from the crusher. Increased density and less required size reduction both contribute to the increase in capacity when the  $F_{10}$  size decreases.

Although Fig. 10a shows a considerable reduction in flakiness for a specific particle size when CSS is decreased, the overall  $FI < 2_{CSS}$  and  $FI < CSS$  is nearly constant. Hence, the effect of CSS depends on the intended screening and use of the products; if the overall particle shape of the full product gradation is of interest, CSS can be increased to achieve a coarser product with less SEC and higher capacity while maintaining the same global FI. However, if the desired quality is related to the material below a certain particle size, reducing CSS will result in a more cubical shape of the product at the cost of increased SEC and reduced capacity. These results are consistent with the conclusions from Bouquety et al. (2007), who also found that crusher setting influences F10 of individual size fractions, but not the global FI.

Briggs and Evertsson (1998) concluded that efficient size reduction and shape improvement are not possible at the same time, which could imply a positive correlation between the flakiness index and reduction ratio. However, in the current data, no correlation was found between the reduction ratio and particle shape.

#### 4.3. Reduced feed rate

The reduced feed rate corresponded to operating the crusher with a throughput of about half of the capacity. The tests where the feed rate was lowered had the lowest power draw, but the production is inefficient due to the low throughput. The power draw measured for these tests will be affected by the material flow through the crusher not being constant.

The top size of the product was not affected by the feed rate, but the PSD curve is steeper when the feed rate is reduced. The results are ambiguous for fines/lower size because the amount of fines was reduced for the 100/400 mm feed material when feed rate was reduced, while it remained unchanged for the 100/300 mm feed material. The PSD curves show that there is more material in the sizes above CSS when the feed rate is reduced.

As the throughput is reduced by about 50%, the reduced material density in the crusher results in less particle-to-particle crushing; hence, the material passing through the crusher will be subject to fewer

crushing events. Reducing the feed rate results in a more flaky product for all particle sizes below 50 mm. The increase is largest for material smaller than 25 mm. Yet for the most coarse particles (50–125 mm), FI is instead reduced when the feed rate is lowered. Eloranta (1995) stated that choke feeding is necessary to obtain good particle shape. The current results indicate that the trend is the same for a single-stage crushing process using a jaw crusher; the shape is improved at the high feed rate.

The reduced feed rate was tested with feed materials where  $d = 100$  mm and CSS at 40 mm for 100/300 mm feed and 70 mm for 100/400 mm feed. Thus, there was no material smaller than CSS present in the feed in these tests.

#### 4.4. Reduced crusher speed

Reducing the crusher speed results in an increased SEC (Fig. 4b), while the PSD curve is steeper (Fig. 6). The particle shape is shifted (Fig. 10d) similarly as described by Bengtsson (2009); smaller particles have higher flakiness. SEC is increased as a result of both a reduced throughput and an increased power draw. Guimaraes et al. (2007) found that energy consumption increased when the amount of fines produced increased, but in the current data, the amount of finer material is not increased when energy consumption increases. The results indicate that some of the additional energy consumed when crusher speed is reduced can go towards particle shape improvement for the larger particles, not additional size reduction. These results are, however, limited in that the smallest particle size measured in the current dataset is 1 mm. There could be variations in fines content below this size, which would not be detected by the chosen analysis.

Eloranta (1995) found that increased crusher speed would improve particle shape, i.e. decrease flakiness index. Both Bengtsson and Eloranta note that although altering crusher speed has some effect on the particle shape, the changes become small compared to the impact of other parameters. This is true also for the current dataset; particle shape is more affected by changes in feed gradation, crusher setting or feed rate than crusher speed.

#### 4.5. Flakiness index

For the tests where fines are present in the feed, some of the material assessed after crushing will have passed through the crusher without any size reduction. The improved particle shape when fines are present in the feed could raise the question of whether the feed material had lower FI than the crushed material. As no shape characterisation of the material was conducted prior to crushing, this question can not be examined using the present data. However, Bengtsson (2009) did find that feed shape did not affect product shape.

The flakiness index is found to be higher for the smaller particles of a distribution, corresponding to the results from Bouquety et al. (2007). Bengtsson and Evertsson (2006) found that the size range close to the crusher setting had the best particle shape, identified by an increasing FI above CSS. In the current dataset (Fig. 10a), no increase is seen for the largest particles. On the other hand, 12.5–16 mm is identified as the size range where the particles are most flaky.

A deviation from the FI standard is that also larger particles than described in the standard procedure ( $> 100$  mm) was measured in the present data. The calculation of the flakiness index is a weighted average of all individual fractions; thus, the comparison between different materials are affected by their top size. Bouquety et al. (2007) note that differences in flakiness in smaller fractions are hidden by the weighting in the calculation of the global FI. Due to the nature of the particle size distribution and the set division into size fractions, the weight of the smallest fractions are considerably smaller than the weight of the largest fractions. For the samples tested in the current dataset, the median weight for the 4–5 mm fraction was 2138 g, while the median weight for the 80–100 mm fraction was 34,926 g.

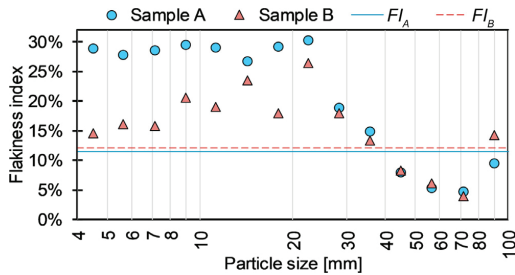


Fig. 20. Comparison of individual fraction  $FI$  (points) for two test materials of similar  $FL_{4-100}$  (lines).

The example in Fig. 20 illustrates the dominating effect of the larger fractions. In this example, sample A has a  $FI$  higher than or equal to sample B in all fractions except the one analysed using the 50 mm bar sieve. Still, due to the mass of the coarsest fractions, the result is that the standard  $FL_{4-100}$  is very similar.  $FI$  is lower for sample A (11.5) than sample B (12.1) even though the difference in particle shape for the smaller individual fractions is considerable, where sample A have the highest  $FI$  values. It is clear that the weighted average calculation hides differences in the smaller particle sizes.

In further research on this topic, alternative methods for calculation of  $FI$  for wide gradations should be investigated. The current standard calculation is reliable for narrow size fractions, but for gradations including the full size range from 4 to 100 mm, differences in particle shape can be hidden. Particle shape is the property most visibly affected when crushing parameters are changed. To investigate the effect of such changes, it is necessary to analyse individual size fractions and not only the weighted average for all sizes.

#### 4.6. Mechanical tests

##### 4.6.1. Preparation of samples

22/125 mm is a common gradation for subbase materials in Norway. The general practice for mechanical testing of such large-size aggregates is to collect a 30 kg sample of the available aggregate (e.g. hand specimens) and prepare the 10–14 mm test portion by laboratory crushing as described in Section 2.2.3. From the results found in Fig. 13, it is apparent that the practice of sample preparation by laboratory crushing affects the reported results. These results match the conclusions from Räsänen and Mertamo (2004) who also found that laboratory crushing resulted in shape properties which were not representative of full-scale crushing conditions.

The lack of relationship between LA results for primary and laboratory crushed aggregates in Fig. 15 shows that the laboratory crushing not only improves the test results, but also does not preserve the ranking between stronger and weaker samples. As this experiment is limited to one rock type only, the span of qualities measured is limited with  $LA_{primary}$  varying from 24.2 to 31.0.

The general assumption that the results from mechanical tests are an expression for geological properties of the material is refuted, as it is clear that production methods affect the mechanical properties of the material. Thus, mechanical strength should not be assumed constant for all products produced from a specific rock deposit. It is generally accepted that the mechanical properties of an aggregate are improved from each crushing stage because weak minerals are worn off. Hence, there is a risk of overrating the quality of an aggregate when the tested samples are laboratory crushed twice after primary crushing. A sample processed in such a way should not be considered representative for the quality of primary crushed aggregates. When the difference in test result due to sample preparation is as big as 26%, there is a clear risk of ranking alternative available materials wrongfully if the sample

preparation is not identical for all samples.

##### 4.6.2. Relation to particle shape

Both Andersson and Öjeborn (2014), Benediktsson (2015) and Cook et al. (2017) found mechanical properties to be related to flakiness. In the current dataset, both LA and  $M_{DE}$  show poor correlation to  $FI$  (Fig. 17). Benediktsson (2015) found that the relationship is stronger when  $FI$  is compared to the remaining material in the original test portion size. For the current data, this is true for  $LA_X$ , while there is no improvement in the correlation between  $M_{DE_X}$  and  $FI$ . Our data show that a decreasing  $FI$  for the test portion results in more material left in the original test fraction after the LA test. However, these relations can not explain more than about 50% of the variation in LA, so clearly, other factors influence the degradation in the LA test besides particle shape. Particle shape and product gradation are highly correlated, as seen in Fig. 12b, so these factors should not be combined in the prediction of  $LA_X$ .

In the current dataset, the largest amount of flaky particles was found in the size range used for mechanical testing. The samples used for laboratory crushing was in the 63–90 mm size range and had a considerably lower  $FI$ . Furthermore, the two-stage laboratory crushing process is also designed to provide well-shaped products. Based on the presented literature, the difference in particle shape can contribute to the large difference in mechanical properties for primary crushed and laboratory crushed aggregates (Fig. 13).

##### 4.6.3. Relation to gradation

$M_{DE}$  is related to the gradation of the feed material through  $F_{10}$  (Fig. 19). Increasing  $F_{10}$  leads to a decrease in  $M_{DE}$ ; i.e. coarser material in the feed results in higher resistance to abrasion. A possible explanation is that fine material can pass through the crusher with low or no size reduction, leading to a high amount of uncrushed particles in the  $M_{DE}$  test portion. When the  $F_{10}$  size is high, the material tested for  $M_{DE}$  has been subject to a bigger size reduction. Although the span of  $F_{10}$  is large, the variation in  $M_{DE}$  is very small, so the increase in abrasion for smaller feed sizes will not likely have any practical consequences.

There is no correlation between Los Angeles abrasion and micro-Deval wear, neither for primary crushed nor laboratory crushed aggregates. The differences in gradation of the test portions after testing, as seen in Fig. 14, show that different degradation mechanisms are applied and that the two tests are quantifying separate properties. Important differences between the tests are that water is present in the micro-Deval test, and the detrimental forces are higher in the LA test. The findings from Fladvad et al. (2017) indicate that LA is more commonly used as a quality requirement than  $M_{DE}$ . Considering the moisture level in the tests, the  $M_{DE}$  test could be considered better suited to assess aggregates for unbound use, as moisture will be present in the road structure.

One could assume that the amount of material remaining in the original size after testing is a more valuable parameter than the amount of material broken down to 1.6 mm or smaller. However, both Los Angeles and micro-Deval are empirical tests where requirements are set with reference to practical experience (Erichsen et al., 2011). The amount of material broken down from 10–14 mm to smaller than 1.6 mm might not have practical value on its own, but it is related to general experience with the abrasion and fragmentation of unbound aggregates. It is however seen both in the present data and by Erichsen (2015) that a more extensive analysis of the sample gradation after mechanical testing provides valuable knowledge about the degradation properties of the tested material.

#### 4.7. Implications of feed gradation

Including fines in the feed during crushing improves particle shape and reduces specific energy consumption, but can result in a particle size distribution including excess fines, thus requiring an extra screening process to obtain a valuable product gradation. What is gained by a high crushing capacity may be lost due to the need for further processing. The product yield, or the proportion of valuable products vs by-products, has not been part of this study. A simple single-stage crushing plant can be used for various products and the definition of valuable products and by-products depends on the applications. Generally, a high fines content is undesirable because the aggregate material becomes sensitive to moisture and frost.

Moisture content is generally considered an important factor for the stability and compactability of unbound aggregates, as pointed out by e.g. Coronado et al. (2011). However, moisture sensitivity is closely related to the full gradation of the aggregate, and cannot be related to the limited size gradation used in the mechanical tests in the present research. Cook et al. (2017) found that particle shape affects the packing density of unbound aggregates. The full-scale tests conducted in this study shows that both gradation and particle shape can be widely modified by adjusting the production process. A single-stage crushing process including screening equipment can be adjusted to produce aggregates adapted to the gradation suitable for the application.

#### 4.8. Future work

In order to systematically use the knowledge gathered from the full-scale tests, the results should be implemented in models for predicting crusher operation and product quality. The dataset produced in this study could be used to calibrate or validate the model presented by Johansson et al. (2017) regarding capacity, power draw, SEC and particle size prediction.

The data presented here is limited to a single rock type and a single jaw crusher. A natural continuation of this research would be to extend the test programme to include several rock types of varying strength and brittleness. Another possibility is to include other jaw crushers to assess the effect of crusher geometry.

### 5. Conclusions

The full-scale parameter study allowed for a range of feed material sizes, reduction ratios and crusher operation parameters to be combined. The subsequent quality assessment was conducted using laboratory tests for particle shape and resistance to wear and fragmentation. From the results, the following conclusions can be drawn:

- Particle shape is the quality parameter most affected by variations in the crushing process. The maximal product particle size is highly dependant on the setting of the crusher, so for comparison of particle shape for full gradations, the size range analysed should be related to crusher setting (CSS).
- To investigate the effect of changing crusher parameters, analyses of particle shape of individual particle size fractions is necessary in addition to the full size range. The calculation method for flakiness index hides variation of particle shape within a product gradation, increasingly for wider gradations.
- Products in a specific particle size have lower flakiness when produced at a lower CSS. However, when flakiness for the full gradation below CSS ( $FI <_{CSS}$ ) is analysed,  $FI$  is independent of CSS.
- Reduced crusher speed increases the specific energy consumption of the crushing process by 50–150%, depending on  $F_{10}$ . Additionally, the product becomes less well-graded.
- The lower size of the feed material ( $d$  and  $F_{10}$ ) has a significant impact on the product particle shape.  $FI$  for individual fractions in the sizes 4–50 mm is 2.5–4 times higher when  $d = 180$  mm

compared to  $d = 0$  mm

- Reducing the feed rate results in a less well-graded product, and increases the flakiness for particles smaller than the crusher setting.  $FI$  for individual fractions in the size range 4–50 mm increases by on average 26% when the feed rate is reduced.
- The poor particle shape produced using low feed level and single-graded feed (180/400 mm) shows that inter-particle crushing is a prerequisite for cubical shape.
- Mechanical strength should not be assumed constant for all products produced from a specific rock deposit. Also, mechanical properties are highly affected by sample preparation; laboratory crushed samples are not representative of primary crushed aggregates.
- The amount of material remaining in the original test portion size after the LA test ( $LA_X$ ) is more closely related to the aggregate gradation and particle shape than the standard  $LA$  value.

The aim for the parameter study was to investigate whether previous research results regarding crusher operation and aggregate quality are valid also for a simple single-stage jaw crusher operation on large-size aggregates. In response to the original hypothesis the results show that crushing efficiency and product quality in terms of particle shape can be controlled. The quality of construction aggregates can be optimised by adjustments to the production process, even for a single-stage crushing process. In order to improve mechanical properties, several crushing steps are needed.

#### Declaration of Competing Interest

The authors declare that they have no known competing financial interests or personal relationships that could have appeared to influence the work reported in this paper.

#### Acknowledgements

The study is financed by the Norwegian Public Roads Administration, Metso Minerals and the Research Council of Norway through the industrial innovation project *Use of local materials* (project No. 256541). This article constitutes a part of the main author's PhD degree at Department of Geoscience and Petroleum, NTNU – Norwegian University of Science and Technology.

The field work was conducted at Metso Minerals' test plant in Tampere, Finland during May and June of 2017. The laboratory work took place at the laboratory of Norwegian Public Roads Administration in Trondheim, Norway during 2017 and 2018.

The authors would like to thank workers at Metso Minerals and Norwegian Public Roads Administration for valuable contributions to the field and laboratory work. Thanks also to master student Nils Arne Fjeldstad Luke who took care of a portion of the laboratory testing.

#### References

- Andersson, E., Öjertborn, S., 2014. Estimation of Rock Quality in Road Projects from Pre-Study to Aggregate (Master thesis). Chalmers University of Technology.
- Benediktsson, S., 2015. Effects of Particle Shape on Mechanical Properties of Aggregates (Master thesis). Norwegian University of Science and Technology.
- Bengtsson, M., 2009. Quality-Driven Production of Aggregates in Crushing Plants (Phd thesis). Chalmers University of Technology.
- Bengtsson, M., Evertsson, C.M., 2006. An empirical model for predicting flakiness in cone crushing. Int. J. Miner. Process. 79 (1), 49–60. <https://doi.org/10.1016/j.minpro.2005.12.002>.
- Bouquet, M., Descantes, Y., Barcelo, L., de Larrard, F., Clavaud, B., 2007. Experimental study of crushed aggregate shape. Constr. Build. Mater. 21 (4), 865–872. <https://doi.org/10.1016/j.conbuildmat.2005.12.013>.
- Brace, W.F., 1961. Dependence of fracture strength of rocks on grain size. In: The 4th U.S. Symposium on Rock Mechanics (USRMS). American Rock Mechanics Association. <https://www.onepetro.org/conference-paper/ARMA-61-099>.
- Brattli, B., 1992. The influence of geological factors on the mechanical properties of basic igneous rocks used as road surface aggregates. Eng. Geol. 33 (1), 31–44. [https://doi.org/10.1016/0013-7952\(92\)90033-U](https://doi.org/10.1016/0013-7952(92)90033-U).
- Briggs, C., Evertsson, C., 1998. Shape potential of rock. Miner. Eng. 11 (2), 125–132.

- [https://doi.org/10.1016/S0892-6875\(97\)00145-3](https://doi.org/10.1016/S0892-6875(97)00145-3).
- Cook, C.S., Tanju, B.F., Yavuz, A.B., 2017. Effect of particle shape on durability and performance of unbound aggregate base. *J. Mater. Civ. Eng.* 29 (2). [https://doi.org/10.1061/\(ASCE\)MT.1943-5533.0001752](https://doi.org/10.1061/(ASCE)MT.1943-5533.0001752). 04016 221.
- Coronado, O., Caicedo, B., Taibi, S., Correia, A.G., Fleureau, J.M., 2011. A macro geo-mechanical approach to rank non-standard unbound granular materials for pavements. *Eng. Geol.* 119 (1–2), 64–73. <https://doi.org/10.1016/j.enggeo.2011.02.003>.
- Eloranta, J., 1995. Influence of Crushing Process Variables on the Product Quality of Crushed Rock (Ph.D. thesis). Tampere University of Technology, Tampere, Finland.
- EN 1097-1, 2011. Tests for mechanical and physical properties of aggregates - Part 1: Determination of the resistance to wear (micro-Deval) EN 1097-1:2011. European Committee for Standardization, Brussels, Belgium.
- EN 1097-2, 2010. Tests for mechanical and physical properties of aggregates - Part 2: Methods for the determination of resistance to fragmentation EN 1097-2:2010. European Committee for Standardization, Brussels, Belgium.
- EN 13242, 2007. Aggregates for Unbound and Hydraulically Bound Materials for Use in Civil Engineering Work and Road Construction EN 13242:2002 + A1:2007. European Committee for Standardization, Brussels, Belgium.
- EN 13285, 2018. Unbound mixtures - Specifications EN 13285:2018. European Committee for Standardization, Brussels, Belgium.
- EN 933-1, 2012. Tests for geometrical properties of aggregates - Part 1: Determination of particle size distribution - Sieving method EN 933-1:2012. European Committee for Standardization, Brussels, Belgium.
- EN 933-3, 2012. Tests for Geometrical Properties of Aggregates - Part 3: Determination of Particle Shape - Flakiness Index EN 933-3:2012. European Committee for Standardization, Brussels, Belgium.
- Erichsen, E., 2015. Plotting aggregate degradation results from the Los Angeles test on a triangular diagram: proposal of a new quality ranking for aggregates. *Bull. Eng. Geol. Environ.* 74 (2), 667–671. <https://doi.org/10.1007/s10064-014-0655-z>.
- Erichsen, E., Ulvik, A., Sævik, K., 2011. Mechanical degradation of aggregate by the Los Angeles-, the Micro-Deval- and the nordic test methods. *Rock Mech. Rock Eng.* 44 (3), 333–337. <https://doi.org/10.1007/s00603-011-0140-y>.
- Erichsen, E., Ulvik, A., Wolden, K., Neeb, P.R., 2008. Aggregates in Norway - Properties defining the quality of sand, gravel and hard rock for use as aggregate for building purposes. In: Slagstad, T. (Ed.), *Geology for Society*, Geological Survey of Norway Special Publication, 11. Geological Survey of Norway, Trondheim, Norway, pp. 37–46. [http://www.ngu.no/upload/Publikasjoner/Specialpublication/SP11\\_LO.pdf](http://www.ngu.no/upload/Publikasjoner/Specialpublication/SP11_LO.pdf).
- Fladvad, M., Aurstad, J., Wigum, B.J., 2017. Comparison of practice for aggregate use in road construction - results from an international survey. In: Loizos, A., Al-Qadi, I., Scarpas, T. (Eds.), *Bearing Capacity of Roads, Railways and Airfields: Proceedings of the 10th International Conference on the Bearing Capacity of Roads, Railways and Airfields (BCRRA 2017)*, June 28–30, 2017, Athens, Greece. CRC Press, Athens, Greece. pp. 563–570, ISBN 9781138295957.
- Guimaraes, M., Valdes, J., Palomino, A., Santamarina, J., 2007. Aggregate production: fines generation during rock crushing. *Int. J. Miner. Process.* 81 (4), 237–247. <https://doi.org/10.1016/j.minpro.2006.08.004>.
- Johansson, M., Bengtsson, M., Evertsson, M., Hulthén, E., 2017. A fundamental model of an industrial-scale jaw crusher. *Miner. Eng.* 105, 69–78. <https://doi.org/10.1016/j.mineng.2017.01.012>.
- Lee, E., 2012. Optimization of Compressive Crushing (Ph.D. thesis). Chalmers University of Technology, Göteborg, Sweden.
- Miskovsky, K., Tabora Duarte, M., Kou, S., Lindqvist, P.A., 2004. Influence of the mineralogical composition and textural properties on the quality of coarse aggregates. *J. Mater. Eng. Perform.* 13 (2), 144–150. <https://doi.org/10.1361/10599490418334>.
- Norwegian Public Roads Administration, 2014. Håndbok N200 Vegbygging [Manual N200 Road construction]. Statens vegvesen Vegdirektoratet, Oslo, Norway [https://www.vegvesen.no/\\_attachment/188382/binary/980128?fast\\_title=Tidligere+utgave%3A+Håndbok+N200+Vegbygging+2014+%2821+MB%29.pdf](https://www.vegvesen.no/_attachment/188382/binary/980128?fast_title=Tidligere+utgave%3A+Håndbok+N200+Vegbygging+2014+%2821+MB%29.pdf).
- Norwegian Public Roads Administration, 2016. Håndbok R210 Laboratorieundersøkelser [Manual R210 Laboratory tests]. Statens vegvesen Vegdirektoratet. ISBN 9788272076930. URL [https://www.vegvesen.no/\\_attachment/185231/binary/1276518?fast\\_title=Håndbok+R210+Laboratorieundersøkelser+%2811+MB%29.pdf](https://www.vegvesen.no/_attachment/185231/binary/1276518?fast_title=Håndbok+R210+Laboratorieundersøkelser+%2811+MB%29.pdf).
- Norwegian Public Roads Administration, 2018. Håndbok N200 Vegbygging [Manual N200 Road construction]. Statens vegvesen Vegdirektoratet, Oslo, Norway ISBN 978-82-7207-723-4. [https://www.vegvesen.no/\\_attachment/2364236/binary/1269980?fast\\_title=Håndbok+N200+Vegbygging+%2810+MB%29.pdf](https://www.vegvesen.no/_attachment/2364236/binary/1269980?fast_title=Håndbok+N200+Vegbygging+%2810+MB%29.pdf).
- NS 3468, 2019. Coarse materials of stone for use in civil engineering works - Specification NS 3468:2019. Standards Norway, Lysaker, Norway.
- Räisänen, M., Mertamo, M., 2004. An evaluation of the procedure and results of laboratory crushing in quality assessment of rock aggregate raw materials. *Bull. Eng. Geol. Environ.* 63 (1), 33–39. <https://doi.org/10.1007/s10064-003-0218-1>.

## Performance of unbound pavement materials in changing moisture conditions

Marit Fladvad & Sigurdur Erlingsson

Fladvad, M. & Erlingsson, S. (2020). Performance of unbound pavement materials in changing moisture conditions. In Chabot A., Hornych P., Harvey J., Loria-Salazar L. G. (eds) *Accelerated Pavement Testing to Transport Infrastructure Innovation*. Lecture Notes in Civil Engineering, vol 96. Springer. doi: 10.1007/978-3-030-55236-7\_8

This paper is not included due to copyright

## **Modelling the response of large-size subbase materials tested under varying moisture conditions in a heavy vehicle simulator**

Marit Fladvad & Sigurdur Erlingsson

*Submitted to Road Materials and Pavement Design*

Fladvad, M. & Erlingsson, S. (2020). Modelling the response of large-size subbase materials tested under varying moisture conditions in a heavy vehicle simulator. Submitted manuscript.

This paper is awaiting publication and is not included in NTNU Open



**Permanent deformation modelling of large-size unbound pavement materials tested in a heavy vehicle simulator under different moisture conditions**

Marit Fladvad & Sigurdur Erlingsson

*Submitted to Road Materials and Pavement Design*

Fladvad, M. & Erlingsson, S. (2020). Permanent deformation modelling of large-size unbound pavement materials tested in a heavy vehicle simulator under different moisture conditions. Submitted manuscript.

This paper is awaiting publication and is not included in NTNU Open

ISBN 978-82-326-4962-4 (printed ver.)  
ISBN 978-82-326-4963-1 (electronic ver.)  
ISSN 1503-8181